Dissertation

Inflammatory Response to Continuous Subcutaneous Insulin Infusion Systems and the Effect on Insulin Absorption

submitted by

Dipl. Ing. Jasmin Renée HAUZENBERGER, BSc.

for the Academic Degree of

Doctor of Philosophy (PhD)

at the

Medical University of Graz

Department of Internal Medicine

Division of Endocrinology and Diabetology

under the Supervision of

Prof. Dr. Thomas R. PIEBER

2017

Statutory Declaration

I hereby declare that this thesis is my own original work and that I have fully acknowledged by name all of those individuals and organizations that have contributed to the research for this thesis. Due acknowledgement has been made in the text to all other material used. Throughout this thesis and in all related publications I followed the “Standards of Good Scientific Practice and Ombuds Committee at the Medical University of Graz“.

Graz, September 1, 2017

Jasmin Hauzenberger, e.h.

DISCLOSURES

Parts of this thesis have been published in

> Hauzenberger JR, Hipszer BR, Loeum C, McCue PA, DeStefano M, Torjman MC, Kaner MT, Dinesen AR, Chervoneva I, Pieber TR, Joseph JI. (2017) *Detailed Analysis of Insulin Absorption Variability and the Tissue Response to Continuous Subcutaneous Insulin Infusion Catheter Implantation in Swine.* Diabetes Technol Ther. doi: 10.1089/dia.2017.0175

The wording and figures have been adapted to fit the scope of this thesis.

The following persons have contributed actively to the results of this thesis and have explicitly agreed to the use of their data in my thesis:

1. Asslaber Martin, Department of Pathology, Medical University of Graz, Austria;
   Contribution: Lead pathologist; sectioned, stained and analyzed tissue samples for Study III.
2. Chervoneva Inna, Department of Pharmacology and Experimental Therapeutics, Sidney Kimmel Medical College, Thomas Jefferson University, Philadelphia, PA, USA;
   Contribution: Carried out large parts of the statistical analyses for Study I.
3. DeStefano Mark, Animas Corp., West Chester, PA, USA;
   Contribution: Planned and co-coordinated Study I. Helped with manuscript preparation (DTT 2017).
4. Dinesen Alek R., Department of Anesthesiology, Jefferson Artificial Pancreas Center, Sidney Kimmel Medical College, Thomas Jefferson University, Philadelphia, PA, USA;
   Contribution: Helped with animal work, tissue excision, slide scanning and data interpretation in Study I and Study II.
5. Hipszer Brian R., Department of Anesthesiology, Jefferson Artificial Pancreas Center, Sidney Kimmel Medical College, Thomas Jefferson University, Philadelphia, PA, USA;
   Contribution: Major contributor in Study I. Planned study, carried out animal work, acquired and organized data and did the first rough analysis of Study I. Helped with manuscript preparation (DTT 2017).

6. Joseph Jeffrey I, Department of Anesthesiology, Jefferson Artificial Pancreas Center, Sidney Kimmel Medical College, Thomas Jefferson University, Philadelphia, PA, USA;
   Contribution: Principal investigator, initiator and planner of Study I and Study II. Major scientific input for the planning of Study III. Contributed to composition of manuscript (DTT 2017).
7. Kaner Mahmut T., Department of Anesthesiology, Jefferson Artificial Pancreas Center, Sidney Kimmel Medical College, Thomas Jefferson University, Philadelphia, PA, USA;
   Contribution: Helped with animal work, tissue excision, slide scanning and data interpretation in Study I and Study II.
8. Loeum Channy, Department of Anesthesiology, Jefferson Artificial Pancreas Center, Sidney Kimmel Medical College, Thomas Jefferson University, Philadelphia, PA, USA;
   Contribution: Lab management at TJU; IACUC composition and animal work for Study I and Study II.
9. McCue Peter A., Department of Pathology, Thomas Jefferson University, Philadelphia, PA, USA;
   Contribution: Lead pathologist; sectioned, stained and analyzed tissue samples for Study I.
10. Münzker Julia, Division of Endocrinology and Diabetology, Medical University of Graz, Austria
    Contribution: Helped with animal work, tissue excision, slide scanning and statistical data analysis in Study III.
11. Torjman Marc C., Department of Anesthesiology, Jefferson Artificial Pancreas Center, Sidney Kimmel Medical College, Thomas Jefferson University, Philadelphia, PA, USA
    Contribution: Senior scientist at TJU, contributed in animal work and carried out large parts of the statistical analyses of Study I and Study II.

I have obtained written permission to reproduce figures and/or tables published in:

- Pickup JC, Mattock M, Kerry S (2002) Glycaemic control with continuous subcutaneous insulin infusion compared with intensive insulin injections in patients with type 1 diabetes: meta-analysis of randomised controlled trials. Br Medica J 324:705–711. (= *Figure 4*)
- Seereiner S, Neeser K, Weber C, et al (2010) Attitudes towards insulin pump therapy among adolescents and young people. Diabetes Technol Ther 12:89–94 6p. doi: 10.1089/dia.2009.0080 (= *Figure 6*)

ACKNOWLEDGEMENTS

I, Jasmin Hauzenberger, received funding from the Austrian Science Fund FWF (W1241) and the Medical University of Graz through the PhD Program Molecular Fundamentals of Inflammation (DK-MOLIN). I received further funding from the *BOSCH-Forschungsstiftung, Stiftung zur Förderung von Wissenschaft in Forschung und Lehre* (Deutsches Stiftungszetrum GmbH).

I would like to first and foremost thank my supervisor Thomas Pieber for always believing in this project, even in times I didn't, and for teaching me the art of selling vacuum cleaners. I look forward to the projects ahead!

Thank you to my lovely co-workers of the BRUT, especially Julia and Petra, for all your scientific inspiration and motivation over countless cups of coffee and Dinkelknöpfe. A special thanks to Verena Zachhuber, for making sure my experiments went smoothly and my results were reproducible. Thank you, Martin Hajnsek, for adopting me in the first year of my PhD and not only giving me a project but also a desk in your office.

I am forever grateful to have been able to work with the inspiring and energetic Jeffrey Joseph in Philadelphia, the city that became my second home. Your endless lessons on life, science and business are accompanying me every step of the way.

Thank you to Agnes, Isabella and Carolina – without you I would have quit this PhD a long time ago. You are the most beautiful, smart and inspiring women I know.

Thank you to my family, especially my parents, who never seize to believe in me. And lastly, to my partner in life and crime, Dominik, who has had to endure my ups and downs these past 4 years - thank you for sticking around and dealing with me, you always help me put everything in perspective.

TABLE OF CONTENT

ABBREVIATIONS

ADA	American Diabetes Association
ANOVA	Analysis of variance
AP	Artificial pancreas
AUC	Area under the curve
AUC_{GIR}	Area under the glucose infusion rate curve
BG	Blood glucose
BW	Body weight
cDNA	Complementary DNA
CGM	Continuous glucose monitor
C_{max}	Maximum plasma insulin concentration
CSII	Continuous subcutaneous insulin infusion
CVC	Central venous catheter
D-20	20 % Dextrose solution
D-50	50 % Dextrose solution
EASD	European Association for the Study of Diabetes
ELISA	Enzyme-linked immunosorbent assay
FBGC	Foreign body giant cell
FBR	Foreign body response
FDA	Food and Drug Administration
GIR	Glucose infusion rate
GOx	Glucose oxidase
H&E	Hematoxylin and eosin
HbA1c	Glycated hemoglobin
IL	Interleukin
IV	Intravenous(ly)
MIQE	Minimum Information for Publication of Quantitative Real-Time PCR Experiments
mRNA	Messenger RNA
n.s.	Not statistically significant
PD	Pharmacodynamics
PK	Pharmacokinetics
qPCR	Quantitative real-time PCR
SC	Subcutaneous(ly)
TGF-β	Tissue growth factor beta
TJU	Thomas Jefferson University, PA, USA
t_{max}	Time to maximum plasma insulin concentration
TNF-α	Tumor necrosis factor alpha
tPA	Tissue plasminogen activator
VAMP	Venous Arterial Blood Management

LIST OF FIGURES

LIST OF TABLES

LIST OF EQUATIONS

ZUSAMMENFASSUNG

Typ-1-Diabtes ist eine Autoimmunerkrankung, bei welcher die Betazellen der Pankreas vom körpereigenen Immunsystem zerstört werden. Patienten sind von externer Insulingabe abhängig und etwa eine Million dieser Patienten verwenden eine Insulinpumpe und einen kontinuierlichen subkutanen Insulininfusionskatheter (CSII), um den Diabetes zu kontrollieren. Die Variabilität der Insulinresorption nimmt über die Tragedauer des Katheters zu und es wird deshalb empfohlen, den Katheter alle 2 bis 3 Tage durch einen neuen zu ersetzen. Die zugrundeliegenden Mechanismen, die für die Variabilität der Insulinresorption verantwortlich sind, sind nach wie vor ungeklärt und Daten hierzu sind rar. Diese Arbeit hatte zum Ziel, die Entzündungsreaktion auf CSII-Katheter und die pharmakokinetische Variabilität des Insulins in zwei verschiedenen Tiermodellen (Schwein und Hund) zu untersuchen. Die Insulinresorption sowie die Gewebsreaktion wurden über einen Zeitraum von bis zu 7 Tage Tragedauer systematisch untersucht. Die Insulinresorption war, verglichen mit Tag 1, am 5. und 6. Tag Tragedauer besser, aber zeigte eine erhöhte Variabilität. Das Setzen und Tragen des Katheters führte zu einem akuten lokalen Trauma und zur Ausbildung einer Barriere aus Zellen und Gewebstrümmern entlang des Stichkanals. Die Ergebnisse dieser Arbeit zeigen, dass flexible Teflonkatheter mit stumpfem Ende besser verträglich sind, als starre Stahlkatheter mit scharfer Spitze. Das Hausschwein stellt gegenüber dem Hund ein besseres Modell für die humane Wundheilung dar. Die Entzündungsreaktion muss für die zukünftige Entwicklung neuer CSII-Katheterdesigns berücksichtigt werden.

ABSTRACT

Type 1 diabetes is an autoimmune disease manifested in the destruction of beta cells of the pancreas. Patients are dependent on external insulin administration and approximately 1 million manage their diabetes with an insulin pump and a continuous subcutaneous insulin infusion (CSII) catheter. Variability of insulin absorption from a CSII catheter increases over wear-time and thus catheters are recommended to be replaced every 2-3 days. Mechanisms responsible for variable insulin absorption are poorly understood and only limited data is available. This thesis aimed to elucidate the inflammatory response to CSII catheters and the pharmacokinetic variability of insulin in 2 different animal models (swine and dog). Insulin absorption and tissue response were systematically evaluated over up to 7 days of catheter wear-time. Insulin absorption was better on days 5 and 6 of wear-time compared to day 1, however, variability increases. The insertion and maintenance lead to an acute local trauma and the formation of a layer of cell and tissue debris along the insertion channel. The results of this thesis show that flexible Teflon with a blunt end is better tolerable than rigid steel with a sharp tip. Based on the tissue histology and composition of skin and subcutaneous adipose tissue, the swine is a better model for human wound healing compared with the dog. The inflammatory response needs to be taken into account for future CSII catheter design.

1. INTRODUCTION

Insulin pump therapy, also known as continuous subcutaneous insulin infusion (CSII), is a therapeutic method to control blood glucose in patients with impaired beta cell function and decreased or no insulin production. The majority of patients on CSII therapy suffer from the auto-immune disease type 1 diabetes but also a small percentage of patients with advanced stages of type 2 diabetes use insulin pumps. CSII therapy mimics the beta-cell function by infusing rapid-acting insulin into the subcutaneous tissue at adjustable rates via an electromechanical pump [1, 2].

1.1 HISTORY OF INSULIN PUMP THERAPY

In 1963, Dr. Arnold Kadish designed the first insulin pump to be worn as a backpack (Figure 1). In this design, both glucagon and insulin were infused intravenously (IV).

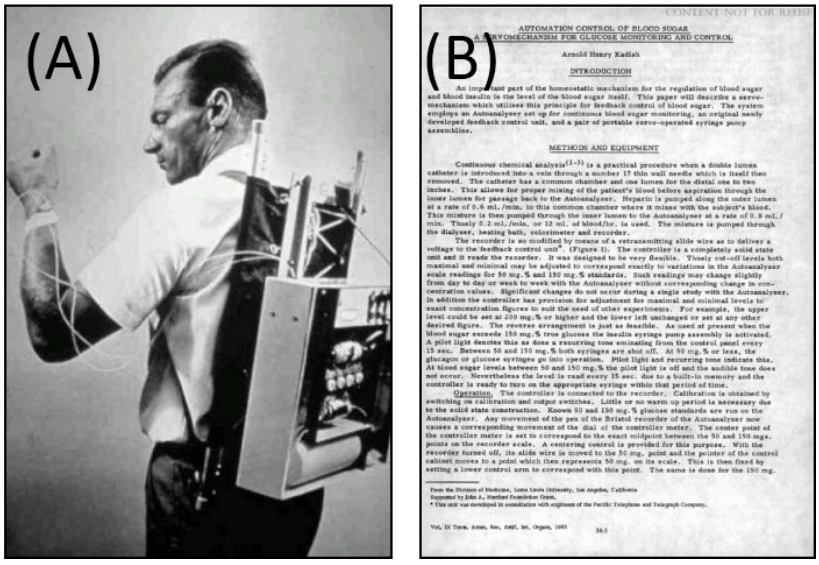

Figure 1: **(A)** Kadish wearing the first dual-hormone pump as a backpack. **(B)** First page of Kadish's publication in *Transactions - American Society for Artificial Internal Organs*, April 1963

In 1974, Gérard Slama and colleagues showed that open-loop IV insulin infusion using a portable pump held in a shoulder bag produced good glycemic control in type 1 diabetes [3]. Professor Harry Keen in London was the first to suggest

subcutaneous (SC) infusion of short-acting insulin to improve metabolic control and avoid the risks associated with long-term IV infusion (e.g. thrombosis). Together with his student John Pickup he went on to develop CSII therapy in the form of a battery-powered, 159 g miniature syringe - the "Mill Hill Infuser" (Figure 2) [4]. This pump became commercially available in 1976. Patients were able to implant a butterfly steel needle themselves to infuse insulin into the subcutaneous tissue of the abdomen.

Figure 2: The "Mill Hill Infuser" (top) and with the casing removed (bottom) showing the syringe drive [5].

In 1978, Dean Kamen improved Kadish's model to a more wearable version and commercialized the first pump which was known as the “Big Blue Brick” in the medical community. Unfortunately, this model lacked features necessary for safe insulin delivery and required a screwdriver to adjust dosage. Kamen sold his company “AutoSyringe” to Baxter Health Care in 1981, when he was only 30 years old.

Pump therapy remained not very user-friendly throughout the 1980s. They were heavy and large and reserved only for the most difficult-to-manage cases of diabetes. By the 1990s pumps became easier to handle, both in size and technology, and ensured greater safety and better blood sugar control for patients. Pumps advanced over the years and received bonus features such as an integrated bolus calculator. This feature advises patients on optimal meal boluses based on the carbohydrate content of the meal and the target blood glucose,

taking into account the remaining insulin from the previous bolus. The idea of a closed-loop artificial pancreas evolved, in which the insulin pump and a continuous glucose monitor communicate automatically, mimicking the function of a healthy pancreas [6–14].

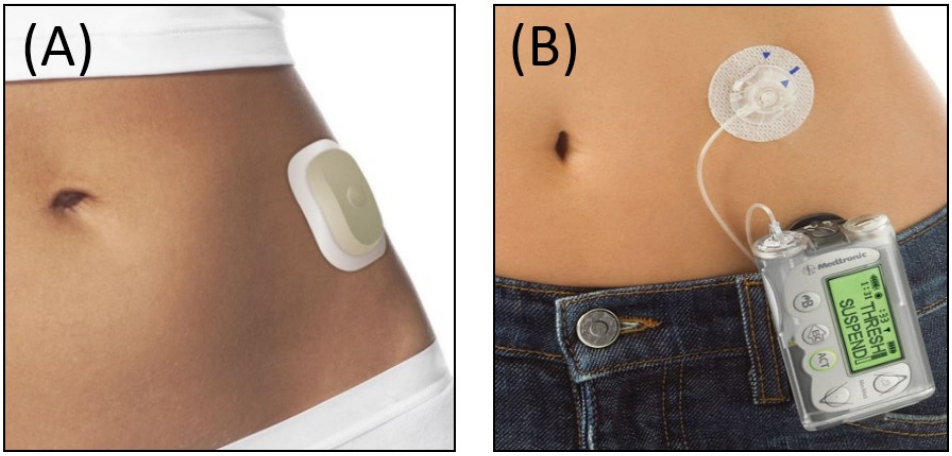

Figure 3: Insulin pumps. **(A)** Patch pump on weight-bearing adhesive. (from: http://www.medicaldevice-developments.com) **(B)** Tethered pump with insulin infusion set. (from: http://www.edinburghdiabetes.com/pump-patients/)

Modern battery-powered insulin pumps contain an insulin reservoir and a computerized control mechanism that is linked to a motor. There are two designs available of the modern insulin pump: patch pumps and tethered pumps. The patch pump reservoir is applied directly to the skin via an adhesive with the insulin infusion catheter attached to the pump and adhesive (Figure 3A). The cannula is inserted via an automated inserter. An example for a patch pump is the Omnipod (Insulet, Billerica, MA, USA). The majority of pumps are tethered, where the insulin reservoir in the pump is connected to a subcutaneous insulin infusion (CSII) catheter via plastic tubing (“infusion set”). The catheter consists of a cannula, a hub to which the tubing can be connected and an adhesive that keeps the catheter in place when the cannula is implanted subcutaneously (Figure 3B). The cannula can be of either a flexible (e.g. Teflon) or a rigid (e.g. steel) material, is between 6 and 13 mm long and is inserted either angled (30°) or straight (90°), depending on the manufacturer's specifications. It can be inserted into the subcutaneous tissue of the abdomen, upper arm, or thigh either manually or by a spring-loaded inserter. Rapid-acting insulin is infused at a basal rate throughout the day and during sleep but set to a higher bolus right before meals. Most pumps now feature a bolus

calculator as well as a function reporting the amount of insulin that is still left in the body from a previous bolus (“insulin on board” monitor function).

1.2 Advantages of Insulin Pump Therapy

In 1993 the Diabetes Control and Complications Trial (DCCT) Research Group published a report on the benefits of tight glucose control [15]. 1,441 insulin dependent patients free of cardiovascular complications at baseline were randomized into 2 groups in a multicenter trial: conventional versus intensive diabetes treatment. By the end of the follow-up of an average of 6.5 years, almost twice as many patients on conventional therapy with loose glucose control had microvascular complications compared with the intensive therapy group [15]. They concluded that tight glucose control delays the onset of diabetic nephropathy (damage to the kidneys), neuropathy (damage to the nerves) and retinopathy (damage to the retina) caused by continuously elevated blood glucose levels.

This tight control of BG levels is more easily achieved when using and insulin pump compared to multiple daily injections (MDI). According to several randomized trials, hypoglycemic events are reduced by 50-80% [16–20] and the needed daily insulin dose by 14 % [21]. Meta-analyses from 2002 and 2007 clearly showed the superiority of insulin pump therapy above multiple daily injection (Figure 4) [21, 22]. Jeitler *et al.* concluded that CSII therapy can reduce HbA1c levels significantly without increasing the number of hypoglycemic events [22]. Although another meta-analysis form 2012 [23] found no statistically significant superiority of CSII therapy in terms of e.g. HbA1c, the authors concluded that insulin pump therapy indeed can be associated with a higher overall quality of life compared with MDI.

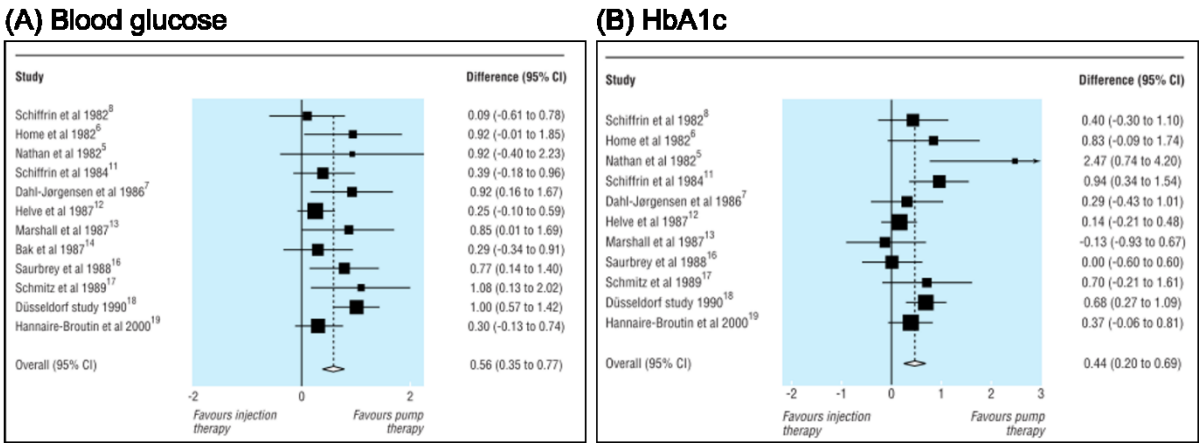

Figure 4: Meta-analysis of 12 studies regarding the standardized mean differences (95% confidence interval) in **(A)** blood glucose concentration and in **(B)** percentage of glycated hemoglobin (HbA1c) during CSII therapy compared with multiple daily injections. (*From: Pickup et al., British Medical Journal 2002* [21])

1.3 The Weak Link of Insulin Pump Therapy

Despite recent improvements in CSII catheter design and method of insertion, the insulin infusion set (catheter + hub + tubing) remains the weak link of an insulin infusion system for the management of type 1 diabetes [24–26]. In fact, issues with the infusion set constitute the greatest number of pump-related recalls by the US Food and Drug Administration (FDA) [24]. In a randomized controlled trial of 256 “pumpers”, more than two-thirds of participants reported at least one incidence of infusion set occlusion and/or unexplained hyperglycemia (see 1.3.1) per month [27].

The success of therapy depends on the reliability and the consistency of insulin absorption from day to day [6, 7, 28]. Insulin bolus guidelines assume a similar profile of insulin uptake by the subcutaneous tissue and the circulation for a healthy prandial response, but this is seldom achieved among patients [10, 29]. The variability of insulin pharmacokinetics increases over time and patients are instructed to replace their infusion set every 2 (steel) to 3 (Teflon) days to avoid unexpected hypo- or hyperglycemia due to variable and less reliable insulin absorption into the circulation [25, 26, 30–36]. Moreover, commercially available Teflon CSII catheters are prone to insertion and mechanical failure such as dislodgment, kinking, and catheter occlusion with blood, tissue or precipitated insulin, adding to the risk of uncontrolled insulin delivery [37, 38]. The intra-patient

coefficient of variation for absorption is said to be approximately 25 % day-to-day and as high as 50 % among patients [32, 39].

In a joint statement, the American Diabetes Association (ADA) and the European Association for the Study of Diabetes (EASD) turned the attention to the gap between the low number of publications on insulin flow blockage and actual number of CSII-related adverse events reported in an FDA database [24]. The issue with studies in insulin pump therapy lies in the fact that the research is often based on patient questionnaires leading to biased data. Adverse events such as blockage or occlusion may be subject to interpretation [40].

1.3.1 Steel or Teflon?

Due to the lack of profound scientific evidence, the choice of CSII catheter material is widely based on personal preference or experience. Further factors include the opinion of the endocrinologist or diabetes educator, and the coverage of CSII therapy by the insurance which varies among countries [41–43]. While in the United States about 90 % of “pumpers” use Teflon sets, 25 % of patients in Europe use steel sets [40, 41, 44]. In Germany, using a steel set is more common than anywhere else in Europe or the United States. About 40-45 % of patients choose steel over Teflon [44]. This may be attributed to the fact that steel cannulas are easier to insert and are less likely to kink. Patients using steel cannulas report better metabolic control, less variable insulin absorption and less unexplained hyperglycemia [41, 45]. In a survey by Pickup *et al.* in 2014 with 92 patients, 64 % of all Teflon sets failed due to kinking, 54 % due to blockage and 26 % due to lipohypertrophy (Figure 5). Subjects wore infusion sets for a mean of 3 days [46].

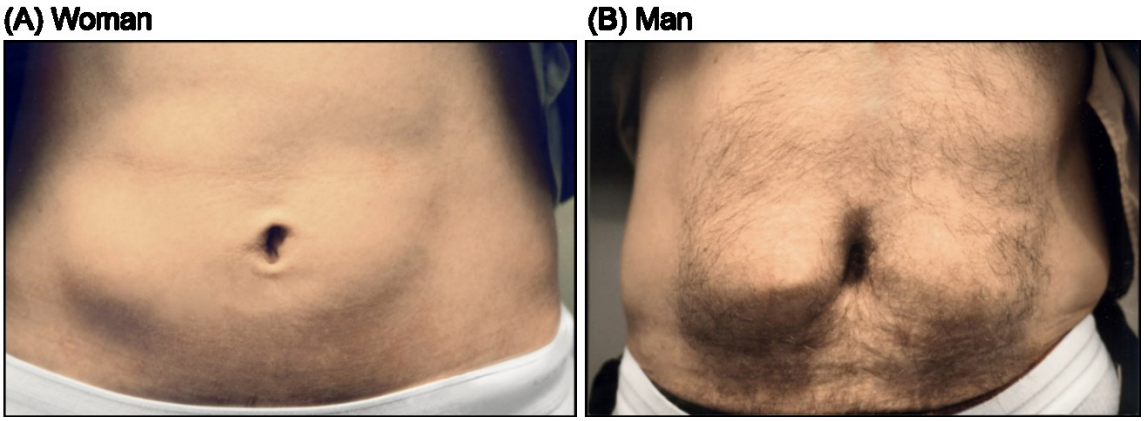

Figure 5: Examples of lipohypertrophy after frequent use of the same injection site in **(A)** a female and **(B)** a male patient. (From: http://www.mylife-diabetescare.com/mylife-diabetes-knowledge-tissue-hardening.html)

In a German 2010 study in 432 pediatric patients [47], the authors observed no difference in number of adverse events between the Teflon and steel group. 83 % of complications occurred before the end of day 2 of wear-time. Interestingly, they did not see the complication rate increase with wear time > 2 days. The complication rate was significantly increased ($p < 0.05$) when the site was disinfected which does not seem intuitive. Catheter obstruction was the most common adverse event observed in this study (33 %). In another study comparing steel and Teflon sets, the strongest predictor for reliability was the individual patient rather than catheter material [37]. 30 % of sets failed due to hyperglycemia and an inadequate correction dose; 13 % reported pain at the infusion site and 10 % of sets were pulled out by accident. In this study, patients wore the set for an average of 7 days [37].

1.3.2 Unexplained Hyperglycemia and Silent Occlusions

A blood glucose level > 250 mg/dl that does not decrease by at least 50 mg/dl one hour post correction bolus, is considered an unexplained hyperglycemic event. According to diabetes experts, unexplained hyperglycemia remains "under-reported, under-estimated and under-discussed", and causes increased psychological burden which ultimately leads to the discontinuation of CSII therapy. [40]. Van Bon *et al.* reported that approximately 65 % of patients in a 13-week study period had at least one episode of unexplained hyperglycemia and/or

infusion set occlusion per month. Of note, only 30 % of occlusion cases resulted in an alarm by the pump. The time to an actual occlusion alarm depends on the set basal rate, the length of the tubing and the pump model [27, 48]. Unexplained hyperglycemic events that do not result in an occlusion alarm could be explained by silent occlusions. Silent occlusions, also known as unexpected flow interruption, are events in which the in-line pressure in the tubing and cannula rises constantly for 30 minutes but does not result in an alarm by the pump [40].

1.3.3 Reasons for Discontinuation of Pump Therapy

It has not gone unnoticed by both physicians and the pharmaceutical industry that 18 % of patients who had previously switched from MDI to pump therapy discontinue CSII therapy after a couple of years [49, 50]. The reasons are manifold, including not only technical difficulties or skin irritation from long-term catheter usage, but also personal reasons such as seeing the pump as a constant reminder of the disease or lack of family support (Figure 6) [51].

	Frequency/number of responses (%)			
Reason for stopping therapy	*Highly agree*	*Agree*	*Disagree*	*Highly disagree*
Pump is bothersome during the summer	13/18 (72.2%)	2/18 (11.1%)	2/18 (11.1%)	1/18 (5.6%)
Catheter slips out during physical activity	10/18 (55.6%)	5/18 (27.8%)	2/18 (11.1%)	1/18 (5.6%)
Pump is bothersome during sport	10/18 (55.6%)	3/18 (16.7%)	2/18 (11.1%)	3/18 (16.7%)
Catheter insertion is more unpleasant than injecting	11/20 (55%)	4/20 (15%)	3/20 (10%)	2/20 (20%)
Pump feels like a foreign body	10/19 (52.6%)	4/19 (21.1%)	3/19 (15.8%)	2/19 (10.5%)

Reasons are reported where >50% respondents highly agree with the statement.

Figure 6: List of most common reasons for discontinuation of pump therapy among adolescent patients. (*From: Seereiner et al, DST 2010* [51])

1.4 The Artificial Pancreas

Artificial pancreas (AP) systems combine continuous glucose monitoring, computer algorithms and insulin delivery pumps with the goal to improve both glycemic control and quality of life of patients with type 1 diabetes. AP systems ranging from pump suspension when BG levels are low to complex fully-automated systems are being developed and/or improved for diabetes management by numerous groups in both academia and industry [52, 53].

1.4.1 CONTINUOUS GLUCOSE MONITORING

Continuous glucose monitoring (CGM) refers to a minimally invasive sensor based glucose concentration measurement in the interstitial fluid of the subcutaneous tissue [54]. Commercially available CGM devices detect changes in the electric current due to changes in glucose concentration in the subcutaneous adipose tissue via a cannula-type electrode. This electrode can, for instance, be coated with the enzyme glucose oxidase (GOx). GOx catalyzes a redox reaction in which upon contact with the substrate Glucose, 2 electrons are transferred to its cofactor FAD. FAD in turn is reduced to FADH which is then oxidized by the final electron acceptor oxygen. Oxygen is reduced to hydrogen peroxide (H_2O_2) and 2 electrons are transferred to the electrode to which the enzyme is bound (Figure 7).

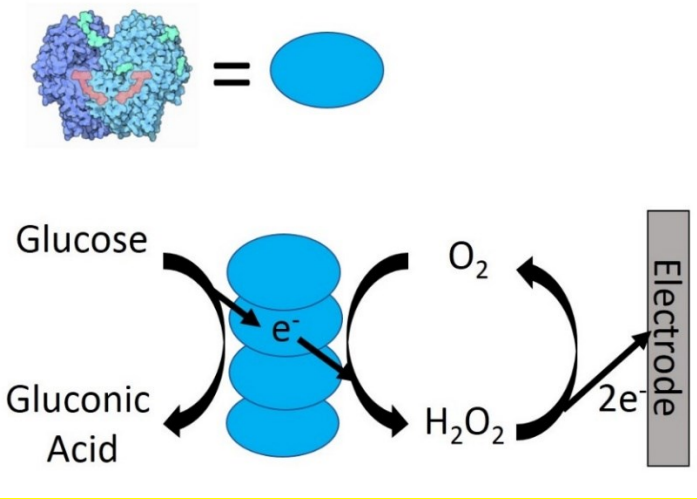

Figure 7: Redox reaction of glucose oxidase (GOx) in the presence of glucose and oxygen. This reaction requires the co-factor FAD which is marked light pink in the dimeric enzyme structure in the upper left corner.

Most CGM devices on the market require regular calibration by finger stick glucose measurement. Due to the constant improvement of system accuracy, both European and United States regulatory bodies have now allowed the independent use of CGM for insulin dosing without additional calibration. The Abbott Freestyle Libre was CE-marked in 2014 and the Dexcom G5 approved by the FDA in 2016 [55, 56]. BG measurements made by the Dexcom G5 can be used for insulin dosing without additional finger stick measurement [55]. The Abbot Freestyle Libre

was the first CGM-like system approved for 2 weeks of wear-time without additional finger stick measurements and factory-calibration only [56].

1.4.2 Types of Artificial Pancreas Systems

Up until now, the fully automated artificial pancreas has not yet been introduced to the market. In the available systems, the patient still has to approve some changes in insulin infusion. The two successful implementations of AP systems are explained in the following. Moreover, attempts have been made to combine both glucose sensor and insulin delivery in one device ("single-port"), reducing the burden of multiple insertions for a functioning AP system [57–61]. A recent meta-analysis including 24 studies showed that any type of AP system increases time in BG target range by almost 13 % ($p < 0.0001$), equivalent to 172 minutes per day [62].

Low-glucose suspend systems

In these systems, the CGM and insulin pump both work on an operator-approved basis, meaning that the modulation of basal insulin does not occur automatically and autonomously. When BG falls below a pre-set value the pump sounds an alarm. If the patient does not react to the alarm, the pump will shut off insulin delivery automatically for a certain period of time. A low-glucose suspend feature can minimize the risk of and the time spent in hypoglycemia, especially during sleep [63–65].

While in Europe the first device to use CGM data to actively affect insulin delivery (MiniMed Veo, Medtronic Inc.) has been marketed in 2009, the Food and Drug Administration (FDA) in the United States approved the first AP system (MiniMed 530G System, Medtronic Inc.) only in 2013. The MiniMed Veo was successfully tested in a large study by Bergenstal *et al.* [63]. The authors report that in the intervention group the low-glucose suspend feature significantly reduced nocturnal hypoglycemic events by more than 30 % without affecting mean glycemic control.

Sensor-augmented, operator approved systems

The second generation of the artificial pancreas, so-called “Treat-to-Target” or “closed-loop” systems (MiniMed Paradigm 640G, Medtronic Inc. and Vibe, Animas, West Chester, PA, USA) combine an insulin pump, a CGM and a smartphone to fully close the loop in insulin delivery. The sensor-augmented pumps are more sophisticated then the low-glucose suspend systems and feature the dynamic regulation of basal insulin delivery. The pump automatically adjusts basal (but not bolus) insulin delivery to achieve a preset target BG concentration. However, the patient needs to make adequate adjustments at mealtimes, setting the insulin bolus manually and needs no ensure proper CGM calibration by regular finger stick measurement. Thabit *et al.* published the results of the first successful study on the home use of sensor-augmented pump therapy in 2015 [66]. The relative burden of hypoglycemia (BG < 63 mg/dl) was reduced significantly by almost 40 % when using the AP system and the overall glucose control was improved [66].

1.4.3 Hurdles in AP Technology

The future generation of AP systems is a fully automated insulin closed loop system in which the manual mealtime bolus and the calibration of the CGM are eliminated. Nonetheless, additional research is necessary to develop a fully automated system to replace beta-cell function.

Daily insulin requirements can vary largely in patients with type 1 diabetes [52, 67]. Patients may need only one-third of the insulin than they had needed the day before or vice versa. The intra-patient variability is said to be 20 % during the day and 30 % at night [67]. Mealtime prediction algorithms are difficult to develop as patients might have different eating and exercise patterns every day [53, 65]. Although AP systems can counteract these variations by continuously adjusting insulin delivery, their performance is further hampered by either slow and variable insulin absorption rates into the circulation and/or inaccuracy of the CGM device [68].

The significant lag of the pharmacodynamic effect of insulin on the BG concentration presents a challenge in the development of adequate AP algorithms

[52, 53, 65]. Even when rapid-acting insulin is delivered subcutaneously, insulin absorption rates into the circulation can be slow and variable and it is especially important to consider the remaining “insulin on board” that may accumulate in a depot subcutaneously and reach the blood stream much later [52, 53, 65]. Therefore, not only the fast onset but also a much shorter offset (i.e. shorter duration of action) need to be considered for future insulin formulations. The development of ultra-fast insulins is currently underway to improve absorption kinetics [69]. Joseph *et al.* have tested the use of additives to insulin to enhance insulin absorption (see Study II in this thesis).

Considering the fact that subcutaneous insulin infusion will remain the route of choice possibly for the next decade, an in-depth and systematic evaluation of the inflammatory tissue reaction to insulin infusion catheters is of utmost importance to develop a fully-automated AP for the treatment of diabetes.

1.5 THE INFLAMMATORY RESPONSE TO INSULIN INFUSION CATHETERS

Since external delivery of insulin requires the introduction of a foreign body into the adipose tissue, insulin absorption variability may be caused by the inflammatory processes happening in the immediate environment of the cannula. When a biomaterial, such as an insulin infusion catheter, is present in the tissue, the regular wound healing process is altered [70]. The insertion of a catheter causes the disruption of capillaries, lymphatic vessels, and connective tissue, all of these triggering inflammation [6, 30, 32, 71–74]. The disruption of vessels leads to the activation of platelets which immediately adhere to the damaged vessel wall as well as the cannula. Fibrinogen is cleaved to fibrin to help the activated platelets form a blood clot (Figure 8) [73, 74].

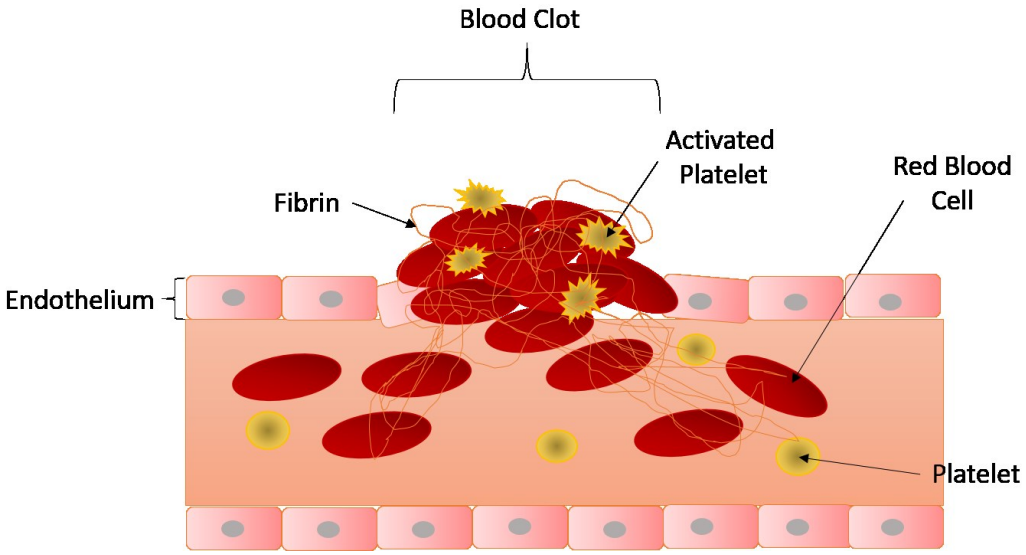

Figure 8: Blood clot formation after damage to the endothelium.

Fibrin, in turn, is sensed by phagocytes and launches the inflammatory response. Activated platelets release growth factors into the interstitial fluid which together with albumin, but also fibrinogen, fibronectin and proteins of the complement system adhere to the foreign body within the first minute after catheter insertion [75, 76]. This protein layer is inconsistent, undefined and can consist of more than 200 different intact and denatured proteins [77, 78]. This is usually not the case in nature. Naturally, such protein adhesion would occur in a very specific, oriented way with only a few proteins involved. An unspecific layer of proteins alarms the body that there is an "invader" present that needs to be attacked and/or walled off [79, 80].

Within the first hour after insertion, neutrophils, monocytes and fibroblasts are recruited which then interplay and form a provisional matrix along the shaft of the catheter [73, 74, 81, 82]. This step initiates the acute inflammation which lasts for about 2 days. The complement system attracts and activates granulocytes and monocytes (that usually stay dormant in the blood steam) and induces the release of reactive oxygen species, cytokines and chemotactic factors. Monocytes adhere to the material surface and differentiate into macrophages [74]. Macrophages serve as the main "orchestrators" in this healing process [80]. They clean up the wound (phagocytosis), which may contain foreign material, bacteria, and dead cells, and start to permanently release cytokines (interleukin-1-beta, tumor

necrosis factor alpha, interleukin-6, interleukin-8) to recruit and activate more monocytes, fibroblasts and endothelial cells, which convert the fibrin clot into a highly vascularized granulation tissue [81].

Fibroblasts recruited by macrophages move up the cytokine concentration gradient and start synthesizing and depositing collagen in order to remodel the extracellular matrix destroyed by catheter insertion [70, 73, 83]. As a result, the wound is closed and scar tissue is formed. In the late stages of acute inflammation (3-4 days), macrophages, frustrated by their inability to digest the invader, fuse to form Foreign Body Giant Cells (FBGCs) and remain attached to the catheter. Macrophages release matrix metalloproteinases and their inhibitors to modulate the cytokine concentration around the foreign body [70, 84].

Depending on the type of macrophage, further host defense by phagocytosis and release of proteases takes place (“defense” macrophage type M1) or tissue repair (fibrinogenesis, angiogenesis) and immunoregulation (“repair” macrophage type M2) [73, 74, 82, 85]. A dysregulation of M2 macrophages, which is the case when a foreign body is present, leads to fibrosis [74]. Fibrosis and encapsulation mark the final step of the foreign body response (FBR), about 3 weeks after implantation. The rate of collagen formation has now exceeded that of degradation. This isolation of the foreign body against the environment in a collagenous bag is the body’s last defense; the immune system has given up digesting the material. Macrophages and FBGCs remain inside the capsule. Contrary to physiological wound healing, the FBR persists for as long as the material remains in vivo [74, 84, 85]. This fibrous encapsulation presents an issue in the development of fully implantable medical devices such as glucose sensors. Figure 9 gives an overview over the processes explained in this chapter.

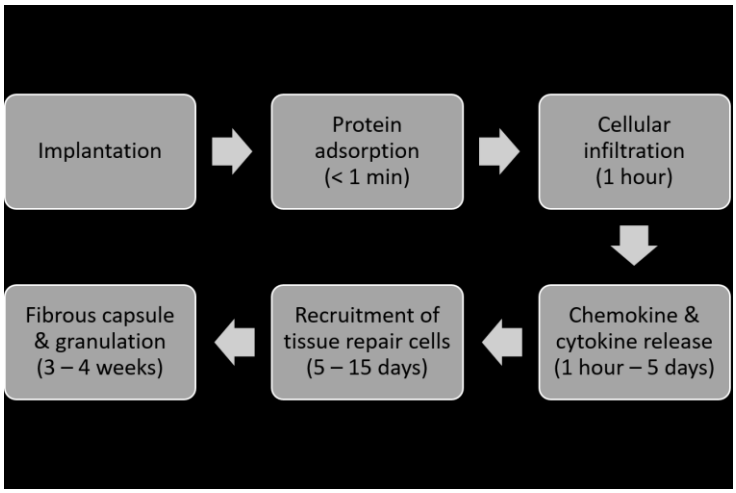

Figure 9: Rough timeline from acute inflammation (within seconds) to foreign body response (> 2 weeks).

1.5.1 BIOMATERIALS AND THE 510(K)

Surface structure and surface science are both critical aspects in biotechnology and biomimetics. Current biomaterials that are declared "biocompatible" by regulatory bodies still end up walled off from the surrounding tissue by a 50-200 µm thick collagenous, avascular capsule, independent of material and surface structure [80]. Therefore, no matter the (bio-) material, cells and proteins of the immune system will recognize it as foreign, attach, and trigger the inflammatory response. Macrophage recognition and attachment depends on the material size, stiffness, topography, and surface chemistry. All of these factors determine the severity of the acute inflammatory and the foreign body response [74, 86–88]. The greater the surface-to-volume ratio, for instance, the more likely macrophages are to attach and the more fibrosis is caused by the implantation [86]. Biomaterials currently in use are predominantly hydrophobic which makes it easy for plasma proteins to attach via hydrophobic interactions [74, 89]. Micropatterns such as random grooves and ridges facilitate cell attachment and enhance the inflammatory response [90]. Thus, macrophages prefer rough, hydrophobic surfaces and sharp edges.

To this day, biomaterials remain fairly unregulated for market entry. This is especially interesting since insulin formulations (like any drug) are heavily regulated. The following is an excerpt from the American Food, Drug and Cosmetic Act from the Food and Drug Administration (FDA):

"Section 510(k) of the Food, Drug and Cosmetic Act […] allows FDA to determine whether the device is equivalent to a device already placed into one of the three classification categories. Thus, "new" devices […] can be properly identified. […] [M]edical device manufacturers are required to submit a premarket notification if they intend to introduce a device into commercial distribution for the first time or reintroduce a device that will be significantly changed […]. Such change or modification could relate to the design, material, chemical composition, energy source, manufacturing process, or intended use."

In short, a device or material that is introduced to the pharmaceutical market needs to be merely equivalent to a previously legally marketed device. It does not need additional preclinical or clinical testing to determine possible negative effects on e.g. drug delivery. It has been discussed whether clinical trials and preclinical proof of concept studies together with tighter regulations on medical devices should be implemented.

1.6 GAPS IN RESEARCH

Although it has been shown that CSII therapy improves the overall management of diabetes, the management of BG is still challenging and the catheter remains the weak link [21, 22, 24]. Patients struggle with insulin absorption variability and dermatological complications due to frequent catheter insertion [25, 32, 41, 72]. Even though single-port concepts for closed-loop AP systems have been proposed, the difference in wear-time of a CSII catheter and a CGM sensor proposes a major hurdle in the development [57]. To understand the underlying mechanisms of insulin absorption variability and/or failure, the inflammatory response to insulin infusion catheters needs to be systematically evaluated. This knowledge may help with the development of better tolerable materials and shapes and may thus increase wear-time of catheters substantially. To study these immunological effects, fresh tissue is needed and therefore an ideal animal model for human wound healing needs to be considered. This thesis deals with the development and optimization of in vivo methods to study inflammatory processes and insulin absorption variability.

2. AIMS AND HYPOTHESIS

This thesis focuses on the validation of different methods and animal models to test biomaterial tolerability over time and the impact of the inflammatory response on insulin absorption variability. The inflammatory response to different catheter types is systematically evaluated with and without insulin infusion. Furthermore, intra- and inter-subject variability of insulin absorption into the circulation is analyzed, compared and discussed. The following 3 studies are based on the hypothesis that the acute inflammatory response to insulin infusion catheters is responsible for variable insulin absorption.

2.1 STUDY I: IN-DEPTH ANALYSIS OF THE PHARMACOKINETICS (PK) OF LISPRO INSULIN AND THE TISSUE RESPONSE TO CSII CATHETERS (SWINE MODEL, THOMAS JEFFERSON UNIVERSITY, PA, USA)

The goal of this pilot study was to determine the mechanisms leading to failure and variability of CSII catheter performance. Insulin absorption pharmacokinetics (PK) and tissue response to 2 different CSII catheter designs implanted in 6 swine for 5 days were analyzed. A new, experimental catheter design was evaluated for equivalence or superiority to a commercial Teflon CSII catheter. Both catheters were tested for the occurrence of pump occlusion alarms and insulin leakage (due to catheter obstruction or tissue changes).

2.2 STUDY II: THE EFFECT OF CO-INFUSION OF THROMBOLYTIC AGENTS AND APPLICATION OF VIBRATION ON INSULIN PK/PD AND TISSUE HISTOLOGY (CANINE MODEL, THOMAS JEFFERSON UNIVERSITY, PA, USA)

Based on the results of Study I, this study aimed to evaluate whether insulin absorption improves upon administration of tissue plasminogen activator (tPA) or streptokinase. Furthermore, the effect of vibration on the rate of insulin absorption was tested. The study was conducted in 13 non-diabetic canines and each animal

underwent a 7-day study period. The primary objective of this study was to compare the time of onset, time to maximum concentration, and blood glucose (BG) lowering effects of a commercial insulin formulation (lispro, Humalog U-100) to insulin in combination with tPA, streptokinase and/or vibration. The secondary aim was to compare the histology of the tissue surrounding the CSII catheters of insulin infusion only to insulin plus fibrinolytic medication.

2.3 Study III: Comparison of the Inflammatory Response to Steel and Teflon CSII Catheters Using Histopathology and Quantitative Real-Time PCR (Swine Model, Medical University of Graz, Austria)

This animal pilot study aimed to systematically assess the inflammatory response to the 2 most commonly used catheter materials in insulin pump therapy: steel and Teflon. The choice of material is largely based on personal experience or preference rather than empirical data. The goal was to histopathologically assess if the area of inflammation around catheters differed significantly in size and inflammatory cell density and draw conclusions whether one material was the superior choice over the other. To do so, commercially available steel and Teflon CSII catheters were implanted into the subcutaneous adipose tissue of 10 farm swine for 1, 4 and 7 days.

3. MATERIALS AND METHODS

3.1 LIST OF MATERIALS

3.1.1 INSULIN INFUSION SETS, INSULIN PUMP, CGM AND INSULIN ANALOGUES

- Medtronic MiniMed Quick-set Paradigm (Teflon) and Sure-T (Steel), 6 or 9 mm (Medtronic plc, Dublin, Ireland)
- Medtronic Quick-Serter (Medtronic plc, Dublin, Ireland)
- Insulin pump: Medtronic Paradigm (Medtronic) or Animas One-touch Ping (Animas Corp., West Chester, PA, USA)
- Insulin: Lispro/Humalog (Ely Lily, Indianapolis, IN, USA)
- CGMs:
    - SEVEN PLUS (DexCom, Inc., San Diego, CA, USA)
    - Platinum G4 (DexCom, Inc., San Diego, CA, USA)
    - iPro®2 Professional CGM (Medtronic plc, Dublin, Ireland)
    - Guardian RT (Medtronic plc, Dublin Ireland)

3.1.2 SUPPLIES FOR ANIMAL STUDIES

- Regular soap and alcohol wipes
- Chlorhexidine applicator: ChloraPrep™ (Becton Dickinson, NJ, USA)
- Kinesiology tape: Leukotape K (BSN medical, Vienna, Austria)
- Stockinette: tg soft (Lohmann & Rauscher GmbH, Vienna, Austria)
- Vest for insulin pumps (Lomir Biomedical Inc., Notre Dame de l'Ile Perrot, Quebec, Canada)
- Medical Dressing: Tegaderm™ (3M medical, St. Paul, MN, USA) or OPSITE (Smith & Nephew, London UK)
- Central venous catheters: CP2 vascular access ports (Access Technologies, IL, USA)
- Battery powered pump for D-20 infusion: Ipump Pain Management System (Baxter MN, USA)
- Blood sampling: VAMP PLUS System (Edwards Lifesciences Corp., Irvine, CA, USA)

3.1.3 THROMBOLYTIC AGENTS

- Streptokinase from β-hemolytic *Streptococcus* (Sigma-Aldrich, St. Louis, MO, USA)
- Tissue Plasminogen Activator: cathflo® activase® (Genentech, San Francisco, CA, USA)

3.1.4 SAMPLING FOR mRNA ANALYSIS

- 2 ml Eppendorf tubes, disposable scalpels and forceps
- RNA stabilizing solution: RNA*later*® (Sigma-Aldrich, St. Louis, MO, USA)
- Cleaning supplies: RNAse *AWAY*™ wipes or spray (Thermo Fisher Scientific Inc., Waltham, MA, USA)

3.1.5 mRNA ISOLATION AND qPCR

- MagNALyser Green Beads (Roche Applied Science, Penzberg, Germany)
- QIAzol Reagent (QIAGEN, Venlo, Netherlands)
- RNeasyMiniKit (QIAGEN, Venlo, Netherlands)
- Reverse Transcriptase Kit (AppliedBiosystems®, Thermo Fisher Scientific Inc., Waltham, MA, USA)

- Primers for porcine cytokines (Sigma-Aldrich, St. Louis, MO, USA)
- LightCycler® 480 SYBR Green I Master (Roche Applied Science, Penzberg, Germany)
- LightCycler® 480 Multiwell plate 384, clear (Roche Applied Science, Penzberg, Germany)

3.1.6 HISTOLOGY – SAMPLING

- Insulin pump: Medtronic Paradigm (Medtronic plc, Dublin, Ireland)
- Insulin reservoir prefilled with methylene blue dye
- 4 % buffered formaldehyde
- Others: scalpel, surgical scissors, specimen containers with screw-top

3.1.7 HISTOLOGY – GROSSING AND PROCESSING

- Micromesh Biopsy Cassettes (Thermo Fisher Scientific Inc., Waltham, MA, USA)
- Rotating microtome: Leica SM2000R (Leica Biosystems, Wetzlar, Germany)
- Others: Microscope Slides, Slide Covers, Ethanol, H&E stains, Trichrome and Reticulin staining kit

3.1.8 DEVICES

- MagNALyser (Roche Applied Science, Penzberg, Germany)
- Tissue Processor: Tissue-Tek® VIP™ (Sakura Finetek Germany GmbH) and Shandon Citadel 1000 (Thermo Fisher Scientific Inc., Waltham, MA, USA)
- Automated slide stainer and coverslipper: Tissue Tek® Prisma & Film (Sakura Finetek Germany GmbH)
- Image capturing device (high-throughput microscope): Aperio ScanScope (Leica Biosystems, Wetzlar, Germany)
- Microtome: Microm, HM355S (Thermo Fisher Scientific Inc., Waltham, MA, USA)
- PCR Cycler: LightCycler® 480 System (Roche Applied Science, Penzberg, Germany)
- Glucose analyzer: YSI-2300STAT Plus™ (Yellow Springs Instruments, Yellow Springs, OH, USA)

3.1.9 SOFTWARE

- Primer design: Primer3Plus (http://www.bioinformatics.nl/cgi-bin/primer3plus/primer3plus.cgi)
- qPCR analysis: LightCycler® 480 Software (Roche Applied Science, Penzberg, Germany)
- Histology analysis: Aperio ImageScope (Leica Biosystems, Wetzlar, Germany)
- Add on for Excel: PKSolver Add-in [91]
- Statistics: GraphPad Prism Software 5.0

3.2 Study I: In-Depth Analysis of the Pharmacokinetics (PK) of Lispro Insulin and the Tissue Response to CSII Catheters (Swine Model, TJU)

An observational study was performed in 6 non-diabetic ambulatory female farm swine (*sus scrofa domesticus*, 68.5 ± 3.6 kg) evaluating the insulin absorption variability over 5 days of catheter wear time and the morphological changes in the tissue caused by catheter insertion and maintenance.

3.2.1 CSII Catheters

In this study, the commercially available Animas inset^{TM} (Teflon, 90° insertion angle, “C”) was compared to an experimental catheter from Animas Corp. (metal, approximately 60° insertion angle, “N”). The commercial catheter contained a 6 mm Teflon cannula (0.5 mm in diameter) connected to a plastic platform (hub) which was attached to the skin via an adhesive base. The Teflon cannula needed a 27-gauge steel guiding needle in order to be inserted at a 90° angle through the skin and subcutaneous tissue and a spring-loaded introducer to apply insertion force (Medtronic Quick-serter). After insertion, the guiding needle was removed and discarded. The experimental catheter had an open clam-shell design plastic hub with an adhesive base for attachment to the skin. Closing the hub manually guided the sharp tip of the thin, flexible needle through the skin into the subcutaneous tissue at an insertion angle of approximately 60°.

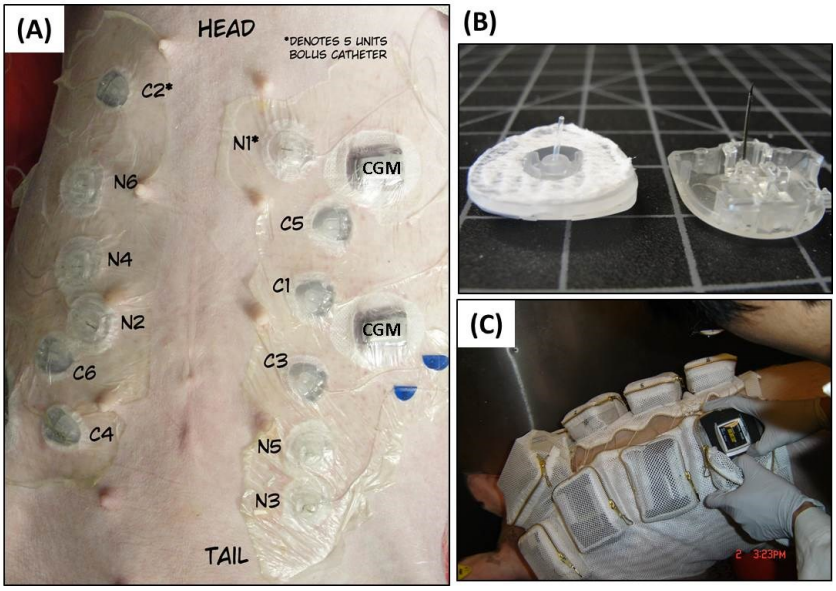

Figure 10: Catheter insertion and animal vests. **(A)** 6 commercial catheters (C) and 6 experimental ("new") catheters (N) were inserted into the abdominal subcutaneous tissue of each animal. Catheters used for the PK study are marked with an asterisk. Two continuous glucose monitors (CGM) were inserted into the subcutaneous tissue of each swine (Dexcom SEVEN) to monitor the concentration of tissue fluid glucose. **(B)** *Left:* Animas inset™ (C) with 6 mm Teflon cannula and insertion needle removed; *right:* experimental catheter (N) with curved cannula with sharp tip. **(C)** To avoid dislodgement, catheters were covered with medical adhesive. Each CSII was connected to a commercial insulin pump that was then stored within the pockets of a custom animal vest. The pocket by the neck housed a battery powered pump that continuously infused glucose solution into a central venous catheter for 5 days.

3.2.2 In Vivo Procedures

The protocol was approved by the Institutional Animal Care & Use Committee of Thomas Jefferson University, Philadelphia, PA. Central venous catheters (CVC) were implanted into the left Innominate Vein (for blood sample acquisition) and the distal Superior Vena Cava (for glucose infusion) under general anesthesia induced via isoflurane inhalation and aseptic surgical technique. The CVC ports were flushed with a low-dose heparin solution every 1-3 days using a Huber needle. One week later (= day 1 of the study), swine were anesthetized and their abdomen shaved, washed and disinfected. 6 commercially available CSII catheters (C) and 6 experimental ("new") CSII catheters (N) were randomly inserted into the subcutaneous abdominal tissue of each swine (Figure 10). Battery-powered insulin pumps containing saline or insulin filled reservoirs were connected to 4 commercial and 4 experimental catheters and catheters were infused for 5 days using the same basal/bolus pattern of delivery. Two commercial and 2 experimental catheters were primed with saline and inserted without connecting an

insulin pump. Insulin was continuously infused through C1, C2, N1, and N2 at a slow basal rate (4 x 0.2 units/hour/catheter = 0.8 units per hour) for 5 days. CSII were covered with Tegaderm™ adhesive bandages to avoid catheter loss due to animal movement. 8 insulin pumps were secured within the pockets of a custom vest (Lomir Biomedical, Inc., Figure 1). For the PK study, either C1/N1 or C2/N2 received a bolus of 5 units of insulin on the day of insertion (day 1), as well as 3 and 5 days later. Saline was continuously infused through C3, C4, N3, and N4 at 0.2 units/hour for 5 days (Table 1).

Table 1: Infusion protocol overview. Catheter location and designated infusion was randomized for each animal (n=6). A total of 36 commercial and 36 experimental catheters were inserted.

Catheter no.	Infusion	Catheter no.	Infusion
C1	Insulin (PK+basal)	N1	Insulin (PK+basal)
C2	Insulin (PK+basal)	N2	Insulin (PK+basal)
C3	Saline	N3	Saline
C4	Saline	N4	Saline
C5	None	N5	None
C6	None	N6	None

The swine were given 2 hours of rest to recover after anesthesia. A stable baseline was established for approximately 30 minutes (3-5 blood glucose values) before infusing a 5-unit bolus of insulin into a commercial or experimental catheter in a randomized order. To minimize the risk for hypoglycemia, blood glucose was loosely clamped at approximately 100-160 mg/dl for 3-4 hours adjusting the intravenous infusion of a solution of 50 % dextrose (D-50), using a battery powered pump. CVC blood samples were obtained every 10 minutes for approximately 2 hours, followed by every 15 minutes for 1 hour and blood glucose measured in duplicate on a glucose analyzer. Blood glucose was furthermore monitored with a continuous glucose monitoring (CGM) device implanted in the subcutaneous tissue (SEVEN PLUS, Dexcom Inc.) which was regularly calibrated with the CVC blood sample glucose values. Plasma was stored at -80 °C for subsequent insulin concentration analysis by Enzyme-linked Immunosorbent Assay (ELISA). After approximately 3 hours, a second baseline was established for 30 minutes before administering a second insulin bolus (5 U) through the alternating catheter and procedures were repeated as for the first PK study. During the PK studies, animals were able to move around (stand up, lie down) and frequently received snacks such as apples or biscuits which made the study of

insulin pharmacodynamics and tight clamping impossible. Three and 5 days after catheter insertion, 2 additional PK studies were performed on each day, always using the same CSII catheter as on day 1. Thus, each animal served as its own control.

3.2.3 INSULIN PHARMACOKINETICS (PK)

Insulin concentrations in plasma were analyzed using a porcine ELISA and an Iso-insulin ELISA kit (Mercodia AB, Uppsala, Sweden) by the company PreClinOmics, Inc. (Indianapolis, IN). By subtracting porcine insulin from total insulin concentration, the lispro insulin concentration in the blood could be calculated. The 3-5 baseline values before bolus (t = 0) were averaged and this value subtracted from all subsequent insulin concentrations. The area under the insulin concentration curve was calculated for 60 (AUC60) and 160 minutes (AUC) using the linear trapezoidal approximation (Figure 11, Equation 1) and the PKSolver add-in for Microsoft Excel [91]. Furthermore, maximal plasma insulin levels (Cmax) and time-to-peak (tmax) were determined (Figure 11). The inter- and intra-subject coefficient of variation (CV) was calculated for AUC, AUC60, C_{max} and t_{max} for each day and across all study days.

Equation 1. Trapezoidal rule for the AUC between bolus (t = 0) and 160 minutes (t = 160).

$$dt = t_2 - t_1$$

$$AUC_{(t1,t2)} = \frac{1}{2}(C_1 + C_2)dt$$

$$AUC_{total} = \sum AUC_{(tx,ty)}$$

$$\int_{t=0}^{t=160} f(t)dt \approx \sum_{n=0}^{n-1} \frac{1}{2}(C_n + C_{n+1})(t_{n+1} - t_n)$$

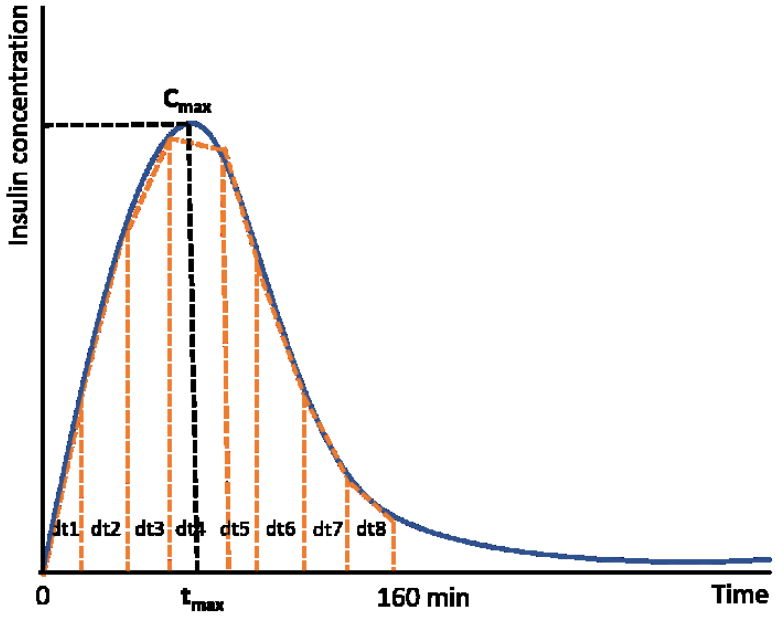

Figure 11: Graphic explanation of the trapezoidal approximation for the AUC between t=0 and t=160 minutes. The AUC is made up of several trapezoids between given time intervals (intermitted orange lines). C_{max} = maximum insulin concentration and t_{max} = time to maximum insulin concentration.

3.2.4 TISSUE HISTOLOGY

After completion of the second PK study on day 5, swine were euthanized by an IV overdose of potassium chloride. The vest, stockinette and medical adhesive were removed and a 5 U bolus (50 µl) of methylene blue dye (methylthioninium chloride), was infused into each commercial and experimental catheter. By doing so, it was determined whether morphological changes in the tissue inhibited the flow of fluid (insulin or dye) into the adjacent tissue and would force the blue dye to take the path of least resistance up the catheter shaft and onto the skin. If dye accumulated in the hub, the problem of flow interruption was attributed to a malfunction of the tubing or an obstructed catheter.

The skin and subcutaneous tissue surrounding the catheters was excised using scalpel, surgical scissors, and forceps. Tissue plugs were immediately transferred into 10 % buffered formaldehyde where they were dehydrated for 3 days (“fixation”) while not removing the CSII catheter. Thereafter, the catheter was removed and the tissue plug grossed to expose the insertion channel for targeted sectioning of paraffin embedded tissue (Figure 12).

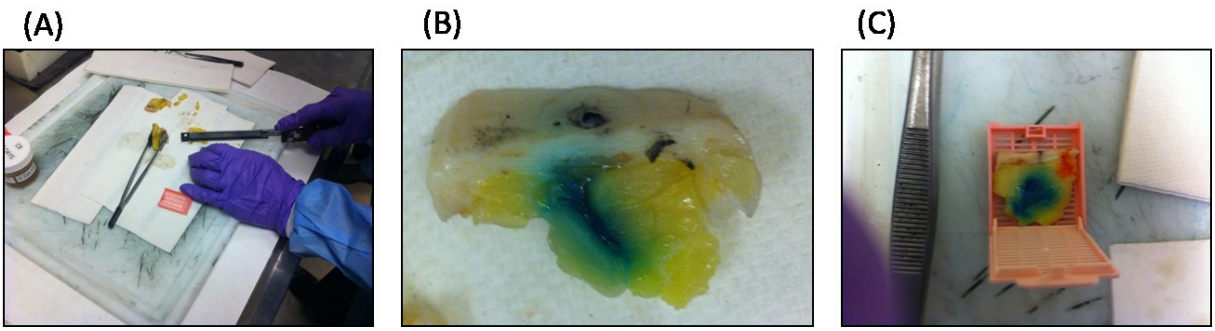

Figure 12: Grossing of fatty tissue exposing the insertion channel. **(A)** Tools used for grossing include a sharp knife, paddle forceps and a cutting board. **(B)** Insertion channel containing blue dye exposed; insertion hole marked with black ink on skin. **(C)** Tissue section placed in cassette after grossing. The side to be cut first on the microtome is marked with orange ink.

The tissue was grossed and processed using a long dehydration protocol for fatty tissue ("Breast Program", Table 2). During this dehydration process, water is removed from the specimen in an ethanol series of ascending concentration. Hardened tissue can then easily be embedded in paraffin wax blocks and sectioned on a microtome.

Table 2: "Breast Program" used by the Dpt. of Pathology of Thomas Jefferson University, Philadelphia, PA.

Solution	Time (hh:mm)
Formalin	00:55
Formalin	00:25
EtOH 70 %	00:30
EtOH 95 %	01:15
EtOH 100 %	01:15
EtOH 100 %	01:15
EtOH 100 %	01:30
Xylene	01:15
Xylene	01:30
Paraffin	01:15
Paraffin	01:15
Paraffin	01:30

Depending on the location and angle of the cannula, paraffin blocks were sectioned perpendicular or parallel to the skin surface 4 µm thick. Sections were stained with hematoxylin and eosin (nuclei are stained blue/purple, ECM, cytoplasm and collagen are stained in pink); Masson's Trichrome (collagen/connective tissue is stained blue, muscle fibers and erythrocytes are stained bright red, and cytoplasm is stained pink) and a reticulin stain (type III

collagen is stained silver) using automated stainers (Tissue Tek® Prisma). The stained tissue was analyzed for no, mild, moderate or severe (grades 0, 1, 2, or 3) hemorrhage (bleeding), reticular fiber disruption, fibrin deposition, fat necrosis, and collagen deposition compared with unaffected control tissue. This grading system was newly established by the lead pathologist of this study who pre-defined these criteria before analyzing all samples. The pathologist remained blinded throughout the study. The width (mm) of the debris field was measured in the vicinity of the insertion channel. All analyses were carried out with the AperioScanScope image capture device and ImageScope software (Leica Biosystems). Histology assessments are summarized in Table 3. The alteration of tissue plane topography was considered either regular or irregular, depending on whether planes were pushed downward evenly by catheter insertion force or not.

Table 3: Histology Assessments

Assesment	**Unit/Grade**
Width of debris field	mm
Reservoir geometry	Regular or irregular
Reticular fiber disruption	0, 1, 2, 3
Fibrin deposition in reservoir	0, 1, 2, 3
Collagen deposition at catheter tip	0, 1, 2, 3
Topography of tissue planes along insertion	Regular or irregular
Fat necrosis	0, 1, 2, 3
Hemorrhage at tip base	0, 1, 2, 3

3.2.5 STATISTICAL ANALYSIS

Fisher's exact test was used to evaluate the differences in histology profiles between commercial and investigational catheters. A Chi-squared test was applied to analyze differences in methylene blue dye leakage.

3.3 Study II: The Effect of Co-Infusion of Thrombolytic Agents and Application of Vibration on Insulin PK/PD and Tissue Histology (Canine Model, TJU)

The study and subsequent analysis was set up to examine changes in insulin concentrations over 5 euglycemic glucose clamp studies in 13 dogs (information in

Table 4) after IV and SC insulin administration of a standardized insulin dose. A glucose clamp study with IV insulin administration was first performed in each animal to serve as a reference for the time action profile of SC delivery.

Table 4: Canine information and bolus amount based on weight

Subject ID	Age (months)	Weight (kg)	Bolus amount (Units)	Study Group
D01	11	28.0	2.8	Lispro only
D02	15	30.0	3.0	Lispro only
D03	16	29.5	3.0	Lispro only
D12	19	28.8	2.9	Lispro only
D13	15	27.5	2.8	Lispro only
D04	19	29.0	2.9	Strep bolus
D05	22	28.0	2.8	Strep bolus
D06	19	29.4	2.9	Strep bolus
D07	14	27.5	2.7	Strep bolus + vibration
D08	26	28.0	2.8	tPA bolus
D09	13	29.2	2.9	tPA bolus
D10	23	29.4	2.9	tPA bolus
D11	16	28.5	2.9	tPA bolus + vibration

3.3.1 In Vivo Procedures

Animals arrived at the Thomas Jefferson University (TJU) animal facility one week prior to the first experiment for acclimatization. One week later, an IV insulin infusion clamp experiment was carried out to serve as an internal control (≡ 100 % insulin absorption into the circulation) for each animal. Procedures are listed in Table 5.

Table 5: Study plan for canine PK/PD study.

	Canine	IV PK/PD	SC PK/PD	SC PK/PD	SC PK/PD	SC PK/PD
Study day		-6	1	3	6	7
Week day		Wed	Wed	Fri	Mon	Tue
Control	**1**	IV insulin & glc clamp	CSII & glc clamp	CSII & glc clamp	CSII & glc clamp	CSII & glc clamp
	2	IV insulin & glc clamp	CSII & glc clamp	CSII & glc clamp	CSII & glc clamp	CSII & glc clamp
	3	IV insulin & glc clamp	CSII & glc clamp	CSII & glc clamp	CSII & glc clamp	CSII & glc clamp
tPA	**4**	IV insulin & glc clamp	CSII & tPA & glc clamp	CSII & tPA & glc clamp	CSII & tPA & glc clamp	CSII & tPA & glc clamp
	5	IV insulin & glc clamp	CSII & tPA & glc clamp	CSII & tPA & glc clamp	CSII & tPA & glc clamp	CSII & tPA & glc clamp
	6	IV insulin & glc clamp	CSII & tPA & glc clamp	CSII & tPA & glc clamp	CSII & tPA & glc clamp	CSII & tPA & glc clamp
Strep	**7**	IV insulin & glc clamp	CSII & Strep & glc clamp	CSII & Strep & glc clamp	CSII & Strep & glc clamp	CSII & Strep & glc clamp
	8	IV insulin & glc clamp	CSII & Strep & glc clamp	CSII & Strep & glc clamp	CSII & Strep & glc clamp	CSII & Strep & glc clamp
	9	IV insulin & glc clamp	CSII & Strep & glc clamp	CSII & Strep & glc clamp	CSII & Strep & glc clamp	CSII & Strep & glc clamp
tPA + Vib	**10**	IV insulin & glc clamp	CSII & tPA+Vibration & glc clamp	CSII & tPA+Vibration & glc clamp	CSII & tPA+Vibration & glc clamp	CSII & tPA+Vibration & glc clamp
Strep + Vib	**11**	IV insulin & glc clamp	CSII & Strep+Vibration & glc clamp	CSII & Strep+Vibration & glc clamp	CSII & Strep+Vibration & glc clamp	CSII & Strep+Vibration & glc clamp
Control	**12**	IV insulin & glc clamp	CSII & glc clamp	CSII & glc clamp	CSII & glc clamp	CSII & glc clamp
	13	IV insulin & glc clamp	CSII & glc clamp	CSII & glc clamp	CSII & glc clamp	CSII & glc clamp

3.3.2 CONTROL EXPERIMENTS (DAY -6)

Canine were mildly sedated with an intramuscular injection of acepromazine (0.05-0.2 mg/kg) and transported to the procedure room. Two IV catheters were inserted into the front paws, one for insulin and 20 % dextrose (D-20) infusion, and the other for blood sampling. For the latter, a Venous Arterial Blood Management Protection (VAMP) system was used – a needleless closed blood sampling system (Edwards Lifesciences). An insulin pump was connected to one of the IV catheters and insulin infused at a basal rate of 0.1 units/hour. Blood samples (1 ml) were acquired every 10 minutes for 30 minutes before administering a bolus of insulin at 0.7 units/kg body weight (BW). The D-20 IV infusion was adjusted to clamp BG in the target range of 120 ± 20 mg/dl. For 120 minutes, blood samples were taken every 5 minutes and BG measured using a reference analyzer (YSI 2300 Plus Analyzer). Plasma was placed on

dry ice and later transferred to -80 °C. At the end of the study day, the animals received a meal before being transferred back into their pen.

3.3.3 Preparation for Subcutaneous Insulin PK/PD Studies (day 1)

Canine were mildly sedated (acepromazine) and transported to the procedure room. General anesthesia was induced with isoflurane and spontaneous ventilation with a mask. Fur on the abdomen was shaved with a fine clipper and skin washed with soap and disinfected with alcohol wipes and a chlorhexidine applicator. Two Medtronic Quick-set CSII catheters (6 mm, Teflon) were inserted into the subcutaneous tissue of the abdomen of each adult canine. One of the 2 catheters remained in the tissue as a control while the other was connected to an insulin pump (Medtronic Paradigm™). Three CGM devices were inserted in the subcutaneous adipose tissue to monitor the glycemic status of animals for the duration of the study. The CSII catheters and CGM devices were covered with clear medical adhesive and Kinesiology tape, sparing the hub of the catheter designated for insulin infusion. A stockinette was pulled over the animal's body as well as a customized vest (Lomir Biomedical Inc.) containing a pocket in which the insulin pump was stored (Figure 13). The pump was set to a basal infusion rate of insulin at 0.1 units/hour) and two IV catheters placed in the front paws of the animal before waking it up. One IV catheter was connected to a VAMP system and the other one connected to a D-20 infusion solution.

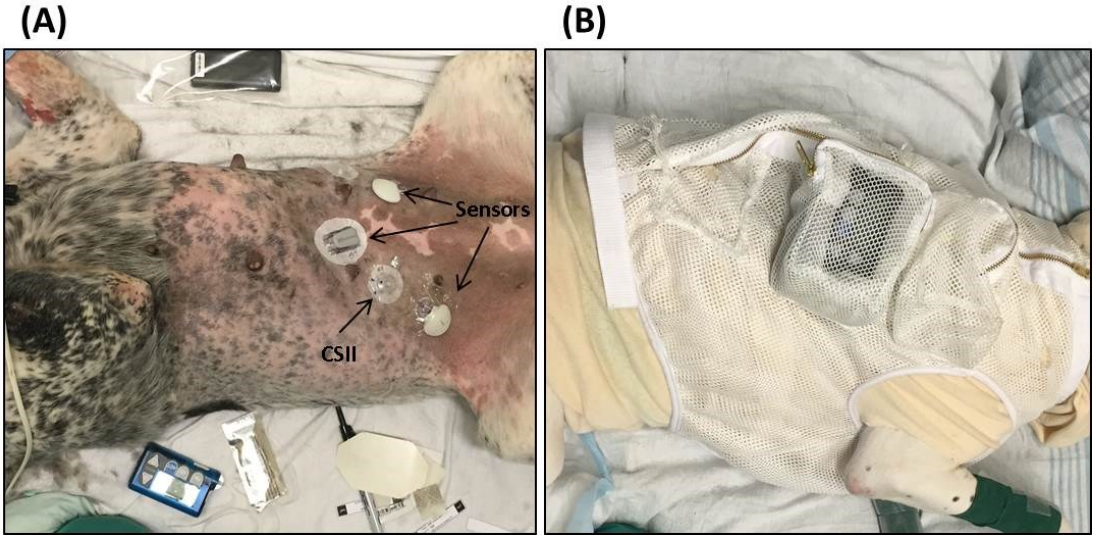

Figure 13: (A) Shaved abdomen with CSII catheter and sensors inserted. Note the difference in skin/fur pigmentation. **(B)** Animal vest containing customized pockets for insulin pumps and CGM signal receivers.

3.3.4 PK CONTROL STUDIES (DAYS 1, 3, 6, AND 7)

The animal was placed on a dog bed on the floor to ensure comfort. A BG baseline was recorded, taking samples every 10 minutes for 30 minutes. An insulin bolus of 0.7 units/kg BW was administered through the CSII catheter and glucose clamped at 105 ± 10 mgl/dl, adjusting intravenous dextrose infusion every 5-10 minutes. Venous blood samples were acquired every 5 minutes for 180 minutes until BG levels remained stable without infusing additional dextrose. The pump was set to basal infusion and the animal given a meal before returning it to the pen.

3.3.5 PK STUDIES WITH THROMBOLYTICS AND/OR VIBRATION

For the intervention studies, 50 µl (1 µg/ml) of tissue plasminogen activator (t-PA; Alteplase, Genentech) or 50 µl (6.25 units; 1 µg/ml) of Streptokinase (Sigma Aldrich) were infused through the CSII catheters 30 minutes prior to each insulin bolus. The streptokinase solution was prepared freshly on each study day. A 10 KU streptokinase powder (Sigma Aldrich) was suspended in 3 ml sterile water using a sterile syringe and needle. Water was injected through a septum on the vial and the vial rolled gently between palms. The entire solution was drawn into a sterile insulin reservoir. The reservoir was connected to tubing designated for Medtronic Sure-T and the plunger was screwed off before placing the reservoir in an insulin pump (Figure 14).

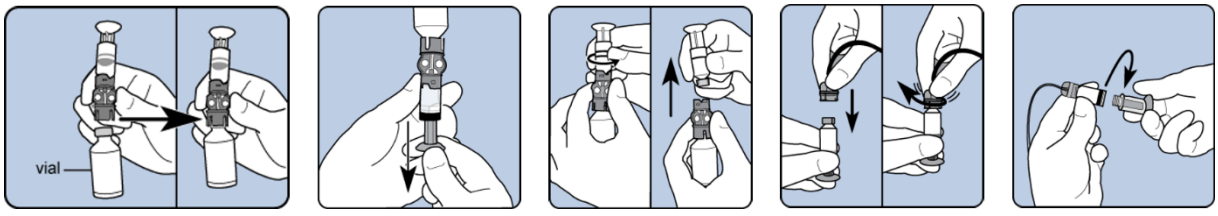

Figure 14: Filling an insulin reservoir with streptokinase (vial). Adapted from: http://www.medtronicdiabetes.co.in/customer-support/device-settings-and-features/utility-settings/fill-reservoir

The hub was cut off of the tubing to insert a short piece of a steel cannula. The cannula was inserted into the septum on top of the catheter hub and a 5 U bolus was injected. The ready-to-use tPA solution was transferred to an insulin reservoir as explained in Figure 14 and injected the same way as streptokinase.

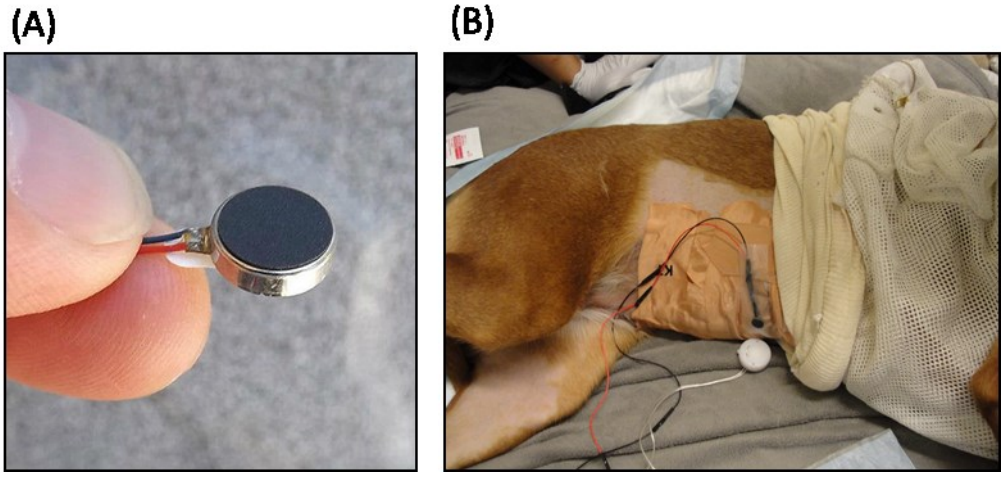

Figure 15: (A) Cell phone vibration motor. The cables are connected to a battery to start the vibration. **(B)** Set-up on a sedated dog. The motor is taped on top of the catheter hub. The white round case contains a button cell battery and an on/off switch.

The effects of thrombolytics plus mechanical vibration of the CSII-catheter were evaluated in canine experiments 10 and 11. A battery powered piezoelectric vibratory mechanism of a cell phone (Figure 15) was mechanically attached to the top of the CSII catheter using a medical adhesive. The CSII catheter and cannula were continuously vibrated for 30 minutes before, during and 30 minutes after each insulin lispro bolus.

3.3.6 Last Day of Study (day 7)

Upon completion of the PK/PD study on day 7, animals were anesthetized and placed on an operating table. Vest, stockinette and medical adhesive were carefully removed. A third CSII catheter was inserted into the subcutaneous tissue to serve as a control for histopathological analysis approximately one hour prior to euthanasia. A 50 µl bolus of blue dye was infused into each CSII catheter using a commercial insulin pump. After completing the infusion of methylene blue dye, the

animal was euthanized. The skin and subcutaneous tissue surrounding each CSII catheter was excised and fixed in 4 % PBS-buffered formaldehyde according to protocols explained in Study I (Chapter 3.2.4).

3.3.7 PHARMACOKINETICS (PK)

Insulin concentration was determined using an insulin lispro specific ELISA. Samples were sent to Mercodia Inc. on dry ice for external analysis. Insulin concentration was plotted against time and the area under the insulin concentration curve determined using the trapezoidal method (Figure 11, Equation 1). The total AUC over 180 minutes and AUC60 over the first 60 minutes was calculated. Maximum insulin concentration (C_{max}) and time to maximum insulin concentration (t_{max}) were determined and compared among animals.

3.3.8 PHARMACODYNAMICS (PD)

The glucose infusion rate was adjusted to body weight using Equation 2. The adjusted GIR was plotted against time (180 minutes) and the area under the GIR curve (AUC_{GIR}) calculated.

Equation 2: Adjusted glucose infusion rate (GIR) to body weight (BW). The dextrose concentration is expressed as a whole number, e.g. 5 or 10.

$$GIR = \frac{IV\ Rate\ \left(\frac{ml}{h}\right) \cdot Dextrose\ Conc\ (\frac{g}{dl}) \cdot 1000(\frac{mg}{g})}{BW\ (kg) \cdot 60(\frac{min}{h}) \cdot 100(\frac{ml}{dl})} = \frac{mg}{kg \cdot min}$$

3.3.9 STATISTICS

AUC, AUC60 and AUC_{GIR} values were tested for normality using the Shapiro-Wilk normality test. One-way analysis of variance (ANOVA) with Bonferroni multiple comparisons post-test was carried out for normally distributed data. Friedman test with Dunn's multiple comparison test was applied to compare non-normally distributed with normally-distributed data. Since ANOVA requires full data sets, all incomplete data sets that did not comprise of all study days (D02, D03, D06) were excluded.

3.4 Study III: Comparison of the Inflammatory Response to Steel and Teflon CSII Catheters Using Histopathology and Quantitative Real-Time PCR (Swine Model, MedUni Graz)

This study aimed to evaluate the difference in inflammatory response to the 2 most commonly used CSII catheter materials (steel and Teflon) and based on these results draw conclusions on the longevity of said catheters. Commercially available insulin infusion sets were inserted into the subcutaneous tissue of 10 female farm swine (*sus scrofa domesticus*) with an average weight of 45 ± 5 kg and maintained for 7, 4 or 1 days of wear-time. This study was carried out at the Institute for Biomedical Research of the Medical University of Graz and was approved by the Austrian Federal Ministry of Science, Research and Economy and performed in consent with Directive 2010/63/EU on the protection of animals used for scientific purposes (BMWFW Gz).

3.4.1 In Vivo Procedures

On day 1 (wear time = 7 days), swine were sedated and shaved on the back and the flanks. The sedative premedication was a combination of the following:

- 0.5 mg/kg Midazolam (Midazolam®)
- 2.5 mg/kg Azaperon (Stresnil®)
- 10 mg/kg Ketamin (Ketasol®)
- 0.2 mg/kg Butorphanol (Butomidor®)

Skin was washed with soap and water, disinfected and covered with a layer of clear medical adhesive, to ensure better adhesion of the catheters and avoid loss of catheters due to movement or friction. Catheters listed in Table 6 were inserted in a randomized manner. The insertion was repeated, if the catheters visibly failed to insert.

Table 6: List of catheter types used in this study with lot numbers and insertion method.

Catheter type	Material	Lot No.	Insertion method
Medtronic Sure-T®, 6 mm	Steel	5099714	Manual
Medtronic Quick-set®, 6 mm	Teflon	5139852	Manual

An insulin pump (Medtronic MiniMed Paradigm™) containing a saline filled reservoir was connected to the hubs of the Teflon CSII catheters directly after insertion. A bolus of 3-4 units was infused to ensure that none of the catheters had kinked during insertion. The tubing was disconnected, the hub closed with a cap and covered with a small piece of medical gauze. Another layer of medical adhesive was applied, followed by Kinesiology tape to firmly secure the catheters and hold them in place over the duration of the study. A stockinette was pulled over the animal and 4 holes cut out for the legs. Sharp edges were padded with cotton (Figure 16).

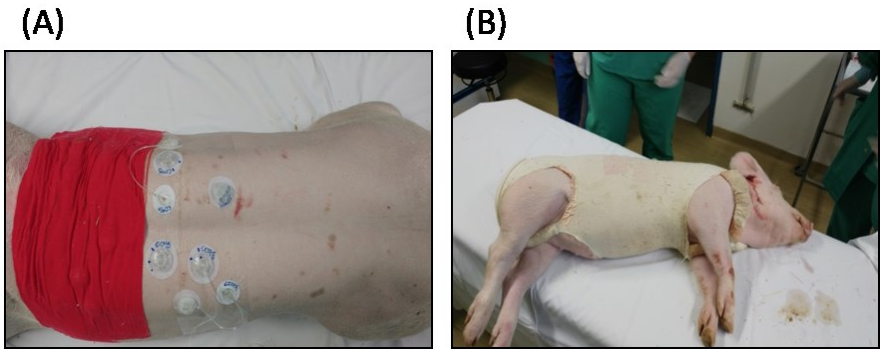

Figure 16: (A) Catheter insertion on day 4 of the study. Catheters of day 1 are covered in Kinesiology tape. (B) Sedated animal wearing padded stockinette.

3 and 7 days after the insertion of the first catheters (4 days and 1 day of wear-time, respectively), the stockinette was removed and all steps except for shaving repeated as described above (Table 7).

Table 7: Experimental setup for study period of 8 days on a Friday-to-Friday schedule. 4 catheters were inserted per time point (n_{total} = 120).

Day no.	**1**	**2**	**3**	**4**	**5**	**6**	**7**	**8**
Week day	Fri	Sat	Sun	Mon	Tue	Wed	Thurs	Fri
Wear-time (d)	**7**			**4**			**1**	
Eperiments	• Sedation • Shaving • Implantation of 4 catheters	Animals allowed to move freely	Animals allowed to move freely	• Sedation • Shaving • Implantation of 4 catheters	Animals allowed to move freely	Animals allowed to move freely	• Sedation • Shaving • Implantation of 4 catheters	• Euthanasia • Tissue excision

Animals were housed in separate pens to ensure that they would not manipulate each other's catheters. Their well-being was monitored and they were able to move around and play with toys in between study days.

On study day 8 the stockinette, Kinesiology tape and medical adhesive were carefully removed to avoid pulling out catheters. Catheters were infused with 4 units of methylene blue dye, using an insulin pump. Occlusion alarms were reported. Animals were euthanized before tissue excision with an IV overdose of potassium chloride.

3.4.2 HISTOLOGY

A block of skin and fatty tissue (approx. 5 x 5 x 2 cm) was removed from around the catheters using a scalpel and surgical scissors. The specimen was placed in 4 % PBS-buffered formalin for 72 hours, leaving the catheter in the tissue. After 3 days, the catheter was removed and the tissue was grossed to locate the region of interest, i.e. the insertion channel (Figure 12). Tissue was processed according to the protocol in Table 8 and embedded in paraffin wax. 3 µm thick sections were stained with the Hematoxylin and Eosin (H&E) using the protocol in Table 9. Nuclei are stained blue or dark purple to visualize lymphocytes, neutrophils, fibroblasts and monocytes, while cytoplasm and collagen are stained pink. Red blood cells are visible as red dots indicating bleeding. Sectioning was repeated 3 times: first to check for the right plane (insertion channel visible or not), second and third for "deeper" layers in the paraffin block (i.e. further away from the center of the insertion channel). The following criteria were analyzed by the pathologist 3 times using a grading system from none to severe, including the following grades:

- 0 = none
- 0.5 = some
- 1 = mild
- 2 = moderate
- 3 = severe

The pathologist remained blinded throughout the analysis.

Table 8: Tissue dehydration protocol. Standard protocol used at the Center for Medical Research, Medical University of Graz, Austria.

	Solution	Time (hh:mm)	Temperature [°C]
1	Formalin 6 %	01:00	40
2	Formalin 6 %	01:00	40
3	EtOH 70 %	01:00	40
4	EtOH 80 %	01:00	40
5	EtOH 96 %	01:00	40
6	EtOH 96 %	01:00	40
7	EtOH 100 %	01:00	40
8	EtOH 100 %	01:00	40
9	Tissue Clear (xylene substitute)	01:00	40
10	Tissue Clear (xylene substitute)	01:00	40
11	Paraffin	01:00	53
12	Paraffin	01:00	53
13	Paraffin	02:00	53
14	Paraffin	02:00	53

Table 9: H&E staining protocol. Protocol used at the Institute of Pathology, Medical University of Graz, Austria in the Tissue Tek Prisma automatic stainer.

	Solution	Time (mm:ss)
1	Xylene	02:00
2	Xylene	02:00
3	EtOH 100 %	02:00
4	EtOH 100 %	02:00
5	Aqua dest.	02:00
6	Hematoxylin	04:00
7	Running tap water	04:00
8	Eosin	02:00
9	EtOH 100 %	02:00
10	EtOH 100 %	02:00
11	EtOH/Xylene	02:00
12	Xylene	02:00

3.4.3 QUANTITATIVE REAL-TIME PCR (QPCR)

For RNA isolation a tissue plug was removed from around the CSII catheter and then grossed down to about 5 mm distance from the cannula. The cylinder-shaped specimen was separated into 2 different parts: around the tip and center of the cannula. The tissue was placed in 2 ml eppendorf tubes containing RNA stabilizing solution and incubated over night at 4 °C. Adipose tissue samples were then transferred to -80 °C for storage until mRNA isolation. Adipose tissue was broken up using Trizol and MagNA Lyser Green Beads and mRNA isolated with the

RNeasy MiniKit (Qiagen). Messenger RNA was transcribed into cDNA by reverse transcriptase PCR using a kit from AppliedBiosystems. Quantitative SYBR green real-time PCR was carried out and analyzed following the MIQE guidelines [92] to measure changes in expression of macrophage marker CD68 and the cytokines interleukin-6 (IL-6), interleukin-8 (IL-8/CXCL8), tumor necrosis factor alpha (TNF-α), transforming growth factor beta (TGF-β) and interleukin-10 (IL-10) using the Roche LightCycler® 480 System. Relative changes in gene expression were calculated using the ΔΔCt method (

Equation **3**). Here, the Ct (cycle threshold) of a target gene is compared with Ct values of reference genes, i.e. genes that are constantly expressed in the cell regardless of environmental influences. The reference genes ribosomal protein 4 (RPL4) and tyrosine 3-monooxygenase/tryptophan 5-monooxygenase activation protein zeta (YWHAZ) were used as internal controls to normalize cellular mRNA data.

Equation 3: Calculating fold-change in gene expression with the ΔΔCq method.

$$\Delta Ct1 = Ct_{C,x} - Ct_{C,hk} \qquad (3.1)$$

$$\Delta Ct2 = Ct_{T,x} - Ct_{T,hk} \qquad (3.2)$$

$$\Delta\Delta Ct = \Delta Ct1 - \Delta Ct2 \qquad (3.3)$$

$$\Delta fold = 2^{-\Delta\Delta Cq} \qquad (3.4)$$

Cq … threshold cycle
T … Traumatized tissue (needle)
C … Control tissue $(no\ needle)$
x … Gene of interest
hk … Reference ("housekeeping") gene
∆fold … gene expression fold change
E…Efficiency of primer pair (ideally 2)

4. RESULTS

4.1 STUDY I: IN-DEPTH ANALYSIS OF THE PHARMACOKINETICS (PK) OF LISPRO INSULIN AND THE TISSUE RESPONSE TO CSII CATHETERS (SWINE MODEL, TJU)

All of the commercial CSII catheters were easily inserted into the subcutaneous tissue using a standardized method. Dimpling of skin during needle/catheter insertion was not observed. Insertion of the experimental CSII catheter was difficult to perform using a standard method. The skin commonly dimpled at the needle tip and closing the catheter head was often difficult, requiring a hard push and snap. A plastic piece commonly herniated from the bottom of the Flex Infuser while closing the head during insertion. The 6 swine tolerated the 30 days of insulin infusion and 36 PK studies without infection or significant hypoglycemia. All of the CSII catheters remained adhered to the skin and insulin, saline and glucose were reliably delivered by the infusion pumps throughout the 5-day study.

4.1.1 DROP-OUTS AND METHYLENE BLUE DYE LEAKAGE

Kinking of one commercial catheter in swine 1 resulted in almost no absorption of insulin in the circulation on days 1 and 3 and some absorption on day 5. Therefore, the respective PK values for calculations of mean, variance and coefficient of variation were omitted, since adequate flow of insulin into the tissue was impaired. Upon infusion of 50 µL of methylene blue dye, leakage into the hub was observed in only 1 out of 36 commercial catheters but 13/36 experimental catheters (see Appendix, Table 23). Of the commercial catheters used for insulin PK studies, none leaked methylene blue dye. Experimental catheters of swine 1, 2 and 6 showed mild or moderate leakage into the hub and produced limited insulin absorption on days 3 and/or 5 (Figure 17).

4.1.2 PHARMACOKINETICS AND INSULIN ABSORPTION VARIABILITY

Results are summarized in Table 10 and Table 11. In general, the intra- (within) and inter- (between) subject variability of PK parameters was lower for the commercial catheter. Between animals, the coefficient of variation (CV) for the area under the curve over the first 60 minutes was lower on day 1 compared with day 5 (Commercial: 25.3 % and 38.0 % respectively; New: 52.2 % and 107.9 %, respectively). Between animals, C_{max} of C was most variable on day 3 compared with days 1 and 5. Insulin absorption from the new catheters was least variable (range 34-124 mU/L*h, inter-subject CV = 52.5 %) on day 1 and most variable on day 3 (range 9-132 mU/L*h, inter-subject CV = 93.8 %). In all experiments, the maximum insulin concentration was reached within the first 60 minutes after bolus administration. Infusion through the experimental catheter resulted in higher maximum insulin plasma concentrations in some animals compared to the commercial catheter. In average, C_{max} values were higher for insulin administration through the experimental catheter but insulin absorption was faster and less variable using the commercial catheter. Insulin absorption was fastest on day 5 of wear-time from the commercial catheter (t_{max} = 12.0 ± 4.5 min), also exhibiting the highest plasma insulin concentration (C_{max} = 114.7 ± 30.1 mU/l). All of the experimental catheters produced the highest AUC60, AUC and C_{max} on day 1, while absorption was slow and low on day 5 of catheter wear-time. The PK data presented here could not be analyzed for statistical significance due to the small number of studies. The averaged PK data for days 1, 3 and 5 is shown in Figure 17 and the individual PK curves are shown in Figure 37.

Table 10: Mean values for AUC, AUC60, C_{max} and t_{max} for both types of CSII catheters on days 1, 3 and 5. (Adapted from Hauzenberger *et al.* 2017 [93])

Catheter type	Day	$\mathbf{AUC}\ (\frac{\mathbf{mU}}{\mathbf{L}}\mathbf{h})$	$\mathbf{AUC60}\ (\frac{\mathbf{mU}}{\mathbf{L}}\mathbf{h})$	$\mathbf{C_{max}}\ (\frac{\mathbf{mU}}{\mathbf{L}})$	$\mathbf{t_{max}}\ \mathbf{(min)}$
Commercial CSII Catheters (C) (n= 5[§] swine)	1	82.7 ± 37.6	50.9 ± 12.9	90.7 ± 26.8	35.0 ± 17.3
	3	63.1 ± 22.8	47.0 ± 25.6	73.9 ± 41.0	20.0 ± 12.2
	5	71.1 ± 29.4	54.9 ± 20.8	114.7 ± 30.1	12.0 ± 4.5
Experimental CSII Catheters (N) (n= 6 swine)	1	68.5 ± 36.0	44.3 ± 23.2	120.0 ± 59.3	43.3 ± 28.8
	3	63.1 ± 51.8	42.7 ± 40.0	115.0 ± 86.2	20.0 ± 6.3
	5	40.1 ± 37.6	29.0 ± 31.3	105.1 ± 87.7	33.3 ± 18.6
Data are provided as mean ± SD, [§]PK from swine 1 excluded due to incomplete insertion of catheter C1.					

Table 11: Coefficients of variation (CV) for inter- and intra-subject variability for each day and over all days.(Adapted from Hauzenberger *et al.* 2017 [93])

CV type	Catheter	Day	CV AUC	CV AUC60	CV C_{max}	CV t_{max}
Between animals	C	1	45.6 %	25.3 %	29.5 %	49.5 %
		3	36.1 %	54.5 %	55.6 %	61.2 %
		5	41.3 %	38.0 %	26.2 %	37.3 %
Between animals	N	1	52.5 %	52.5 %	49.4 %	66.4 %
		3	82.1 %	93.7 %	75.0 %	31.6 %
		5	93.8 %	107.9 %	83.4 %	55.9 %
Between animals	C	all	13.7 %	7.8 %	22.0 %	52.3 %
		all	26.4 %	21.7 %	6.7 %	36.3 %
Within animals	N	all	30.8 %	25.5 %	37.0 %	39.2 %
		all	69.6 %	83.8 %	49.5 %	55.5 %

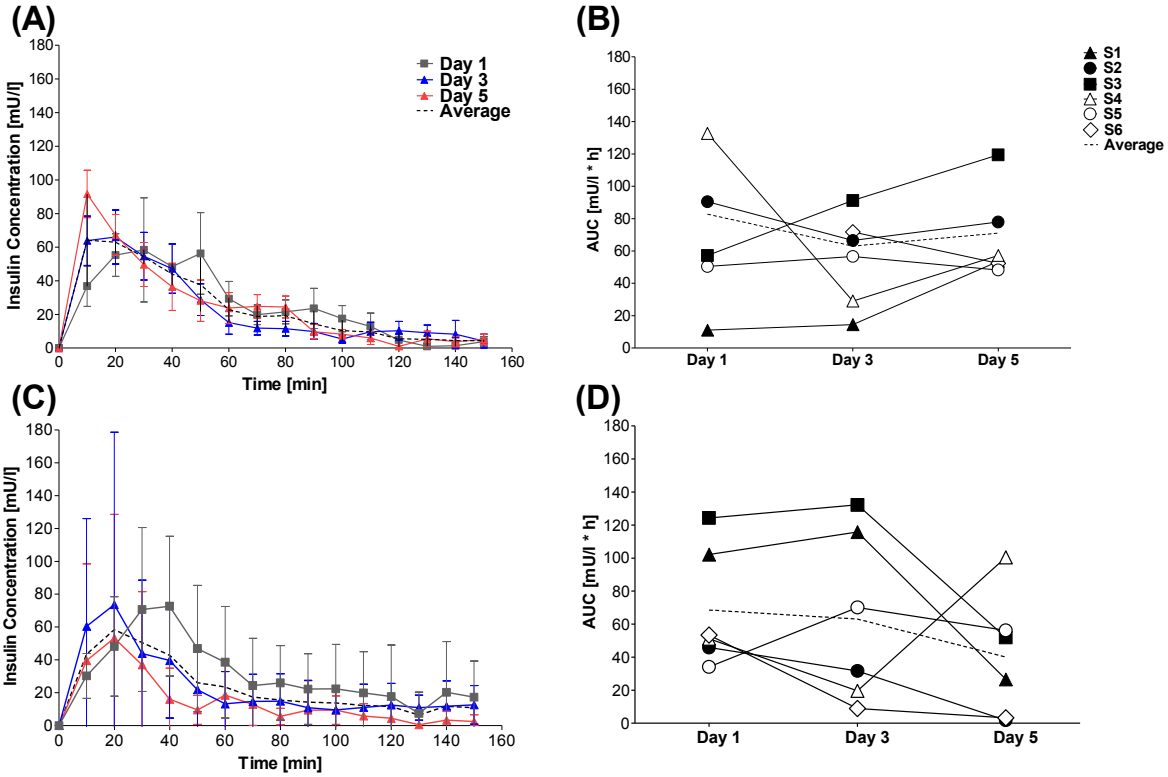

Figure 17: Insulin concentration curves and area under the insulin absorption curve (AUC) over 5 days and 2.5 hours for commercial and investigational catheters. Average insulin plasma concentrations measured after bolus administration through the commercial **(A)** and the experimental **(C)** catheter with SEM bars. Intermitted line represents the average over all 5 days. Panels **(B)** and **(D)** show changes in area under the insulin absorption curve (AUC) over 2.5 hours. Intermitted line represents the average AUC values for 6 swine. Plasma samples could not be obtained on the first day in swine 6 (panel B, white diamonds). (Adapted from Hauzenberger *et al.* 2017 [93])

4.1.3 HISTOLOGY

Table 12 and Table 13 summarize the surgical pathologist's description of the tissue response to CSII catheter implantation for 5 days. A total of 72 samples (36 commercial and 36 experimental) were analyzed. The histology slides revealed a layer surrounding the CSII catheters that varied in thickness, density, continuity, and composition (Figure 18). It contained a heterogeneous mixture of red and white blood cells, fibrin, collagen and damaged cells, connective tissue, and extracellular matrix. All specimens showed severe inflammation regardless of catheter material after 5 days of wear time. Neutrophils and fibroblasts (dark pink cells in H&E stain) migrated towards the traumatized site. The damage of arterioles, capillaries and venules lead to bleeding and thrombus formation (fibrosis), especially around the tip of the catheter (dark red cells in H&E and trichrome stains). The force of insertion destroyed adipocytes leading to fat necrosis and the replacement of fat cells by fresh collagen (light blue compared to existing collagen as darker blue in trichrome stain). Existing collagen fibers were pushed downward and compressed following catheter insertion, destroying the natural distribution of fibers parallel to the epidermis. Re-epithelization down the insertion hole of the catheter was observed on skin surface after 5 days of implantation. Reticular fiber disruption, fat necrosis, hemorrhage, reservoir geometry, tissue topography and size of debris field significantly differed ($p < 0.001$ or $p < 0.05$) between catheter types while fibrin and collagen deposition where similar. The tissue histology surrounding the CSII catheter infused with insulin was similar to the tissue histology surrounding catheters infused with saline or not infused. Insulin infusion significantly increased fibrin deposition in the catheter reservoir (Table 13).

Table 14 summarizes the tissue histology and PK outcomes for each commercial and experimental catheter. The mean AUC and C_{max} were higher and t_{max} shorter for insulin administration through a commercial catheter. Reticular fibrin deposition and fat necrosis was less in tissue specimens surrounding commercial catheters compared with experimental catheters but fibrin deposition was more often (4/5) severe around a commercial catheter.

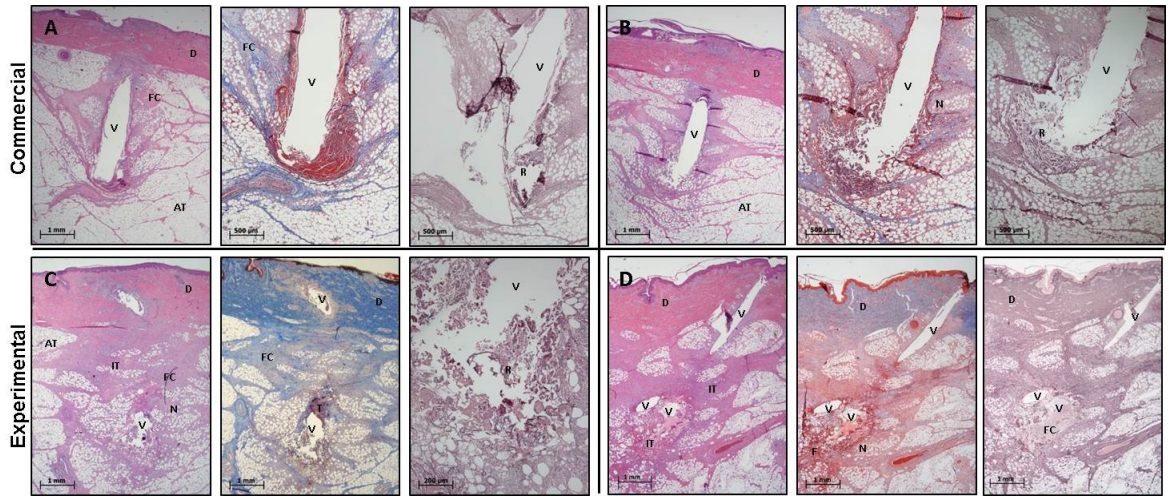

Figure 18: Examples of histopathological staining of subcutaneous adipose tissue (AT) surrounding commercial CSII catheters (panels A and B) and experimental CSII catheters (panels C and D). Tissue sections were stained with with H&E, Masson's Trichrome and Reticulin III (left to right). Void (V), dermis (D), fresh collagen (FC), thrombus (T), fat necrosis (N) reticular fibers (R), inflamed tissue (IT). The (Adapted from Hauzenberger *et al.* 2017, [93])

Table 12: Statistical correlation of catheter type with tissue histology. (Adapted from Hauzenberger *et al.* 2017, Supplementary Data [93])

Inflammatory characteristic	**Cath. Type**	**None**	**Mild**	**Moderate**	**Severe**	
Reticulin Fiber Disruption	C (n=36)	1 (2.8 %)	29 (80.6 %)	6 (16.7 %)	0	***
	N (n=36)	0	6 (16.7 %)	9 (25.0 %)	21 (58.3 %)	
Fibrin Deposition in Reservoir	C	1 (2.8 %)	10 (27.8 %)	15 (41.7 %)	10 (27.8 %)	
	N	0	8 (22.2 %)	21(58.3 %)	7 (19.4 %)	
Collagen Deposition at Tip	C	4 (11.1 %)	26 (72.2 %)	6 (16.7 %)	0	
	N	1 (2.8 %)	23 (63.9 %)	11 (30.6 %)	1 (2.8 %)	
Fat Necrosis	C	1 (2.8 %)	22 (61.1 %)	13 (36.1 %)	0	***
	N	0	7 (19.4 %)	14 (38.9 %)	15 (41.7 %)	
Hemorrhage at Tip Base	C	1 (2.8 %)	27 (75.0 %)	8 (22.2 %)	0	*
	N	1 (2.8 %)	17 (47.2 %)	17 (47.2 %)	1 (2.8 %)	
Changes in Tissue Morphology		**Regular**	**Intermediate**	**Irregular**		
Reservoir Geometry	C (n=35§)	29 (82.9 %)	-	6 (17.1 %)		***
	N (n=36)	11 (30.6 %)	-	25 (69.4 %)		
Topography of Tissue Planes along Insertion	C	30 (85.7 %)	5 (14.3 %)	0		***
	N	1 (2.8 %)	19 (52.8 %)	16 (44.4 %)		
		Depth (mm) ± SD				
Debris Field (mean)	C	3.2 ± 1.1				***
	N	4.9 ± 1.4				

Values are provided with % of a total of 36 catheters in brackets, §changes in tissue morphology for Swine1-C1 not possible to evaluate due to incomplete, superficial insertion of catheter, ***p < 0.001, *p < 0.05, significant difference between catheter types

Table 13: Correlation between type of infusion (insulin, saline, none) and tissue histology. (Adapted from Hauzenberger *et al.* 2017 [93])

	Infusion	None	Mild	Moderate	Severe	
Reticulin Fiber Disruption	Insulin (n=24)	1 (4.2 %)	9 (37.5 %)	6 (25.0 %)	8 (33.3 %)	
	Saline (n=24)	0	13 (54.2 %)	3 (12.5 %)	8 (33.3 %)	
	None (n=24)	0	13 (54.2 %)	6 (25.0 %)	5 (20.8 %)	
Fibrin Deposition in Reservoir	Insulin	1 (4.2 %)	2 (8.3 %)	11 (45.8 %)	10 (41.7 %)	
	Saline	0	9 (37.5 %)	11 (45.8 %)	4 (16.7 %)	*
	None	0	7 (29.7 %)	14 (58.3 %)	3 (12.5 %)	
Collagen Deposition at Tip	Insulin	2 (8.3 %)	16 (66.7 %)	5 (20.8 %)	1 (4.2 %)	
	Saline	2 (8.3 %)	16 (66.7 %)	6 (25.0 %)	0	
	None	1 (4.2 %)	17 (70.8 %)	6 (25.0 %)	0	
Fat Necrosis	Insulin	1 (4.2 %)	5 (20.8 %)	12 (50.0 %)	6 (25.0 %)	
	Saline	0	14 (58.3 %)	5 (20.8 %)	5 (20.8 %)	
	None	0	10 (41.7 %)	10 (41.7 %)	4 (16.7 %)	
Hemmorhage at Tip Base	Insulin	1 (4.2 %)	13 (54.2 %)	10 (41.7 %)	0	
	Saline	1 (4.2 %)	15 (62.5 %)	7 (29.2 %)	1 (4.2 %)	
	None	0	16 (66.7 %)	8 (33.3 %)	0	
Values are provided with % of total n of catheters in brackets, *p < 0.05, significant difference between infusion types						

Table 14: Tissue histology data and corresponding PK values (Day 5) for all CSII catheters used for PK study. (Adapted from Hauzenberger *et al.* 2017, Supplementary Data [93])

Swine	Catheter	Debris Field (mm)	Reservoir Geometry	Reticular fiber disruption§	Fibrin deposition§	Collagen deposition at tip§	Topography of tissue planes	Fat necrosis§	Hemorrh. at tip base§	$AUC(\frac{mU}{L}h)$	$C_{max}(\frac{mU}{L})$	$t_{max}(min)$
2	CC	3.1	regular	1	2	1	regular	1	1	83.29	113.43	10
3	CC	3.3	regular	1	3	1	regular	1	1	119.45	116.16	20
4	CC	1.9	regular	1	3	1	regular	2	2	57.25	156.62	10
5	CC	2.2	regular	2	3	1	regular	2	2	48.26	115.52	10
6	CC	2.6	irregular	2	3	1	interm.	2	2	54.47	71.56	10
Mean ± SD		**2.6 ± 0.6**								**72.54 ± 29**	**114.66 ± 30**	**12.00 ± 4**
1	IC	7.9	irregular	3	2	1	irregular	3	2	28.30	68.17	60
2	IC	3.2	regular	2	2	1	interm.	2	1	1.77	47.10	50
3	IC	6.8	irregular	3	2	1	interm.	2	1	54.83	85.06	30
4	IC	4.3	irregular	3	2	1	interm.	3	2	100.49	269.32	20
5	IC	3.8	irregular	2	1	1	irregular	2	1	57.08	131.09	10
6	IC	4.1	irregular	3	3	0	irregular	3	2	3.27	29.76	30
Mean ± SD		**5.0 ± 1.9**								**40.96 ±38**	**105.08 ± 88**	**33.33 ± 19**
§Ordinal scaling for histology: 0-none, 1-mild, 2-moderate, 3-severe.												

4.2 Study II: The Effect of Co-Infusion of Thrombolytic Agents and Application of Vibration on Insulin PK/PD and Tissue Histology (Canine Model, TJU)

An adult large canine model was used for this study because of previous difficulties obtaining frequent blood samples from the ambulatory large swine for more than 5 days. Though the canines proved easier to work with and obtain viable samples from, the lack of subcutaneous tissue and presence of skeletal muscle and mammary gland tissue may designate them as a poor choice for subject testing. Canine information can be found in

Table 4.

4.2.1 Dislodgement and drop outs

The CSII catheters for insulin delivery and control as well as the 2 CGM sensors of canine D02 became dislodged prematurely (day 5) due to movement of the animal and rubbing against the cage. A new CSII catheter was inserted 24 hours later creating data for an additional PK/PD studies on day 1 in D02 (Day 1 and Day 1R, respectively). Both CSII catheters (insulin and control) and the CGM sensors were pulled out by dislodgment of vest in canine D03. A new CSII catheter was inserted on study day 3 creating an additional PK/PD study for day 1 (Day 1R, Table 15). For canine D06, 2 zero values (insulin concentration = 0 mg/dl) were determined to be outliers and were removed after re-analyzing the samples using ELISA (reduced data skewing). The tissue histology for canine D01 and D022 did not produce histology visualizing the catheter insertion channel and therefore were not included in histology analysis. Overall, histology outcomes were poor and incomplete, rendering the analysis impossible.

Table 15: Summary of PK/PD studies in 13 dogs (D01-D13). Successful studies marked with ✓. If catheter became dislodged, the newly inserted catheter and repeated study is indicated as "= Day 1R". If a new catheter was inserted, the study time line of 1, 3, 6 and 7 days could not be held. Even if PK/PD studies were carried out, the data was included in the data analysis (indicated as n/a). Strep = Streptokinase; tPA = tissue plasminogen activator

	Treatment	**IV**	**SQ Day 1**	**SQ Day 3**	**SQ Day 6**	**SQ Day 7**
		Wed	Wed	Fri	Mon	Tue
D01	Control	✓	✓	✓	✓	✓
D02	Control	✓	✓	✓	n/a	n/a
D03	Control	✓	✓	= Day 1R	n/a	n/a
D12	Control	✓	✓	✓	✓	✓
D13	Control	✓	✓	✓	✓	✓
D04	Strep	✓	✓	✓	✓	✓
D05	Strep	✓	✓	✓	✓	✓
D06	Strep	✓	✓	✓	= Day 1R	n/a
D07	Strep	✓	✓	✓	✓	✓
D08	tPA	✓	✓	✓	✓	✓
D09	tPA	✓	✓	✓	✓	✓
D10	tPA	✓	✓	✓	✓	✓
D11	tPA	✓	✓	✓	✓	✓

4.2.2 PHARMACOKINETICS

There was no statistically significant difference found between C_{max} and t_{max} values on different days of CSII catheter wear-time. C_{max} was significantly higher and t_{max} significantly lower when insulin was administered intravenously (IV) compared to subcutaneous (SC) administration on day 1, 3, 6, and 7 of catheter wear-time (Figure 19). C_{max} and t_{max} did not differ significantly between treatment groups (thrombolytics versus control, not shown). Results are listed in Table 16.

Table 16: Summary of C_{max} and t_{max} values according to treatment group; "All" refers to the average over all groups.

	Treatment	**IV PK**	**SC PK Day 1**	**SC PK Day 3**	**SC PK Day 6**	**SC PK Day 7**
C_{max}	Control	279.8 ± 189.8	16.5 ± 8.6	25.9 ± 10.9	30.4 ± 14.4	17.1 ± 3.1
	Streptokinase	372.3 ± 182.5	21.8 ± 21.3	26.6 ± 8.6	35.9 ± 11.1	21.0 ± 10.6
	tPA	277.8 ± 30.7	11.2 ± 4.0	27.8 ± 14.0	37.1 ± 11.9	23.8 ± 12.4
	All	**307.6 ± 150.3**	**16.5 ± 12.7**	**26.7 ± 10.3**	**34.7 ± 11.4**	**21.0 ± 9.3**
t_{max}	Control	10.0 ± 0.0	56.0 ± 39.1	32.5 ± 37.1	50.0 ± 30.0	36.7 ± 15.3
	Streptokinase	10.0 ± 0.0	110.0 ± 64.8	62.5 ± 44.3	26.7 ± 11.6	20.0 ± 10.0
	tPA	10.0 ± 0.0	72.5 ± 52.5	37.5 ± 9.6	57.5 ± 45.0	50.0 ± 29.4
	All	**10.0 ± 0.0**	**77.7 ± 52.9**	**48.5 ± 32.9**	**46.0 ± 33.1**	**37.0 ± 23.1**

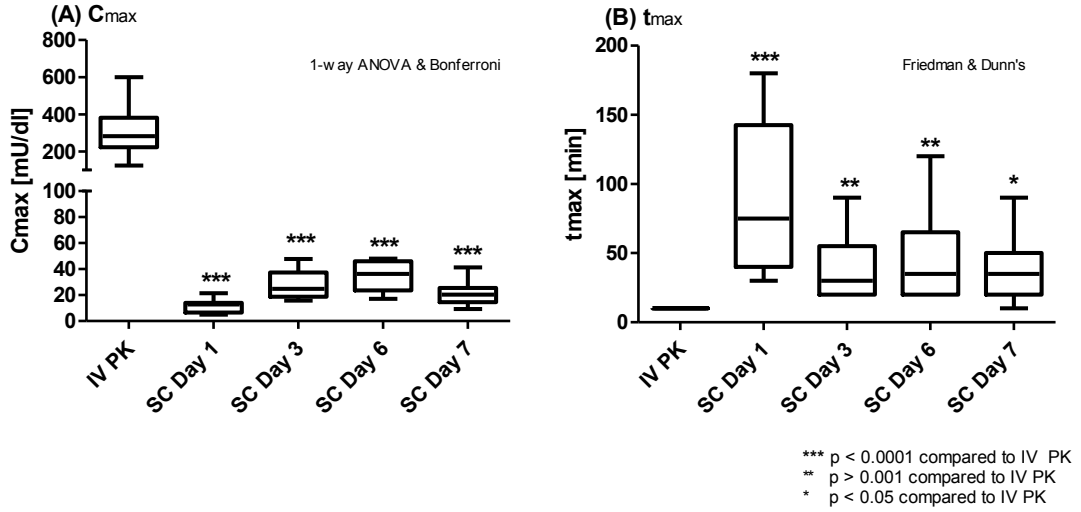

Figure 19: Median values of **(A)** C_{max} and **(B)** t_{max}. The first study was performed using IV insulin infusion while the other 4 studies were performed using a CSII catheter (indicated as IV and SC). The tests & post-tests used for comparison are indicated in the upper right corner of each panel.

The area under the insulin concentration curve was significantly higher when insulin was administered intravenously (Figure 20). The intra-subject (within-animal) coefficient of variation (CV) of AUC was calculated to be 73.9 ± 22.9 %. The inter-subject CVs can be found in Table 17.

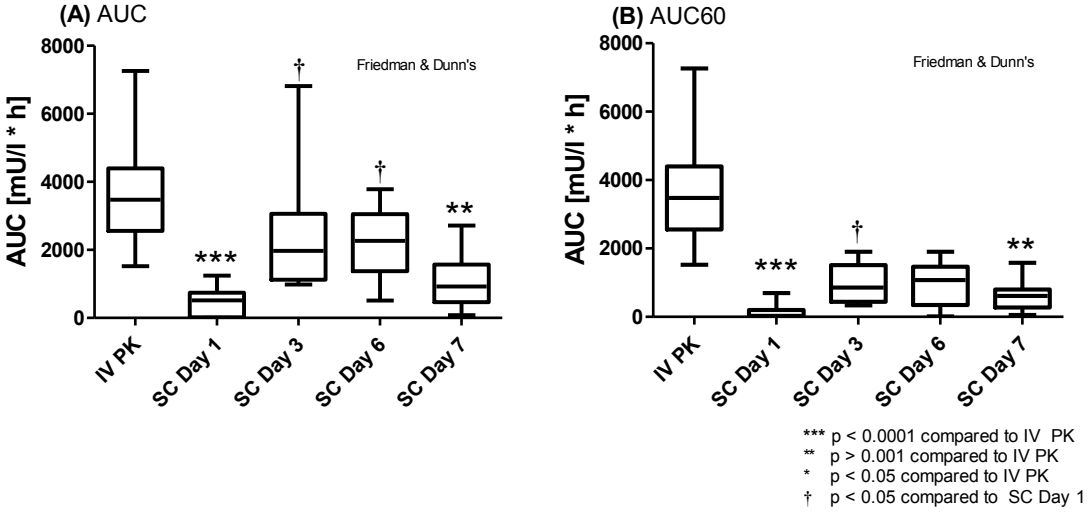

Figure 20: Median values of areas under the insulin concentration curves over **(A)** 180 minutes and **(B)** 60 minutes. The first study was performed using intravenous insulin infusion while the other 4 studies were performed using a CSII catheter (indicated as IV and SC). The tests & post-tests used for comparison are indicated in the upper right corner of each panel.

Table 17: Inter-subject (in between animals) coefficient of variation of AUC for each PK study day.

	inter-subject CV
IV PK	46.9 %
SC Day 1	109.6 %
SC Day 3	79.2 %
SC Day 6	45.3 %
SC Day 7	72.2 %

4.2.3 PHARMACODYNAMICS

The GIRs (mg/kg/min) of days 3 and 6 were significantly higher than on day 1 and day 7 of CSII catheter wear time (Figure 21, Table 18). The dextrose requirements between no vibration and vibration could not be tested for statistical significance as there were only 2 animals in the vibration group. GIR curves for each day of wear-time are shown in Figure 22. There is a trend towards higher glucose requirements, i.e. faster insulin absorption on day 3, when vibration is applied.

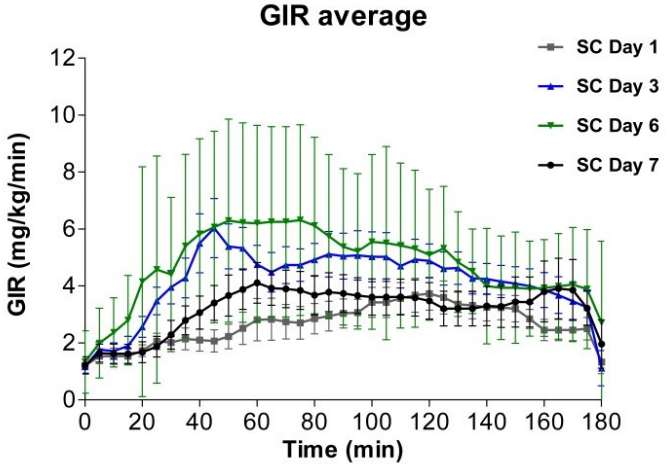

Figure 21: Glucose infusion rate (GIR) of all 13 dogs illustrating the glucose lowering effect of an insulin lispro bolus (0.1 units/kg BW) on day 1, 3, 6, and 7. The GIR represents the amount of 20 % dextrose required to clamp the blood glucose concentration at 105 ± 15 mg/dl. The animals required more glucose following an insulin bolus on days 3 and 6 of catheter wear-time compared to day 1 ($p < 0.0001$), indicating increased insulin absorption. Data are plotted as mean ± SEM.

Table 18: Significant differences between dextrose requirements (GIR) over days of catheter wear time.

Days compared	Significant?
SC Day 1 vs SC Day 3	significantly lower (***)
SC Day 1 vs SC Day 6	significantly lower (***)
SC Day 1 vs SC Day 7	not significant (n.s.)
SC Day 3 vs SC Day 6	significantly lower (**)
SC Day 3 vs SC Day 7	significantly higher (**)
SC Day 6 vs SC Day 7	significantly higher (***)
**p < 0.001, ***p < 0.0001; Dunn's Multiple Comparison Test	

The actual amount of dextrose needed is represented by the area under the glucose infusion curve over time (AUC_{GIR}). The glucose requirement was similar to that of IV insulin infusion on SC days 3, 6, and 7 but significantly lower on SC day 1 ($p < 0.001$). The average intra-subject CV of AUC_{GIR} was 40.1 ± 17.8 %. The inter-subject CVs can be found in Table 19. $t_{max(GIR)}$ of the IV PD experiment was significantly lower (compared to SC PD experiments on day 3 and day 6 (Figure 23).

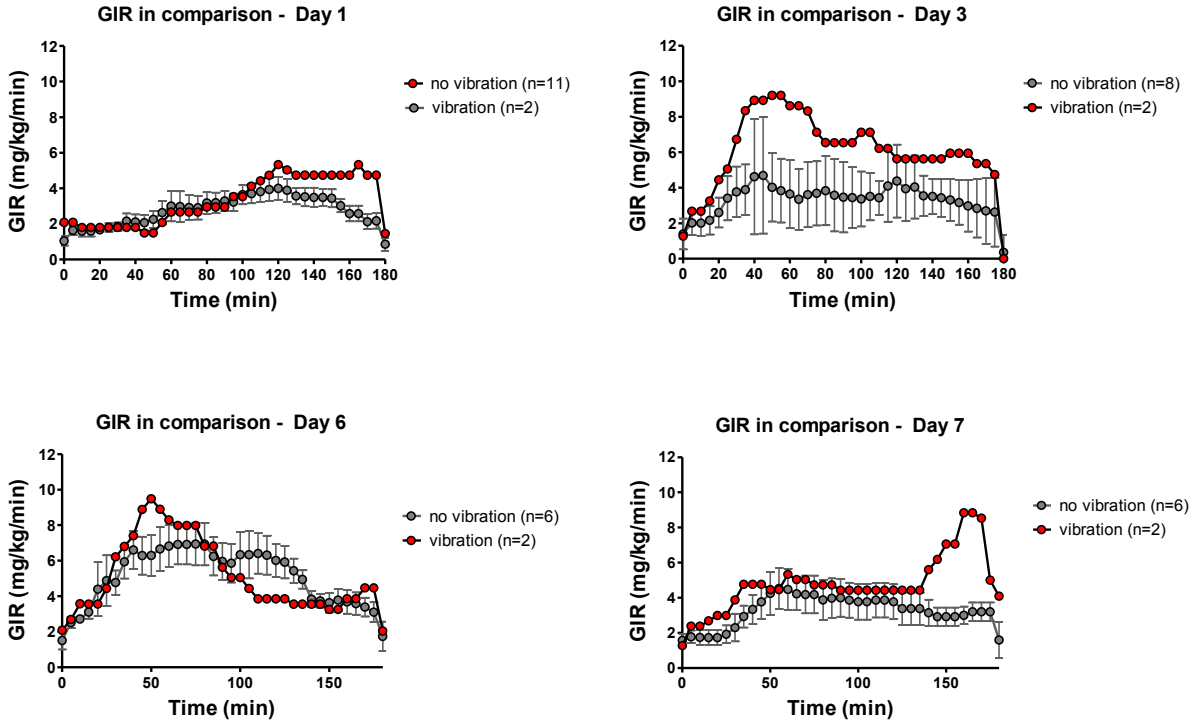

Figure 22: Comparison of dextrose requirements when vibration is applied to the CSII catheter during insulin bolus administration. Data points are plotted as mean ± SEM.

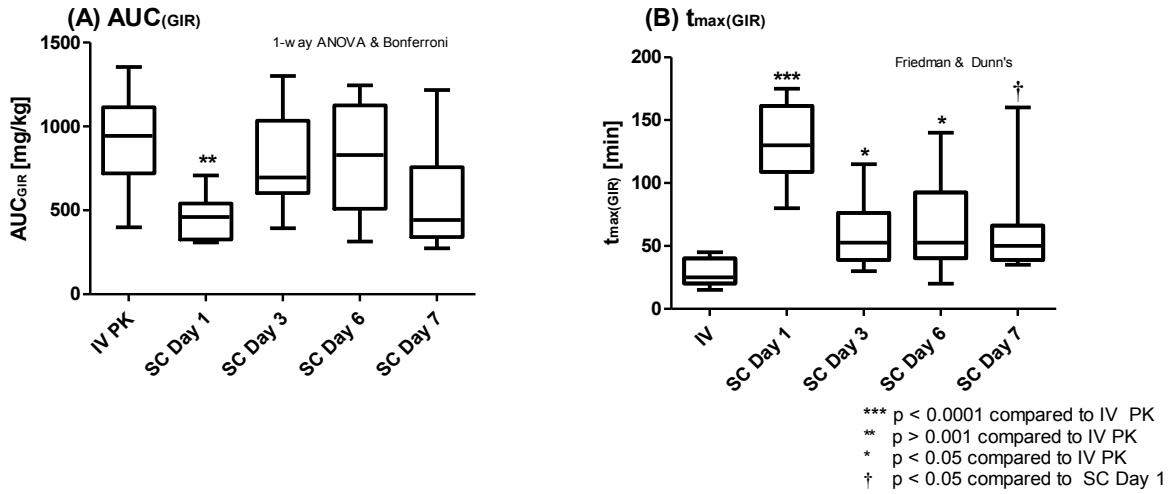

Figure 23: PD data for 13 dogs. **(A)** Median values of areas under the glucose infusion curve over time. **(B)** Median values of time to maximum glucose infusion rate. The first study was performed using intravenous insulin infusion while the other 4 studies were performed using a CSII catheter (indicated as IV and SC). The tests & post-test used for comparison are indicated in the upper right corner. (**p < 0.001; ***p < 0.0001)

Table 19: Inter-subject (in between animals) coefficient of variation of AUC_{GIR} for each PD study day.

	inter-subject CV
IV PK	26.3 %
SC Day 1	29.4 %
SC Day 3	38.3 %
SC Day 6	40.4 %
SC Day 7	59.6 %

4.2.4 TISSUE HISTOLOGY

Locating the insertion channel was extremely difficult in this experiment as canine skin pigmentation differed among subjects and also skin areas. If catheter was inserted in an area where fur and thus skin color was dark brown or black, the insertion channel could not be properly located during tissue grossing. Figure 24 shows representative slides stained with Trichrome or H&E to provide an idea of tissue response of canine to CSII catheter insertion. Samples co-infused with thrombolytic agents showed little to no bleeding in fibrin deposition in the reservoir. Vibrated samples had a slarger debris field. All samples showed layer formation of inflammatory cells and fresh collagen along the insertion channel.

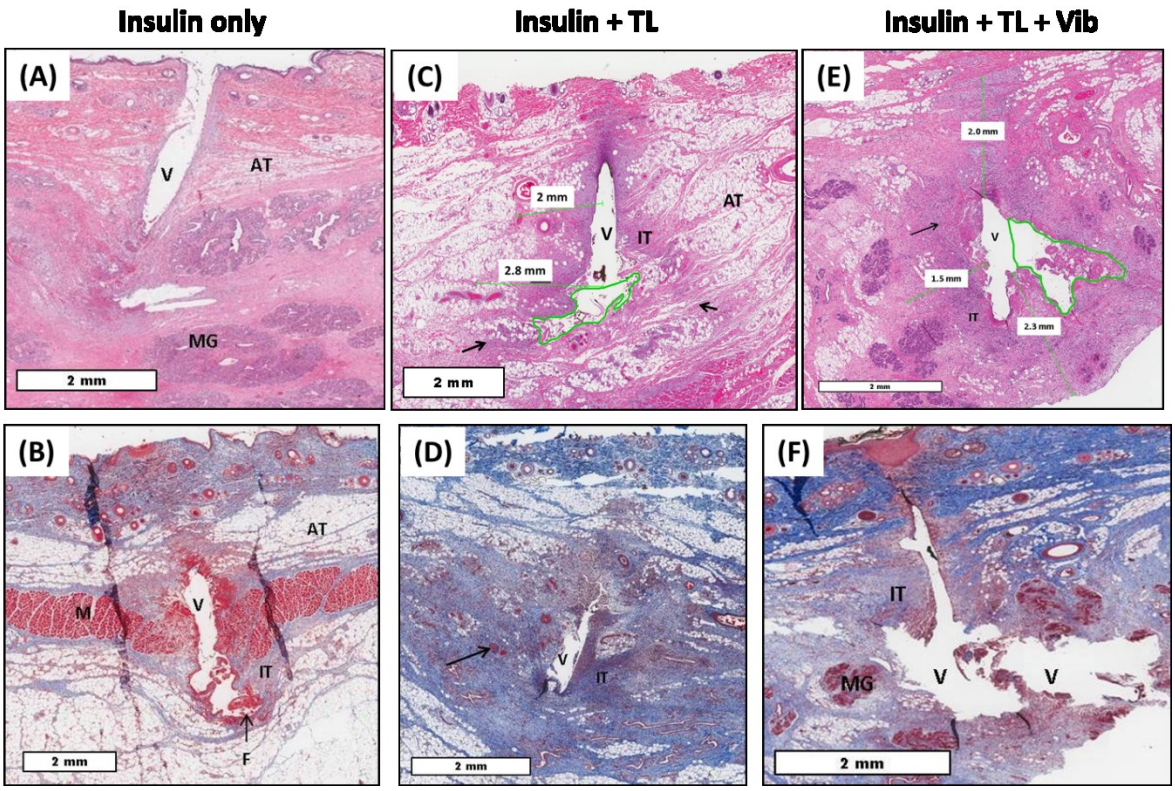

Figure 24: Overview histology - canine study; H&E (top row) and Trichrome (bottom row) stains. **(A)** and **(B)** show the insertion channel of a CSII catheter infused with insulin lispro for 7 days. The void in the specimen (V) illustrates loss of adipose cells, capillaries, and lymph vessels following removal of the 6 mm CSII cannula. The cannula extended through the dermal tissue layer, adipose tissue layer (AT) into a layer of skeletal muscle (M). The CSII cannula is surrounded by a layer of inflammatory tissue (IT) of variable density containing damaged cells, fresh collagen (light blue in Trichrome) and immune cells. There is fibrin (F) deposited on the bottom of the insertion channel. Mammalian glands are indicated as (MG). **(C)** and **(D)** are examples of specimens infused with insulin lispro and thrombolytic (TL) agents (tissue plasminogen activator or streptokinase). The cannula extended through the dermal layer with hair follicles, into a deeper layer of adipose tissue (AT). The void (V) is surrounded by a layer of inflammatory tissue (IT). The arrows point to inflammatory cells (dark purple), that are migrating towards the site of trauma. Distal to the insertion channel is an open area of adipose tissue may be distended connective tissue due to the infusion of insulin. This specimen lacks thrombus or fibrin. **(E)** and **(F)** are representative histology pictures of tissue surrounding a CSII catheter that was infused with a thrombolytic (TL) agent and vibrated at the same time using a cell phone motor. They exhibit a larger area of tissue disruption (V) and a surrounding area of inflammatory tissue (IT) of variable thickness and density. The distal end of this CSII cannula was located within subcutaneous adipose tissue containing many mammary glands (MG)

4.3 Study III: Comparison of the Inflammatory Response to Steel and Teflon CSII Catheters Using Histopathology and Quantitative Real-Time PCR (Swine Model, MedUni Graz)

4.3.1 Drop-outs and occlusion alarms

120 CSII catheters were inserted in total. 4/120 cannulas (2 steel and 2 Teflon) did not push through the layer of clear medical adhesive on the animal's skin. They kinked between the adhesive and the hub and did not insert into the tissue (Figure 25). In 115/120 samples, the insertion channel could be located, the remaining 5 did not produce adequate histology pictures. The drop-out rate for this study was thus calculated to be 7.5 %. Details are listed in Table 20.

Figure 25: Examples of catheters that kinked above adhesive and did not insert into the skin.

Table 20: List of samples rejected after completion of study (drop-outs).

Catheter type	No. of catheters kinked	No insertion channel
Sure-T, 6 mm	2	2
Quick-set, 6 mm	2	3
Total	**4**	**5**

While removing the kinesiology tape and medical adhesive that covered the CSII catheters, some catheters were accidentally pulled out. However, in all instances, the insertion channels could be located without prior methylene dye infusion. Locating the insertion channel was the most crucial part in this study. Localization was most difficult when catheter kinked within the tissue and did not follow an approximately 90-degree insertion angle. A 3- or 4-unit bolus of saline immediately after insertion of Teflon sets did not result in a single occlusion alarm, even for kinked catheters. Before excision on day 8, a 4-unit bolus of methylene blue dye was infused through the Quick-sets. In the Sure-T-sets, the blue dye could not

pass through the connecting hub and into the tubing and it was not possible to carry out this experiment (see arrow in Figure 26). Table 21 summarizes all leakages of blue dye and occlusion alarms. No leakages were observed and 10 % of catheters produced an occlusion alarm.

Figure 26: Image of a Sure-T set with tubing and hub (adapted from: www.diaexpert.de).

Table 21: Overview of blue dye leakage into hub and occlusion alarms on study day 8.

total leakages	0/30	0%
total occlusion alarms *("no delivery")*	3/30	10%

4.3.2 TISSUE EXCISION

Upon removal of skin/adipose tissue specimens, the difference in tissue trauma caused by materials could be observed immediately on the muscle layer. Steel sets caused major inflammation, bleeding and fibrosis after only 4 days of wear-time. This difference was even more pronounced for skin that had a catheter inserted for 7 days (see Figure 27). Figure 28 and Figure 29 show a tissue specimen after formalin fixation that is in the process of being grossed for the embedding in paraffin blocks. Methylene blue dye migrated down the insertion channel and diffused into adipose tissue in the vicinity but did not travel all the way back onto the skin.

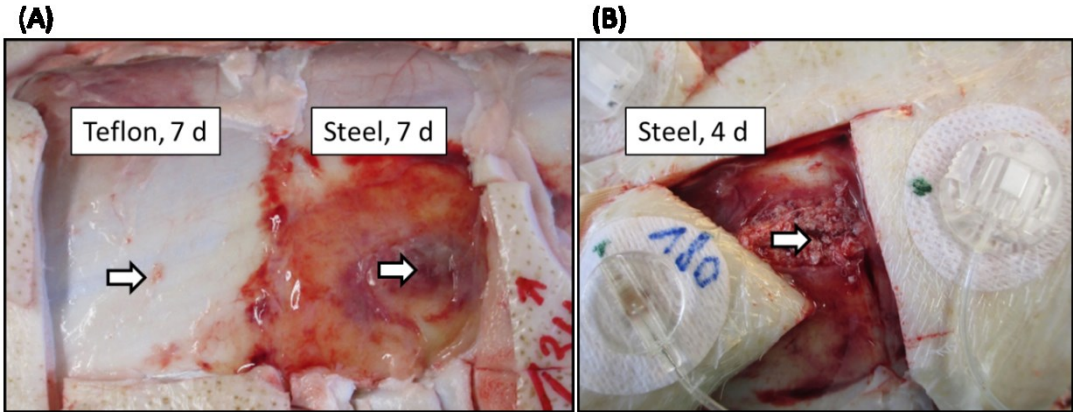

Figure 27: Inflamed fascia after **(A)** 7 and **(B)** 4 days of wear-time. Arrows point at area where cannula tip hit the muscle layer. Area below steel catheters is severely inflamed and exhibits fibrosis.

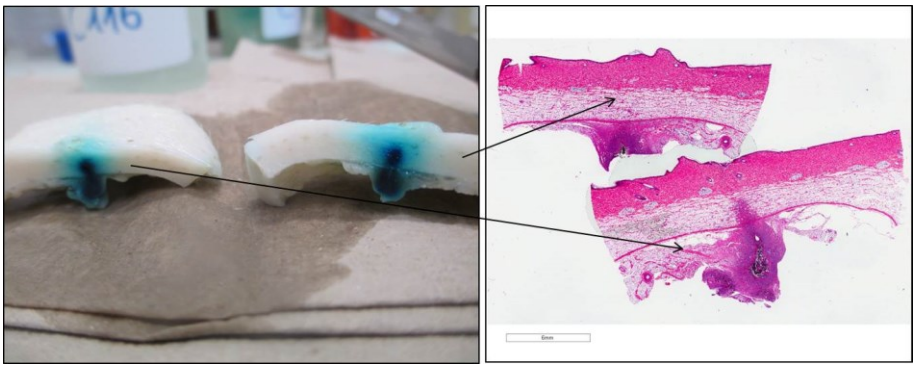

Figure 28: Localization of the insertion channel with methylene blue dye infusion and resulting H&E stains (Teflon, 7 days).

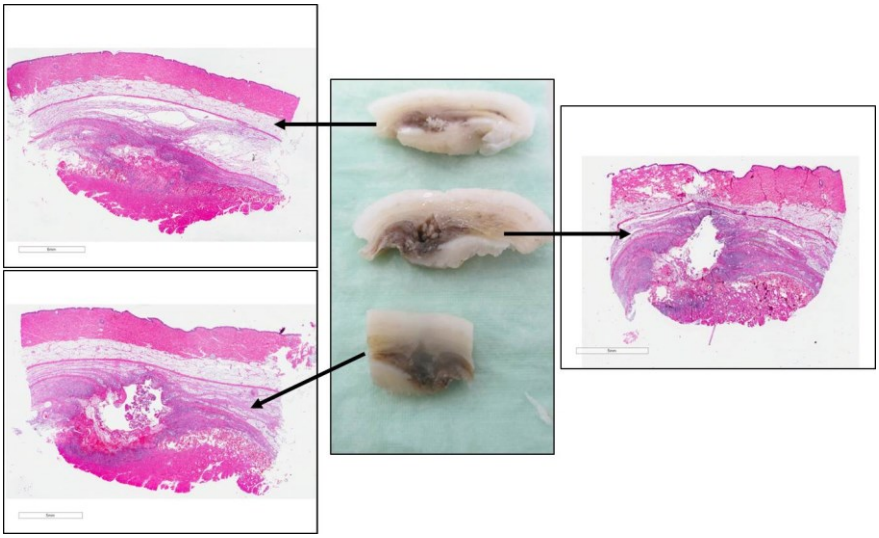

Figure 29: Localization of the insertion channel without methylene blue dye infusion and resulting H&E stains (steel, 4 days).

4.3.3 Histopathological Evaluation of Tissue

Figure 30 shows representative examples of subcutaneous adipose tissue stained with H&E after the removal of the CSII catheters. While the insertion channel in the tissue remained intact in the original shape of the Teflon catheter, the cylindrical void was disrupted and distorted by the steel catheter.

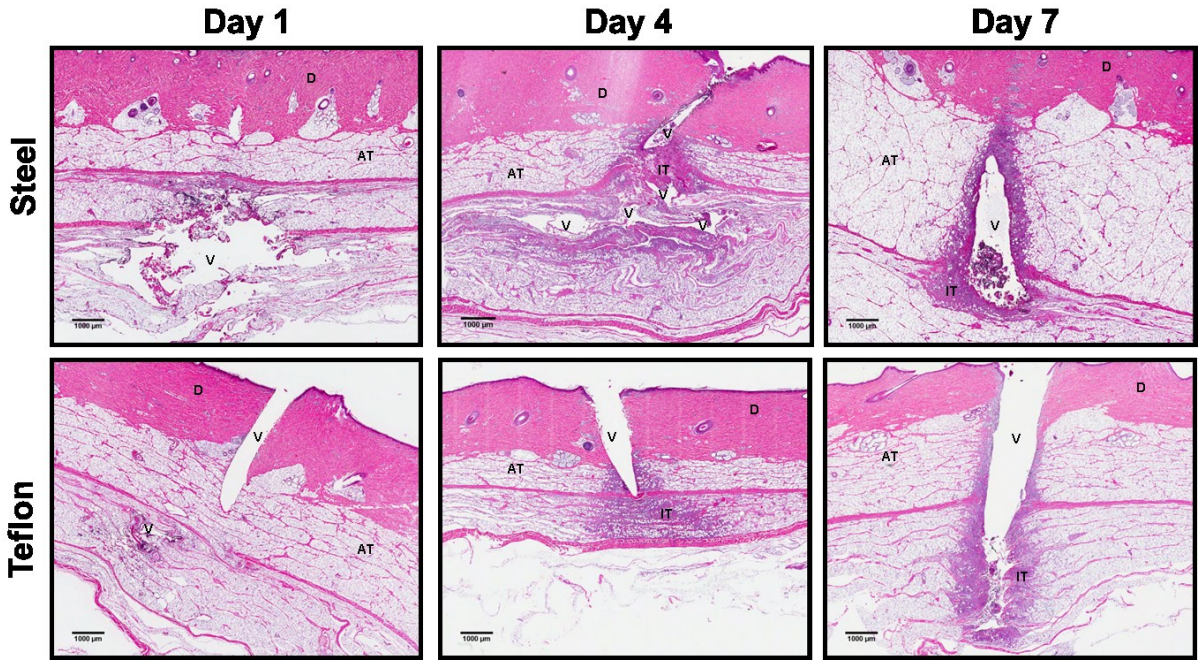

Figure 30: Representative H&E slides of tissue surrounding steel (top row) and Teflon (bottom row) cannulas. The void (V) left by the cannula is distorted around the steel tip but follows the cylindrical shape of Teflon catheters. Inflamed tissue (IT) is characterized by dark purple inflammatory cells and collagen that form a layer along the void. Healthy adipose tissue (AT) and the dermis (D) are indicated.

There was a trend towards larger areas of inflammation around steel catheters ($p = 0.14$) on day 4, characterized by inflammatory cells, fresh collagen and fibrin/red blood cells. All of these formed a layer along the catheter shaft. Interestingly, on day 7 of wear-time the areas around both materials were similar in size. For the remaining histopathological characteristics the same phenomenon could be observed – no differences on day 1 and 7 of wear time, but statistically significant or slight differences on day 4 of wear time (Figure 31). Steel, for example, caused substantially more bleeding, indicated by a 77 % larger area of

fibrin deposition on day 4 compared to Teflon ($p < 0.05$). Overall, fat necrosis was 12 % and inflammation distance 8 % increased around steel catheters. The lowest point of inflamed tissue was observed at 7.6 mm, in average, below epidermis on day 4 for steel while only at 6 mm for Teflon ($p < 0.05$).

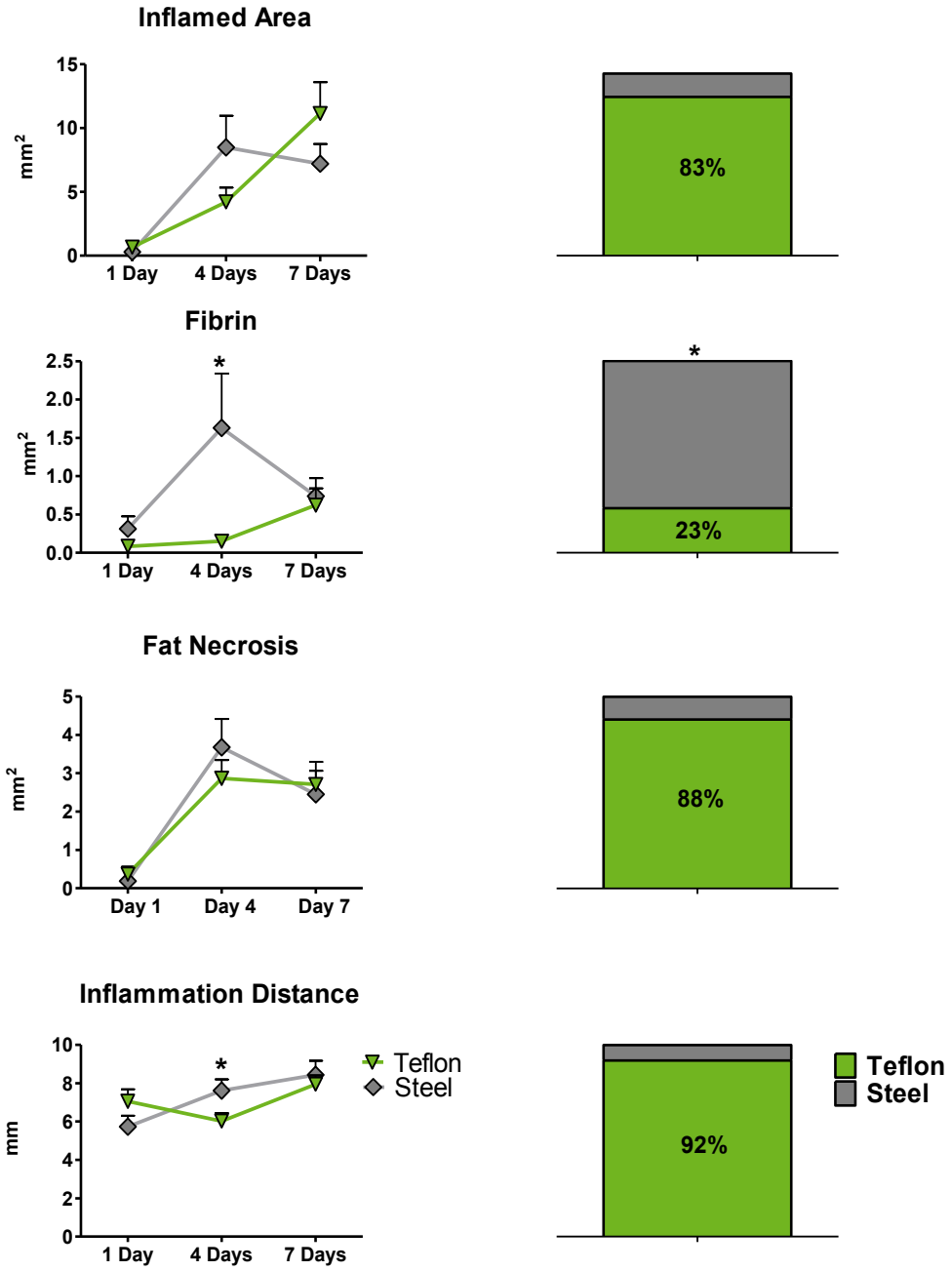

Figure 31: Trend curves over 8 days of wear-time and respective areas under the curve. All AUC values were normalized to Sure-T catheters, considering trauma caused by steel equals maximum trauma (100 %). (*$p < 0.05$; unpaired t-test for normally distributed data or Mann Whitney U test for non-normally distributed data)

The grading by the pathologist regarding the density of inflammatory cells (*none, some, mild, moderate, severe*) around the insertion channel of steel and Teflon cannulas exhibited statistically significant differences in most cases (Figure 32). Again, the difference was more pronounced on day 4 compared to shorter or longer wear-times. Neutrophil cell density was higher around steel over the first 4 days ($p < 0.0001$) but similar around materials on day 7 of wear-time. Over the first 4 days of wear-time, mononuclear cell infiltrate (including lymphocytes, neutrophils, monocytes and macrophages) was significantly denser around steel CSII catheters than Teflon. Interestingly, this was reversed on day 7 with more Teflon samples graded *moderate* or *severe*.

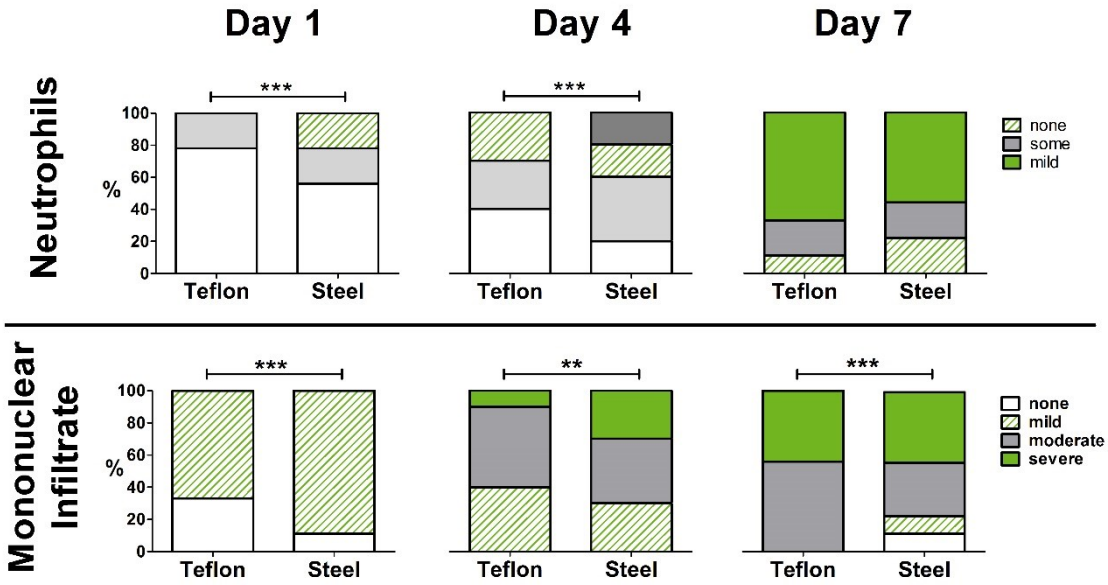

Figure 32: Qualitative grading regarding the density of inflammatory cells around the insertion channel. Top row: neutrophils; bottom row: mononuclear infiltrate (lymphocytes, monocytes, macrophages, neutrophils). (**$p < 0.001$; ***$p < 0.0001$; Chi-square test)

4.2.4 INFLAMMATORY GENE EXPRESSION ANALYSIS

There was a significant increase in gene expression of macrophage marker CD68 between day 1 (almost no increase in expression) and day 7 of wear-time of a Teflon catheter (1.7 ± 0.9-fold vs. 7.2 ± 5.6-fold, $p < 0.05$) and a steel catheter (1.4 ± 1.2-fold vs. 5.2 ± 3.4-fold, $p < 0.005$). IL-6 expression increased substantially within 24 hours of catheter insertion and continuously decreased after. IL-6 gene expression was higher around steel on days 4 and 7 compared to Teflon ($p < 0.05$ and $p = 0.058$, respectively). Although not statistically significant, a trend towards higher IL-8 mRNA levels could be observed on days 1 and 7 of wear-time. TNF-α gene expression was similar between materials over 7 days while TGF-β levels significantly increased over 7 days of wear time around Teflon (2.1 ± 0.3-fold versus 4.7 ± 1-fold, $p < 0.05$). There was a high variability in TGF-β gene expression around steel on day 4 with values ranging from 0.9-fold to 49.7-fold among samples (mean 10.2 ± 5.0-fold). TGF-β mRNA levels in adipose tissue around Teflon on day 4 were more consistent among samples and in average lower than around steel 2.1 ± 0.8-fold, n.s.). A fourfold increase in anti-inflammatory IL-10 gene expression was detected after 1 day of catheter wear-time. Expression remained at this level around both materials throughout wear-time. Mean gene expression changes are shown in Figure 33.

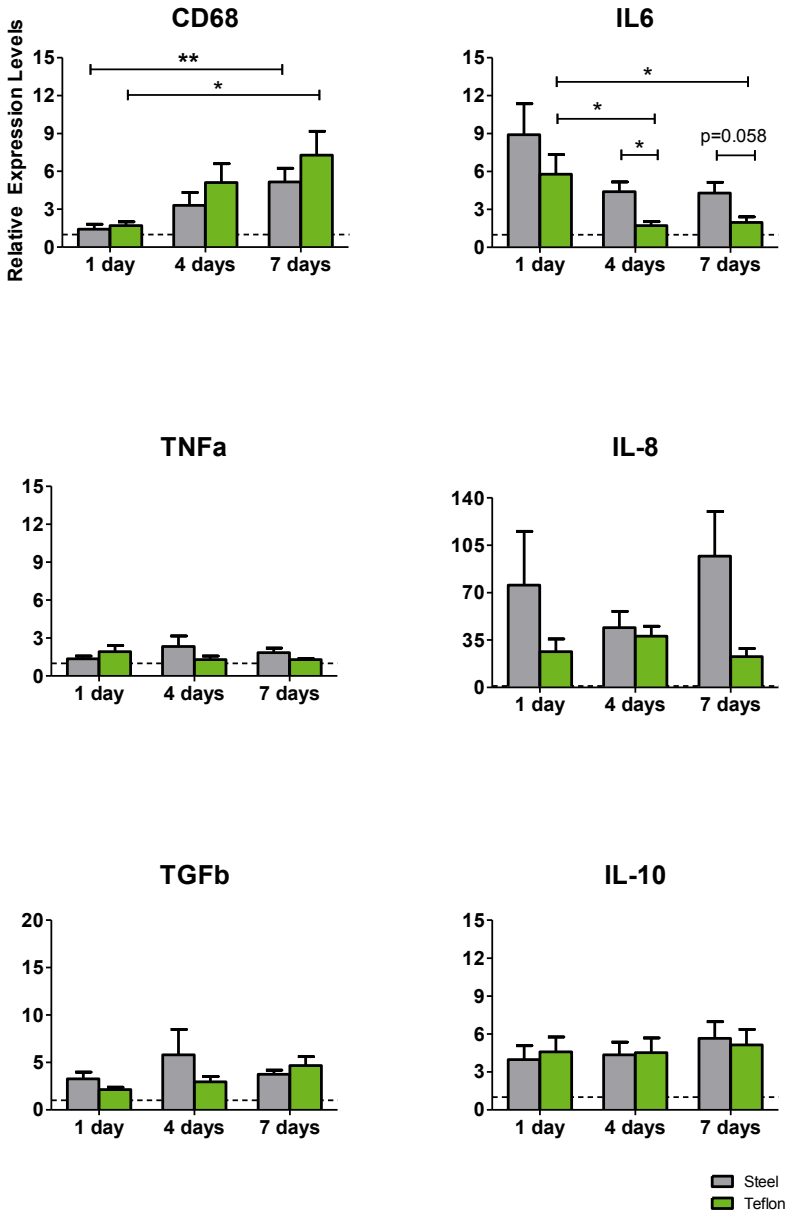

Figure 33: Relative changes in gene expression around steel and Teflon CSII catheters over 7 days. (*p < 0.05, **p < 0.001; Student's t test for normally distributed or Man Whitney U test for non-normally distributed data)

5. DISCUSSION

5.1 STUDY I: IN-DEPTH ANALYSIS OF THE PHARMACOKINETICS (PK) OF LISPRO INSULIN AND THE TISSUE RESPONSE TO CSII CATHETERS (SWINE MODEL, TJU)

This study aimed to assess insulin absorption variability and correlating changes in tissue morphology in a swine model. Two catheters of distinct materials and shapes were studied: a Teflon catheter with 9 mm cannula length (90° insertion angle) and an experimental design consisting of a flexible 9 mm long metal needle with a very sharp tip (approx. 60-degree insertion angle). The resulting pharmacokinetics (PK) and tissue histology were significantly different between catheter types.

The recommended frequency of changing the infusion set is based on the observation that insulin absorption becomes more inconsistent with increasing wear-time [94, 95]. Tight glucose control becomes difficult on days 2-3 after CSII catheter insertion and extended wear-time can lead to infections of the insertion site [26, 37, 96, 97]. In this swine study, the relationship between tissue inflammation, methylene blue dye leakage and the pharmacokinetics of a rapid acting insulin bolus were systematically assessed and analyzed. The acute inflammatory response caused by the introduction and maintenance of a CSII catheter may help understand why insulin fails to be properly absorbed into the surrounding subcutaneous tissue.

5.1.1 INSULIN ABSORPTION VARIABILITY

In this animal study, variability of insulin PK could be observed on all study days, i.e. 1, 3 and 5 days after catheter insertion. Similar variability was observed in other studies and is commonly seen in routine clinical care [25, 26, 98, 99]. The least variability was observed on day 5 of commercial catheter wear-time, a time point seldom reached by patients. Day 5 moreover showed highest C_{max} and AUC60. Currently patients are advised to not wear a CSII set until day 5, which is when insulin absorption may recover if absorption was low on day 3. The day 5

observations are of interest, as current recommendations do not recommend the patient to wear a CSII set until day 5, when insulin absorption may recover. Studies have shown that some patients indeed successfully wear CSII catheters up to 7 days [37, 100]. In contrast, insulin infused through the experimental catheters was absorbed best on day 1 (highest AUC, AUC60, and C_{max}) and fastest on day 3 (t_{max}) of wear-time. The intra- and inter-subject absorption variability was consistently higher for insulin infused through the experimental catheter. Of 36 PK studies, 10 resulted in limited or delayed insulin absorption. Three of the experiments with low absorption on day 5 resulted in pump occlusion alarms and/or leaked dye into the hub of the experimental catheter. The decreased uptake of insulin when administered through the IC may primarily be explained by issues in the connector between catheter and tubing. Methylene blue dye often accumulated in the hub indicating a technical obstruction of insulin flow.

5.1.2 TISSUE TRAUMA

Tissue sections along the insertion channel revealed the extent to which subcutaneous adipose tissue was traumatized by insulin infusion systems. Collagen fibers (light and dark blue in Trichrome stains) were pushed downward and compressed, due to friction between the catheter wall and tissue. Damage to arterioles, capillaries, and venules lead to the formation of a fibrous wall around the catheter shaft. Thrombus, compressed connective tissue, and inflammatory cells that surrounded the catheter shaft may inhibit the diffusion of insulin into the adjacent vascular adipose connective tissue. This continuous or near-continuous layer was observed in many of the tissue specimens analyzed by a surgical pathologist, while others had a discontinuous layer with healthy adipose tissue in the immediate vicinity of the CSII catheter. The tissue debris field adjacent to the catheter shaft lacked functioning capillaries and lymphatic vessels, responsible for the uptake of insulin. In some cases, a bolus infusion of insulin or blue dye migrated upward and stained the skin surface and the CSII catheter adhesive, despite no occlusion alarm from the insulin pump. Methylene blue dye leakage was observed in 3/6 PK experiments with catheter N, all of which showed very little or impaired absorption manifesting in a much lower AUC level than in the other 3 experiments (Figure 17). In these 3 cases, reticular fiber disruption, fibrin

deposition in reservoir and fat necrosis were categorized as moderate or severe by the clinical pathologist, hence suggesting a severely inflamed and disrupted environment. Compared with the tissue response to the experimental catheter, tissue surrounding the commercial catheter had a more regular topography of connective tissue planes, more regular reservoir geometry, a smaller debris field, less reticular fiber disruption, less fat necrosis, and less hemorrhage within the reservoir. Irregular reservoir geometry and irregular topography of tissue planes could be attributed to catheter shape and the forceful manual insertion method. The shape of the IC possibly contributed substantially to the extent of trauma due to its sharp tip which may have continuously disrupted tissue in the vicinity. Round, soft shapes are known to be better tolerated that sharp edges [101, 102]. In general, the Ns produced a similar, yet more pronounced, tissue response independent of infusion type. Interestingly, tissue that was perfused with insulin exhibited significantly more fibrin deposition. It has been postulated by Kraegen and Chisholm that insulin itself could promote fibrin deposition by inhibiting fibrinolysis [103].

5.1.3 FACTORS INFLUENCING PHARMACOKINETICS

The data presented here suggest a faster absorption of insulin at a higher maximum concentration peak on day 5, however, with a higher variability. In average C_{max} values were higher for insulin administration through catheter N than catheter C which could be explained by a higher incidence of hemorrhage and thus a faster flux of insulin into the vasculature due to the rupture of capillaries. There are various factors that lead to different metabolic responses after repeated administration of the same insulin dose. Blood and lymph flow in the vicinity of the cannula are important as insulin is absorbed by capillaries and lymphatic vessels [2, 32, 104, 105]. However, similar insulin levels detected in the blood (pharmacokinetics) may have different BG lowering effects (pharmacodynamics) depending on insulin sensitivity of the cells which can vary from one time point to the other [2, 32]. Factors such as ambient temperature and exercise can have an effect on insulin absorption [39]. Insulin monomers and dimers are mainly absorbed by capillaries in the vicinity of the cannula but a small percentage is absorbed by lymph vessels [105–107]. When insulin is transported into local lymph

nodes it can be either absorbed by capillaries or degraded by proteolytic enzymes [104, 108, 109]. Furthermore, the acute inflammatory response and the infusion of insulin may directly increase local blood flow which may contribute to increased insulin uptake on day 5 of catheter wear-time [72, 97, 110–112]. Both lymph and blood flow as well as degradation within lymph nodes are influential factors for rapid or slow insulin absorption.

5.1.4 "LAYER" FORMATION

The infusion of insulin through an insulin pump leads to the production of a hydrostatic pressure differential between the cannula lumen and the adjacent subcutaneous adipose tissue. Insulin therefore, will choose the path of least resistance and flow along connective tissue planes or upward along the cannula shaft [113, 114]. Slow increases and abrupt decreases in insulin pump back pressure suggest that a bolus dose of insulin may accumulate within the layer of inflammatory tissue, distend the tissue, and then abruptly travel into adjacent tissue through a pathway with lower resistance [114]. It has been shown in micro CT experiments that when insulin first enters the tissue it distributes in a spherical pattern [115]. This pattern, however, can change with varying tissue morphology over the course of catheter-wear-time which in turn could affect absorption. Considering the layer of inflammatory cells, fresh collagen and thrombus observed in this study, insulin distribution may be delayed or even prevented due to accumulation of insulin within this layer.

5.1.5 IMPACT OF CATHETER MATERIAL AND SHAPE

Different materials and the inflammatory response by the tissue can influence insulin pharmacokinetics [37, 116]. The histopathological results show that the commercially available Teflon catheter causes less trauma due to a softer tip and a fast and well-established insertion method using an attached insertion device. The experimental metal catheter (N) with a pointy, sharp tip was not only difficult to insert but tissue response was also significantly more severe after a wear-time of 5 days. It is of interest, that the experimental catheter was made of a flexible

material but caused more trauma. Both manual and supported insertion is prone to insertion failure and the optimal insertion angle is not always reproducible.

5.1.6 LIMITATIONS

This study was limited by the small sample size and the difficulty controlling variables influencing insulin absorption, such as the activity level of the animal or ambient temperature. Blood glucose could not be clamped to determine pharmacodynamics as animals often received snacks to keep distress to a minimum. Localization of the insertion channel often proved difficult and histology did not always reveal a complete picture of tissue trauma. Insulin plasma concentrations were indirectly detected by subtracting swine insulin from total insulin content. This method adds to the overall variability and should be replaced by specific measurement of lispro insulin which was not available at the time. Unfortunately, this indirect calculation adds to the calculated intra- and inter-subject variability.

It has to be noted that inhaled anesthetics such as isoflurane have a major impact on glucose and insulin metabolism. The limitation of this study was the relatively short period of time that passed between general anesthesia on day 1 and the administration of the first insulin bolus. Inhaled isoflurane has been shown to slow down glucose clearance and increase the endogenous glucose production leading to hyperglycemia [117, 118]. Plasma glucose concentrations increase steadily over 2 hours after administration of the anesthetic [119, 120]. This major impact on glucose metabolism has not been properly taken into account in this study. Propofol would be an adequate alternative to isoflurane as it does not affect plasma glucose concentration [120].

Furthermore, the anti-inflammatory properties of heparin need to be considered. The CVC ports were flushed every 1-3 days with heparin solution in order to avoid blockage of the ports. Heparin influences wound healing processes as it mediates granulation tissue formation and fibrosis, and has been further shown to affect angiogenesis [121, 122]. Since this anti-inflammatory effect is systemic [123, 124], the inflammatory response observed in this study may have been hampered by heparin infusion. In future studies, CVC ports should be flushed with 0.9 % saline

solution which has proven to work just as effectively in preventing occlusions [125, 126].

Lastly, the aim of this study was to test the hypothesis whether insulin absorption variability over time correlates with the inflammatory tissue response. This was challenging to statistically evaluate due to the following limitations:

1. The relatively complex statistical procedures that would have had to be applied to test a correlation which would have not been robust enough in this small cohort.
2. The fact that the only histological data available are of day 5 of wear-time, leaving out the information needed for all other days. It is not possible to evaluate histology and PK in combination of the same catheter over wear-time, since the tissue can only be excised at the end of the study.

5.2 Study II: The Effect of Co-Infusion of Thrombolytic Agents and Application of Vibration on Insulin PK/PD and Tissue Histology (Canine Model, TJU)

The results of Study I revealed a layer of inflamed tissue and thrombus around the insertion channel which may function as a mechanical barrier for the distribution of insulin into the tissue and surrounding vasculature. The aim of this canine study was to assess the effect of thrombolytic agents, i.e. drugs that break up and dissolve blood clots, and are used as emergency therapy for stroke and heart attack.

5.2.1 Insulin Absorption

Assuming that insulin administered intravenously is 100 % available to the organism, insulin pump therapy has to account for the fact that only about 60 % of subcutaneously administered insulin reaches the circulation [105, 127, 128]. In this study, bioavailability of insulin ranged from 8 % on day 7 in one dog to 200 % on day 6 in another. Although the area under the curve was larger in some instances compared to the IV PK experiment, a closer look at the individual insulin concentration curves (Appendix Figure 38 and Figure 39) shows that onset of IV insulin was much faster with much higher C_{max} values. In average, bioavailability was 34 % on day 1, 64 % on day 2, 70 % on day 6 and 41 % on day 7 of subcutaneous insulin administration.

The rate of insulin absorption is influenced by external factors such as heat and exercise, but also injection depth, blood flow, injection volume and dispersion play a role [103, 115, 129–131]. Insulin monomeric molecules have a natural tendency to form hydrogen-bond dimers in solution. When zinc ions are present, insulin dimers associate into hexamers with a molecular weight of approximately 35 kDa [132]. Macromolecules larger than 20 kDa may be taken up faster by the peripheral lymphatics than the vasculature. According to literature, the absorption into the lymphatics of subcutaneously injected drugs is greater than 50 % [106, 133].

Rapid-acting insulin analogues, such as lispro and aspart, are genetically modified so that their tendency for self-association into hexamers is reduced, thus

increasing the velocity of uptake into the blood stream [104, 134, 135]. Rapid-acting insulins still have a delayed absorption of approximately half an hour. Insulin absorption in dogs was in general slower than in human models, where the average t_{max} of lispro is 40 minutes on the day of catheter insertion [131, 136, 137]. In the animals t_{max} was 77.7 ± 52.9 minutes on day 1 of subcutaneous bolus administration. Interestingly, t_{max} decreased over wear time to 37.0 ± 23.1 minutes ($p > 0.05$, n.s.). Other groups saw this same effect on t_{max} (decreased) and C_{max} (increased) when testing the influence of CSII catheter wear time on insulin pharmacokinetics [30, 138, 139]. In addition, in the canine study presented here, a significant increase in AUC and AUC60 on days 3 and 6 compared to day 1 was observed. A study by Olsson *et al*. [140], however, contradicted previous studies by claiming unchanged pharmacokinetics over 5 days of wear-time. They speculated that the immediate administration of an insulin bolus after CSII catheter insertion was the reason for delayed insulin absorption. The same could be true for this study. The previously administered anesthesia as well as the short period between insulin catheter insertion and bolus administration could have a hampering effect on insulin pharmacokinetics.

The administration of thrombolytic agents did not have any effect on the insulin absorption into the circulation. In contrast, other approaches of co-administration of absorption enhancing agents (i.e. hyaluronic acid) have been proposed and have successfully accelerated insulin absorption into the circulation [137].

5.2.2 PHARMACODYNAMICS

Glucose requirements were significantly increased on day 3 and day 6 of catheter wear-time compared to day 1 and day 7. Of interest, variability (expressed as SEM) increased over 7 days and was highest on day 6 of wear-time (Figure 21). In a 2009 study by Swan *et al.* [97] the AUC_{GIR} was unchanged over 4 days of wear-time, again indicating that the previously administered anesthesia influenced insulin pharmacokinetics in dogs on day 1.

All IV and SC experiments had a similar AUC_{GIR} but time to maximum glucose infusion rate ($t_{max(GIR)}$) was significantly shorter in IV experiments. This is concordant with a shorter t_{max} in insulin appearance in the plasma when administered IV. $t_{max(GIR)}$ was in average 53 minutes shorter on days 3 (n.s.), 6 (n.s.) and 7 ($p < 0.05$) of wear-time compared to day 1 (119.6 ± 38.4 min).

The subjects that had vibration applied to the CSII catheter before/during/after bolus administration required in average 3 mg/kg/min more dextrose on day 3 (n.s. due to small sample size in vibration group), while requirements were similar on other days. This indicates a faster and better insulin absorption into the circulation due to the disruption of the tissue in the vicinity of the catheter which may have facilitated insulin flow through the interstitial fluid. In order to confirm these findings, the sample size of the vibration group would have to be increased. The following chapter discusses drawbacks of applied vibration in terms of tissue trauma.

5.2.3 TISSUE TRAUMA

Similar to previous results, the CSII catheters inserted and maintained for 7 days caused significant damage to the cells, connective tissue, capillaries, and lymph vessels. All of the specimens had a layer of inflammatory tissue that surrounded the CSII cannula. This layer varied in thickness, density, and continuity. Mechanical vibration tended to disrupt this layer of inflammatory tissue, but had a greater area/volume of damaged subcutaneous tissue. Methylene blue dye did not migrate to the skin surface in any of the CSII catheters. Unfortunately, this study resulted in very limited histology that could not be adequately analyzed. This presents a major limitation in the results.

5.2.4 LIMITATIONS

The main weakness of this pilot study was the small total sample size (n = 13) and the small group sizes (5 control animals, 4 in the tPA group, 4 in the streptokinase group, 2 in the vibration group). There was still a high degree of variability between trials in the same subject and between subjects. One of the biggest variables encountered in this study was the tissue surrounding the site of catheter insertion. Unlike both swine and human tissue, there was skeletal muscle and mammary gland tissue at the site of insertion. Not only does this not represent a similar tissue site for human clinical use, the damage to these additional types of tissue may have caused irregular responses compared to subcutaneous tissue only.

An adult large canine model was used for this study because of previous difficulties obtaining frequent blood samples from the ambulatory large swine for more than 5 days. Though the canines proved easier to work with and obtain viable samples from, the lack of subcutaneous tissue and presence of skeletal muscle and mammary gland tissue may designate them as a poor choice for subject testing.

Furthermore, the attachment and maintenance of CSII catheter adhesives and Tegaderm™ was almost impossible in this animal model. Due to the dense fur that grew back quickly after shaving, none of the adhesives would stick leading to a drop out of 2 of the 5 control animals for further analysis because of catheter loss. The pigmentation of fur and tissue below, made localization of the insertion channel impossible in many cases. An advantage of the swine model is the pink, unpigmented skin that allows easy localization of the trauma.

The first PK/PD study was performed the same day as the CSII catheter was inserted. Most subjects had a blunted response on Day 1 and this may have been due to the residual effects of general anesthesia. Future studies should allow for longer period of time between insertion and the first PK/PD study. The impact of isoflurane on glucose metabolism is discussed briefly in section 5.6.1.

5.3 Study III: Comparison of the Inflammatory Response to Steel and Teflon CSII Catheters Using Histopathology and Quantitative Real-Time PCR (Swine Model, MedUni Graz)

Study I showed that the inflammatory response was different when catheter material was plastic or metal, stiff or flexible and had a sharp tip or not. Therefore, in this pilot swine study the inflammatory response of the adipose tissue to the 2 most commonly used CSII catheter materials was systematically assessed over a wear-time of 1 day, 4 days, and 7 days.

5.3.1 Histopathology

The steel cannula of the Sure-t catheter was not only much stiffer than the Teflon cannula of the Quick-set, it also had a sharp tip to facilitate manual catheter insertion. While the introducer needle of the Teflon catheter had a sharp tip as well, it was immediately removed after insertion, only leaving a blunt flexible cannula in the tissue. The stiffness and sharp tip of the steel cannula continuously ruptured connective tissue and microvasculature, resulting in significantly higher fibrin deposition after 4 days of wear-time. Mononuclear immune cell density (neutrophils, monocytes, macrophages) was significantly more pronounced after 1 day and after 4 days of wear-time around steel. On day 7 of wear-time, the mononuclear infiltrate around Teflon cannulas was more often graded *moderate* or *severe* compared to steel. Published results on the recruitment of inflammatory cells are often contradicting and not always easy to interpret [141, 142]. While Hallab et al. claim a five-fold increase in adhesion strength of macrophages to steel surfaces compared to Teflon [142], Bussutil et al. showed significantly less macrophage and neutrophil adhesion to intraperitoneally implanted steel disks [141]. Cells that adhere to a material, are not automatically activated, making interpretation of data even more difficult [143].

5.3.2 Gene Expression of Inflammatory Markers

The activation of the immune system depends on the release of pro-inflammatory cytokines, such as IL-6, IL-8 and TNF-α by macrophages and other cells adherent to the cannula [74, 144]. IL-6 gene expression levels increased approximately 10-

fold within the first day and were significantly higher around steel cannulas than around Teflon cannulas on days 4 and 7. By day 4, IL-6 levels around Teflon returned to non-traumatized tissue levels. IL-6 is known to be associated with reepithelization and scarring [145]. The continuous tissue disruption caused by the sharp tip of the steel needle could possibly be the reason for continuously elevated IL-6 levels around steel. In concordance with literature [146], the expression of the major chemotactic factor IL-8/CXCL8 is highly elevated after 1 day of wear-time, with a trend towards higher levels around steel. Impaired wound healing due to a foreign body can lead to continuously elevated IL-8 levels [147]. In fact, IL-8 gene expression was 100-fold elevated compared to control tissue on day 7 of wearing a steel catheter and 23-fold higher around Teflon (n.s.).

When tissue is injured, TNF-α production is immediately upregulated to activate phagocytosis [73]. Expression levels were rather low around both steel and Teflon samples (approximately 2-fold) compared with results of a study by Pachler *et al*. The group showed a 25-fold increase in TNF-α protein levels within 8 hours after inserting a Teflon open-flow microperfusion probe subcutaneously [116]. There was no difference in expression between steel and Teflon.

In the course of wound healing, macrophages undergo a phenotype switch from M1 to M2 macrophages and start releasing anti-inflammatory IL-10 and TGF-β [144, 148]. TGF-β is responsible for the reconstruction of tissue and scarring [144]. Its release activates fibroblasts which in turn start to synthesize collagen to lay down new extracellular matrix [144]. Within 1 day of wear-time, TGF-β gene expression is upregulated and steadily increase over 7 days around Teflon ($p > 0.05$). TGF-β levels around steel peak on day 4 of wear time and decrease to levels similar to Teflon by day 7. When a foreign body is present, there is a constant release of reactive oxygen species and degradative enzymes and IL-10 cannot act out its full potential as an anti-inflammatory cytokine [149]. This explains the consistently high level of IL-10 gene expression around both steel and Teflon cannulas.

5.3.3 Impact of Catheter Material and Shape

The 2 catheters used in this study did not only differ in material but also in shape. The Teflon cannula had a larger inner diameter and thicker walls than the steel cannula (29 versus 25 gauge). It has been shown that the shape of the material influences the inflammatory response, i.e. macrophage attachment, suggesting that round shapes elicit a less severe response than shapes with sharp edges [101, 102]. Even though the Teflon cannula was thicker, the elicited inflammatory response was less severe than that of steel. Rounded, flexible and larger objects indeed are better tolerated by the immune system than sharp edges and smaller objects [150]. The stiff steel catheter may have continuously activated the immune response by destroying connective tissue structures by sheer force. Stiffness is another factor known to play a role in material tolerability [151].

Overall, the results of Study III suggest better tolerability of flexible Teflon cannulas with a blunt end over longer periods of wear time. The sharp tip of the stiff steel cannula continuously ruptures connective tissue structures and blood vessels in the vicinity of the insertion channel. The inflammatory response to a foreign body progresses more slowly around Teflon than steel indicating that Teflon is more suitable for longer wear-times.

5.3.4 Limitations

Unfortunately, this study did not allow for continuous insulin infusion since the animals was at high risk of hypoglycemia when multiple catheters are infused. The effect of insulin on the tissue response is not yet fully understood and has only been studied over a couple of hours after catheter insertion [116, 152].

2 Teflon and 2 steel cannulas kinked during our study but neither the infusion of saline not methylene blue dye produced a pump occlusion alarm. Reasons for kinking of the steel cannula could be the considerable amount of force needed to insert the cannula through the medical adhesive and/or the rather rigid swine skin. Unfortunately, there is no way of testing for catheter kinking post insertion.

6. SUMMARY AND OUTLOOK

6.1 AN ADEQUATE MODEL FOR HUMAN SKIN AND ADIPOSE TISSUE

In general, medical research makes use of rodent models as they are low in cost, small in size and thus easy to handle [153]. However, rodents heal through wound-contractions as opposed to reepithelization and their epidermal layer is much thinner than that of humans [153, 154]. This lack of immune contribution to wound healing and the significant difference of the innate and adaptive immune system between rodents and humans adds to the list of reasons, why rodents are not an adequate model for human inflammation of the skin and adipose tissue [154–156].

Although a canine model was used for Study II of this thesis, it has to be mentioned here that the model may not be adequate for human wound healing. The epidermis of dogs is much thinner than that of humans and pigs (10 – 45 µm versus 50 – 120 µm and 70 – 140 µm, respectively) [157, 158]. Canines have a thick fur with 100 – 600 groups of 2 – 15 hairs per cm^2. Holocrine sebaceous glands are arranged in groups around the follicles that are extremely well supplied with blood vessels which is not the case in humans and pigs. This fur is shed seasonally in canine while human continuously shed hair throughout the year [157].

While in swine the lipid layer of the skin is similar in composition to that of humans, it is different in dogs. Lipids of porcine and human skin are composed of triglycerides and free fatty acids while in dogs the lipid layer is made up of cholesterol, wax diesters and cholesteryl esters [157, 159]. The skin itself slides loosely over subcutaneous fascia while in porcine and human skin it is adherent to the underlying structures [154].

The main reason for using dogs in Study II was that these animals are relatively easy to handle. They adapt to the humans in their vicinity and are more cooperative than swine. The veins on the front and hind legs made blood sampling and IV administration of glucose fairly easy. However, due to the difference in (epi-) dermal and subdermal structure and the fact that pigmentation of canine skin

made preparation for histological analysis almost impossible, this animal model seems inadequate for human inflammatory tissue response.

A review by Sullivan and colleagues [158] concluded that porcine studies show a 78 % concordance with human wound healing studies. Rodent and in vitro studies were only 53 % and 57 % concordant with wound healing studies in men, respectively [158]. Pig skin has similar dermal collagen (similar biochemical structure), similar size and distribution of dermal blood vessels and a similar epidermal turn over time as humans [154, 157, 158]. They close wounds through reepithelization and the immune cells in the skin are similar to man [154, 157, 158]. In contrast to humans, however, porcine skin has no eccrine sweat glands, which are limited to the snout and lips of the animal [153, 154, 157, 158].

The pig model is limited by its high cost and the fact that its large size makes it rather difficult to handle. The administration of IV drugs requires surgery for the insertion of infusaports and therefore a skilled veterinarian. Lastly, for subsequent analysis such as immunohistochemical staining, porcine antibodies are difficult to come by.

In conclusion, densely-haired animals such as the dog show morphological and functional characteristics which severely limit the comparison of wound healing with men. The porcine model is the most adequate for human skin and adipose tissue wound healing.

6.2 HUMAN STUDIES

Human studies have been proposed but still raise ethical and methodological issues. Currently the only way to acquire large amounts of human tissue is from patients undergoing elective plastic surgery in which a large pannus of skin and adipose tissue is removed (abdominoplasty). In a small pilot study, 3 patients were recruited and Teflon CSII catheters (9 mm) inserted 4 days, 3 days, 2 days and 2 hours prior to surgery. The patients experienced no additional scarring except scars caused by the surgery itself. The skin flap was grossed and tissue either stained with H&E and Trichrome or mRNA isolated for qPCR. This model is ideal for the analysis of the inflammatory response to a CSII catheter over time but it does not allow for simultaneous insulin infusion since patients recruited are not

necessarily insulin dependent. Recruitment is difficult as the small risk of infection keeps patients from participating as they do not want to risk their scheduled surgery. Figure 34 shows skin and adipose tissue stained with H&E of a human, a swine and a dog.

Figure **35** is a comparison of qPCR results between swine and human tissue. Although the time points are different, the trends of gene expression are comparable.

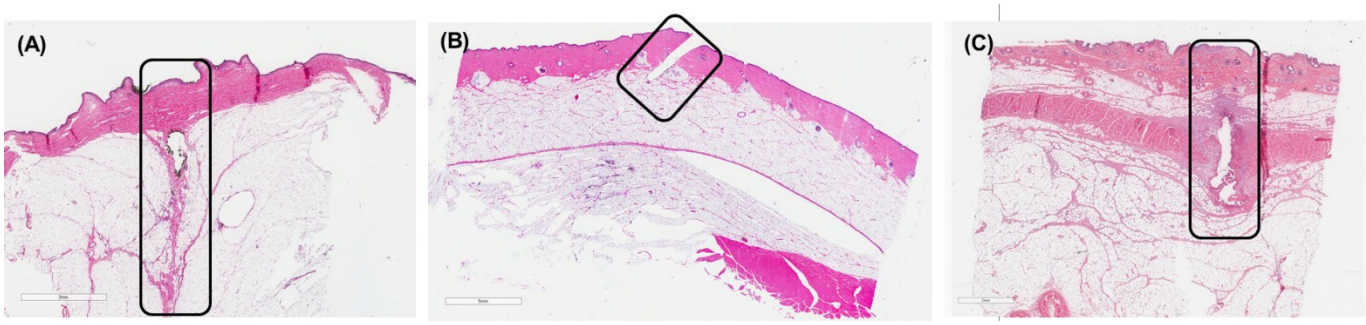

Figure 34: Side by side comparison of skin and adipose tissue stained with H&E. The area of catheter insertion is marked by a rectangle. **(A)** Human skin; **(B)** swine skin; **(C)** dog skin.

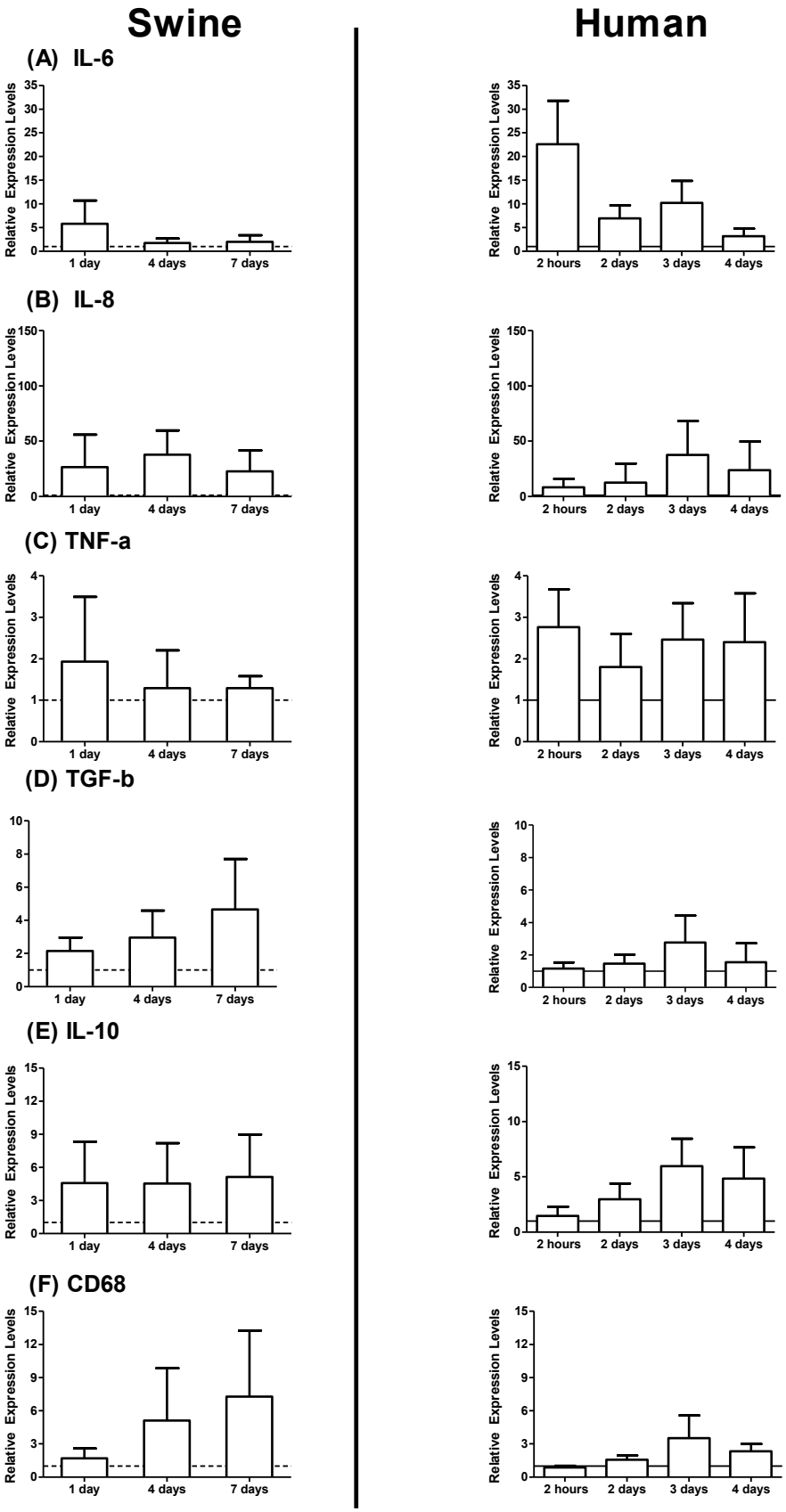

Figure 35: Side by side comparison of swine and human gene expression data over wear time.

6.3 CONCLUSION

Several *in vivo* study designs to assess the underlying mechanisms for failed/impaired insulin absorption have been proposed in this thesis. A combination of PK/PD, histopathology and gene expression analysis is a strong tool to help define specific targets for the development of improved catheters. These improvements may be realized in the form of new anti-inflammatory coatings, softer materials and smooth catheter tips. The studies presented here suggest that the swine is a more adequate model for human wound healing than the dog due to skin structure, hair follicle density and skin pigmentation. Nonetheless, special efforts should be made to develop an optimal, minimally invasive protocol for the study of the impact of insulin infusion systems in a human *in vivo* model.

7. REFERENCES

1. Pickup JC, Keen H, Parsons JA, Alberti KG (1978) Continuous subcutaneous insulin infusion: an approach to achieving normoglycaemia. Br Med J 1:204–7.

2. Pickup JC, Williams G (1997) Textbook of Diabetes, 2nd ed. Blackwell Science

3. Slama G, Hautecouverture M, Assan R, Tchobroutsky G (1974) One to five days of continuous intravenous insulin infusion on seven diabetic patients. Diabetes 23:732–8. doi: 10.2337/diab.23.9.732

4. Williams G, Pickup JC, Keen H (1985) Continuous intravenous insulin infusion in the management of brittle diabetes: Etiologic and therapeutic implications. Diabetes Care 8:21–26. doi: 10.2337/diacare.8.1.21

5. Pickup J (2014) History and use of CSII. Diapedia. doi: 10.14496/dia.8104974815.5

6. Skyler JS (2010) Continuous Subcutaneous Insulin Infusion-an Historical Perspective. Diabetes Technol Ther 12 Suppl 1:S5–9. doi: 10.1089/dia.2010.0068

7. M. James Lenhard GDR (2001) Continuous Subcutaneous Insulin Infusion. Arch Intern Med 161:2293–2300.

8. Kovatchev BP, Renard E, Cobelli C, et al (2014) Safety of outpatient closed-loop control: first randomized crossover trials of a wearable artificial pancreas. Diabetes Care 37:1789–96. doi: 10.2337/dc13-2076

9. Schaeffer NE (2013) Human factors research applied: the development of a personal touch screen insulin pump and users' perceptions of actual use. Diabetes Technol Ther 15:845–54. doi: 10.1089/dia.2013.0098

10. Srinivasan A, Lee JB, Dassau E, Doyle FJ (2014) Novel Insulin Delivery Profiles for Mixed Meals for Sensor-Augmented Pump and Closed-Loop Artificial Pancreas Therapy for Type 1 Diabetes Mellitus. J Diabetes Sci Technol 8:957–68. doi: 10.1177/1932296814543660

11. Cobelli C, Renard E, Kovatchev B (2011) Artificial pancreas: Past, present, future. Diabetes 60:2672–2682. doi: 10.2337/db11-0654

12. Haidar A (2013) The future of care for type 1 diabetes. CMAJ 185:285–6. doi: 10.1503/cmaj.130011

13. Ang KH, Tamborlane W V, Weinzimer SA (2015) Combining glucose monitoring

and insulin delivery into a single device: current progress and ongoing challenges of the artificial pancreas. Expert Opin Drug Deliv 12:1579–1582. doi: http://dx.doi.org/10.1517/17425247.2015.1074174

14. Russell SJ (2016) Progress of artificial pancreas devices toward clinical use: the first outpatient studies. Curr Opin Endocrinol Diabetes Obes 22:106–111. doi: 10.1097/MED.0000000000000142.Progress

15. DCCT (1995) Effect of intensive diabetes management on macrovascular events and risk factors in the diabetes control and complications trial. Am J Cardiol 75:894–903. doi: 10.1016/S0002-9149(99)80683-3

16. Tang Fui SN, Pickup JC, Bending JJ, et al (1986) Hypoglycemia and counterregulation in insulin-dependent diabetic patients: a comparison of continuous subcutaneous insulin infusion and conventional insulin therapy. Diabetes Care 9:221–227.

17. Dahl-Jørgensen K, Brinchmann-Hansen O, Hanssen KF, et al (1986) Effect of near normoglycaemia for two years on progression of early diabetic retinopathy, nephropathy, and neuropathy: the Oslo study. Br Med J (Clin Res Ed) 293:1195–9.

18. Bending JJ, Pickup JC, Keen H (1985) Frequency of diabetic ketoacidosis and hypoglycemic coma during treatment with continuous subcutaneous insulin infusion. Audit of medical care. Am J Med 79:685–91.

19. Boland EA, Grey M, Oesterle A, et al (1999) Continuous subcutaneous insulin infusion. A new way to lower risk of severe hypoglycemia, improve metabolic control, and enhance coping in adolescents with type 1 diabetes. Diabetes Care 22:

20. Bode BW, Steed RD, Davidson PC (1996) Reduction in Severe Hypoglycemia With Long-Term Continuous Subcutaneous Insulin Infusion in Type I Diabetes. Diabetes Care 19:324–327.

21. Pickup JC, Mattock M, Kerry S (2002) Glycaemic control with continuous subcutaneous insulin infusion compared with intensive insulin injections in patients with type 1 diabetes: meta-analysis of randomised controlled trials. Br Medica J 324:705–711.

22. Jeitler K, Horvath K, Berghold A, et al (2008) Continuous subcutaneous insulin infusion versus multiple daily insulin injections in patients with diabetes mellitus: systematic review and meta-analysis. Diabetologia 51:941–951. doi: 10.1007/s00125-008-0974-3

23. Golden, Sherita Hill, Sapir T (2012) Methods for Insulin Delivery and Glucose Monitoring in Diabetes: Summary of a Comparative Effectiveness Review. J Manag Care Pharm 18:1–20.

24. Heinemann L, Fleming GA, Petrie JR, et al (2015) Insulin Pump Risks and Benefits: A Clinical Appraisal of Pump Safety Standards, Adverse Event Reporting, and Research Needs. Diabetes Care 38:dc150168. doi: 10.2337/dc15-0168

25. Heinemann L, Krinelke L (2012) Insulin infusion set: the Achilles heel of continuous subcutaneous insulin infusion. J Diabetes Sci Technol 6:954–964. doi: 10.1177/193229681200600429

26. Schmid V, Hohberg C, Borchert M, et al (2010) Pilot Study for Assessment of Optimal Frequency for Changing Catheters in Insulin Pump Therapy--Trouble Starts on Day 3. J Diabetes Sci Technol 4:976–982. doi: 10.1177/193229681000400429

27. van Bon AC, Bode BW, Sert-Langeron C, et al (2011) Insulin Glulisine Compared to Insulin Aspart and to Insulin Lispro Administered by Continuous Subcutaneous Insulin Infusion in Patients with Type 1 Diabetes: A Randomized Controlled Trial. Diabetes Technol Ther 13:607–614. doi: 10.1089/dia.2010.0224

28. Davies M (2004) The reality of glycaemic control in insulin treated diabetes: defining the clinical challenges. Int J Obes Relat Metab Disord 28 Suppl 2:S14–22. doi: 10.1038/sj.ijo.0802745

29. Linde B (1997) The pharmacokinetics of insulin. In: Pickup JC, Williams G (eds) Textb. Diabetes, 2nd ed. Blackwell Science, pp 32.1–32.14

30. Clausen TS, Kaastrup P, Stallknecht B (2009) Effect of insulin catheter wear-time on subcutaneous adipose tissue blood flow and insulin absorption in humans. Diabetes Technol Ther 11:575–580. doi: 10.1089/dia.2009.0058

31. Kerr D, Hoogma RPLM, Buhr A, et al (2010) Multicenter User Evaluation of ACCU-CHEK(R) Combo, an Integrated System for Continuous Subcutaneous Insulin Infusion. J Diabetes Sci Technol 4:1400–1407. doi: 10.1177/193229681000400615

32. Heinemann L (2002) Variability of insulin absorption and insulin action. Diabetes Technol Ther 4:673–82. doi: 10.1089/152091502320798312

33. McAulay V, Frier BM (2003) Insulin analogues and other developments in insulin therapy for diabetes. Expert Opin Pharmacother 4:1141–56. doi:

10.1517/14656566.4.7.1141

34. Lauritzen T, Faber OK, Binder C (1979) Variation of 125I-Insulin Absorption and Blood Glucose Concentration. Diabetologia 295:291–295.

35. Shetty G, Wolpert H (2010) Insulin pump use in adults with type 1 diabetes-practical issues. Diabetes Technol Ther 12 Suppl 1:S11–S16. doi: 10.1089/dia.2010.0002

36. Pfützner A, Sachsenheimer D, Grenningloh M, et al (2015) Using Insulin Infusion Sets in CSII for Longer Than the Recommended Usage Time Leads to a High Risk for Adverse Events: Results From a Prospective Randomized Crossover Study. J Diabetes Sci Technol 9:1292–8. doi: 10.1177/1932296815604438

37. Patel PJ, Benasi K, Ferrari G, et al (2013) Randomized Trial of Infusion Set Function: Steel Versus Teflon. Diabetes Technol Ther 16:1–5. doi: 10.1089/dia.2013.0119

38. Renard E, Boizel R (2014) Comments on Patel et al.'s "Randomized Trial of Infusion Set Function: Steel Versus Teflon": Early Catheter Failures May Differ According to Teflon Catheter Model. Diabetes Technol. Ther.

39. Binder C, Lauritzen T, Faber O, Pramming S (1984) Insulin Pharmacokinetics. Diabetes Care 7:188–199. doi: 10.2337/diacare.7.2.188

40. Deiss D, Adolfsson P, Zomeren MA, et al (2016) Insulin Infusion Set Use: European Perspectives and Recommendations. Diabetes Technol Ther. doi: 10.1089/dia.2016.07281.sf

41. Heinemann L (2016) Insulin Infusion Sets: A Critical Reappraisal. Diabetes Technol Ther 18:327–333. doi: 10.1089/dia.2016.0013

42. Facchinetti A, Sparacino G, Guerra S, et al (2012) Real-Time Improvement of Continuous Glucose Monitoring Accuracy: The smart sensor concept. Diabetes Care 36:793–800. doi: 10.2337/dc12-0736

43. Heinemann L, Walsh J, Roberts R (2014) We Need More Research and Better Designs for Insulin Infusion Sets. J Diabetes Sci Technol 8:199–202. doi: 10.1177/1932296814523882

44. Walsh J, Roberts R, Weber D, et al (2015) Insulin Pump and CGM Usage in the United States and Germany: Results of a Real-World Survey With 985 Subjects. J

Diabetes Sci Technol 9:1103–10. doi: 10.1177/1932296815588945

45. Reichert D, Weber D, Kaltenheuer M, et al (2013) Realität der Insulinpumpentherapie in Diabetesschwerpunktpraxen: Daten von 1142 Patienten aus 40 diabetologischen Schwerpunktpraxen. Diabetes Stoffwechsel Herz 22:367–375.

46. Pickup JC, Yemane N, Brackenridge A, Pender S (2014) Nonmetabolic complications of continuous subcutaneous insulin infusion: a patient survey. Diabetes Technol Ther 16:145–9. doi: 10.1089/dia.2013.0192

47. Liebner T, Holl R, Heidtmann B, et al (2010) Insulinpumpenkatheter – Komplikationen im Kindes- und Jugendalter. Diabetol und Stoffwechsel 5:P151. doi: 10.1055/s-0030-1253880

48. van Bon AC, Dragt D, DeVries JH (2012) Significant Time Until Catheter Occlusion Alerts in Currently Marketed Insulin Pumps at Two Basal Rates. Diabetes Technol Ther 14:447–448. doi: 10.1089/dia.2011.0259

49. DiMeglio LA, Pottorff TM, Boyd SR, et al (2004) A randomized, controlled study of insulin pump therapy in diabetic preschoolers. J Pediatr 145:380–384. doi: 10.1016/j.jpeds.2004.06.022

50. Ahern JAH, Boland EA, Doane R, et al (2002) Insulin pump therapy in pediatrics: a therapeutic alternative to safely lower HbA1c levels across all age groups. Pediatr Diabetes 3:10–5. doi: 10.1034/j.1399-5448.2002.30103.x

51. Seereiner S, Neeser K, Weber C, et al (2010) Attitudes towards insulin pump therapy among adolescents and young people. Diabetes Technol Ther 12:89–94 6p. doi: 10.1089/dia.2009.0080

52. Heinemann L, Benesch C, DeVries JH (2011) AP@home: a novel European approach to bring the artificial pancreas home. J Diabetes Sci Technol 5:1363–72. doi: 10.1177/193229681100500607

53. Ang KH, Tamborlane W V, Weinzimer SA (2015) Combining glucose monitoring and insulin delivery into a single device: current progress and ongoing challenges of the artificial pancreas. Expert Opin Drug Deliv 12:1579–82. doi: 10.1517/17425247.2015.1074174

54. Rodbard D (2016) Continuous Glucose Monitoring: A Review of Successes, Challenges, and Opportunities. Diabetes Technol Ther 18 Suppl 2:S3–S13. doi:

10.1089/dia.2015.0417

55. (2016) FDA Advisory Panel Votes to Recommend Non-Adjunctive Use of Dexcom G5 Mobile CGM. Diabetes Technol Ther 18:512–516. doi: 10.1089/dia.2016.07252.mr

56. Bailey T, Bode BW, Christiansen MP, et al (2015) The Performance and Usability of a Factory-Calibrated Flash Glucose Monitoring System. Diabetes Technol Ther 17:787–94. doi: 10.1089/dia.2014.0378

57. Hajnsek M, Nacht B, Sax S, et al (2014) The single-port concept: combining optical glucose measurement with insulin infusion. Acta Diabetol 51:883–886. doi: 10.1007/s00592-014-0578-y

58. Rumpler M, Mader JK, Fischer JP, et al (2016) First application of a transcutaneous optical single-port glucose monitoring device in patients with type 1 diabetes mellitus. Biosens Bioelectron. doi: 10.1016/j.bios.2016.08.039

59. Lindpointner, Korsatko, Köhler, Köhler, Schaller, Kaidar, Yodfat, Schaupp, Ellmerer, Pieber R (2010) Use of the Site of Subcutaneous Insulin Administration for the Measurement of Glucose in Patients With Type 1 Diabetes. Diabetes Care. doi: 10.2337/dc09-1532.

60. Ward WK, Heinrich G, Breen M, et al (2017) An Amperometric Glucose Sensor Integrated into an Insulin Delivery Cannula: In Vitro and In Vivo Evaluation. Diabetes Technol Ther 19:226–236. doi: 10.1089/dia.2016.0407

61. Lindpointner S, Korsatko S, Köhler G, et al (2010) Use of the site of subcutaneous insulin administration for the measurement of glucose in patients with type 1 diabetes. Diabetes Care 33:595–601. doi: 10.2337/dc09-1532

62. Weisman A, Bai J-W, Cardinez M, et al (2017) Effect of artificial pancreas systems on glycaemic control in patients with type 1 diabetes: a systematic review and meta-analysis of outpatient randomised controlled trials. Lancet Diabetes Endocrinol 5:501–512. doi: 10.1016/S2213-8587(17)30167-5

63. Bergenstal RM, Klonoff DC, Garg SK, et al (2013) Threshold-based insulin-pump interruption for reduction of hypoglycemia. N Engl J Med 369:224–32. doi: 10.1056/NEJMoa1303576

64. Garg S, Brazg RL, Bailey TS, et al (2012) Reduction in Duration of Hypoglycemia by Automatic Suspension of Insulin Delivery: The In-Clinic ASPIRE Study. Diabetes

Technol Ther 14:205–209. doi: 10.1089/dia.2011.0292

65. Bequette BW (2012) Challenges and Recent Progress in the Development of a Closed-loop Artificial Pancreas. Annu Rev Control 36:255–266. doi: 10.1016/j.arcontrol.2012.09.007

66. Thabit H, Tauschmann M, Allen JM, et al (2015) Home Use of an Artificial Beta Cell in Type 1 Diabetes. N Engl J Med 150917085028008. doi: 10.1056/NEJMoa1509351

67. Ruan Y, Thabit H, Leelarathna L, et al (2016) Variability of Insulin Requirements Over 12 Weeks of Closed-Loop Insulin Delivery in Adults With Type 1 Diabetes. Diabetes Care 39:830–832. doi: 10.2337/dc15-2623

68. Hovorka R (2015) Artificial Pancreas Project at Cambridge 2013. Diabet Med 32:987–92. doi: 10.1111/dme.12766

69. Cengiz E (2013) Closer to ideal insulin action: ultra fast acting insulins. Panminerva Med 55:269–75.

70. Kastellorizios M, Tipnis N, Burgess DJ (2015) Foreign Body Reaction to Subcutaneous Implants. In: Lambris JD, Ekdahl KN, Ricklin D, Nilsson B (eds) Immune Responses to Biosurfaces Mech. Ther. Interv., 1st ed. Springer, pp 93–108

71. Hirsch IRLB, Farkas-hirsch R, Mcgill JB (1992) Catheter Obstruction With Continuous Subcutaneous Insulin Infusion. Diabetes Care 15:593–594.

72. Conwell LS, Pope E, Artiles AM, et al (2008) Dermatological complications of continuous subcutaneous insulin infusion in children and adolescents. J Pediatr 152:622–8. doi: 10.1016/j.jpeds.2007.10.006

73. Anderson JM, Rodriguez A, Chang DT (2008) Foreign body reaction to biomaterials. Semin Immunol 20:86–100. doi: 10.1016/j.smim.2007.11.004

74. Sheikh Z, Brooks PJ, Barzilay O, et al (2015) Macrophages, foreign body giant cells and their response to implantable biomaterials. Materials (Basel) 8:5671–5701. doi: 10.3390/ma8095269

75. Gifford R, Kehoe J, Barnes S, et al (2006) Protein interactions with subcutaneously implanted biosensors. Biomaterials 27:2587–2598. doi: 10.1016/j.biomaterials.2005.11.033

76. Bagnall RD, Arundel PA (1983) A method for the prediction of protein adsorption on implant surfaces. J Biomed Mater Res 17:459–66. doi: 10.1002/jbm.820170306

77. Horbett TA (2013) Chapter II.1.2 - Adsorbed Proteins on Biomaterials. In: Biomater. Sci. (Third Ed. pp 394–408

78. Horbett TA (1993) Chapter 13 Principles underlying the role of adsorbed plasma proteins in blood interactions with foreign materials. Cardiovasc Pathol 2:137–148. doi: 10.1016/1054-8807(93)90054-6

79. Ratner BD (1996) The engineering of biomaterials exhibiting recognition and specificity. J Mol Recognit 9:617–625. doi: 10.1002/(SICI)1099-1352(199634/12)9:5/6<617::AID-JMR310>3.0.CO;2-D

80. Castner DG, Ratner BD (2002) Biomedical surface science: Foundations to frontiers. Surf Sci. doi: 10.1016/S0039-6028(01)01587-4

81. Ratner BD, Bryant SJ (2004) Biomaterials: where we have been and where we are going. Annu Rev Biomed Eng 6:41–75. doi: 10.1146/annurev.bioeng.6.040803.140027

82. Franz S, Rammelt S, Scharnweber D, Simon JC (2011) Immune responses to implants - a review of the implications for the design of immunomodulatory biomaterials. Biomaterials 32:6692–709. doi: 10.1016/j.biomaterials.2011.05.078

83. Morais JM, Papadimitrakopoulos F, Burgess DJ (2010) Biomaterials/tissue interactions: possible solutions to overcome foreign body response. AAPS J 12:188–96. doi: 10.1208/s12248-010-9175-3

84. Sides CR, Stenken J a. (2014) Microdialysis sampling techniques applied to studies of the foreign body reaction. Eur J Pharm Sci 57:74–86. doi: 10.1016/j.ejps.2013.11.002

85. Jones JA, Chang DT, Meyerson H, et al (2007) Proteomic analysis and quantification of cytokines and chemokines from biomaterial surface-adherent macrophages and foreign body giant cells. J Biomed Mater Res A 83:585–96.

86. Mitragotri S, Lahann J (2009) Physical approaches to biomaterial design. Nat Mater 8:15–23. doi: 10.1038/nmat2344

87. Champion JA, Mitragotri S (2006) Role of target geometry in phagocytosis. Proc Natl Acad Sci U S A 103:4930–4. doi: 10.1073/pnas.0600997103

88. Tang L, Hu W (2005) Molecular determinants of biocompatibility. Expert Rev Med Devices 2:493–500. doi: 10.1586/17434440.2.4.493

89. Thevenot P, Hu W, Tang L (2008) Surface chemistry influences implant biocompatibility. Curr Top Med Chem 8:270–80.

90. Parker JATC, Walboomers XF, Von den Hoff JW, et al (2002) Soft-tissue response to silicone and poly-L-lactic acid implants with a periodic or random surface micropattern. J Biomed Mater Res 61:91–98. doi: 10.1002/jbm.10170

91. Zhang Y, Huo M, Zhou J, Xie S (2010) PKSolver: An add-in program for pharmacokinetic and pharmacodynamic data analysis in Microsoft Excel. Comput Methods Programs Biomed 99:306–314. doi: 10.1016/j.cmpb.2010.01.007

92. Bustin SA, Benes V, Garson JA, et al (2009) The MIQE Guidelines: Minimum Information for Publication of Quantitative Real-Time PCR Experiments. Clin Chem 55:611–622. doi: 10.1373/clinchem.2008.112797

93. Hauzenberger JR, Hipszer BR, Loeum C, et al (2017) Detailed Analysis of Insulin Absorption Variability and the Tissue Response to Continuous Subcutaneous Insulin Infusion Catheter Implantation in Swine. Diabetes Technol Ther. doi: 10.1089/dia.2017.0175

94. Schmid V, Hohberg C, Borchert M, et al (2010) Pilot study for assessment of optimal frequency for changing catheters in insulin pump therapy-trouble starts on day 3. J diabetes Sci Technol 4:976–982.

95. Guerci B, Sauvanet JP (2005) Subcutaneous insulin: pharmacokinetic variability and glycemic variability. Diabetes Metab 31:4S7–4S24. doi: 10.1016/S1262-3636(05)88263-1

96. Medtronic Australasia Pty Ltd (2008) Basic troubleshooting tips. http://www.medtronicretiree.com/wcm/groups/mdtcom_sg/@mdt/@ap/@au/@diabetes/documents/documents/contrib_107978.pdf. Accessed 22 Jun 2016

97. Swan KL, Dziura JD, Steil GM, et al (2009) Effect of age of infusion site and type of rapid-acting analog on pharmacodynamic parameters of insulin boluses in youth with type 1 diabetes receiving insulin pump therapy. Diabetes Care 32:240–4. doi: 10.2337/dc08-0595

98. Plum A, Agerso H, Andersen L (2000) Pharmacokinetics of the rapid-acting insulin analog, insulin aspart, in rats, dogs, and pigs, and pharmacodynamics of insulin

aspart in pigs. Drug Metab Dispos 28:155–60.

99. Vlasakakis G, Johnson SL, Lin J, et al (2015) Pharmacokinetics and Tolerability of Exenatide Delivered by 7-Day Continuous Subcutaneous Infusion in Healthy Volunteers. Adv Ther 32:650–661. doi: 10.1007/s12325-015-0222-4

100. Karlin AW, Ly TT, Pyle L, et al (2016) Duration of Infusion Set Survival in Lipohypertrophy Versus Nonlipohypertrophied Tissue in Patients with Type 1 Diabetes. Diabetes Technol Ther 18:dia.2015.0432. doi: 10.1089/dia.2015.0432

101. Matlaga BF, Yasenchak LP, Salthouse TN (1976) Tissue response to implanted polymers: The significance of sample shape. J Biomed Mater Res 10:391–397. doi: 10.1002/jbm.820100308

102. Salthouse TN (1984) Some aspects of macrophage behavior at the implant interface. J Biomed Mater Res 18:395–401. doi: 10.1002/jbm.820180407

103. Kraegen EW, Chisholm DJ Pharmacokinetics of insulin. Implications for continuous subcutaneous insulin infusion therapy. Clin Pharmacokinet 10:303–14. doi: 10.2165/00003088-198510040-00002

104. McLennan DN, Porter CJH, Charman SA (2005) Subcutaneous drug delivery and the role of the lymphatics. Drug Discov Today Technol 2:89–96.

105. Yang YJ, Hope ID, Ader M, Bergman RN (1989) Insulin Transport across Capillaries Is Rate Limiting for Insulin Action in Dogs. J Clin Invest 84:1620–1628.

106. Charman SA, McLennan DN, Edwards GA, Porter CJ (2001) Lymphatic absorption is a significant contributor to the subcutaneous bioavailability of insulin in a sheep model. Pharm Res 18:1620–1626.

107. Porter CJ, Charman SA (2000) Lymphatic transport of proteins after subcutaneous administration. J Pharm Sci 89:297–310. doi: 10.1002/(SICI)1520-6017(200003)89:3<297::AID-JPS2>3.0.CO;2-P

108. Charman SA, McLennan DN, Edwards GA, Porter CJH (2001) Lymphatic Absorption Is a Significant Contributor to the Subcutaneous Bioavailability of Insulin in a Sheep Model. Pharm Res 18:1620–1626.

109. Ader M, Poulin RA, Yang, Yeon J, Bergman RN (1992) Dose-Response Relationship Between Lymph Insulin and Glucose Uptake Reveals Enhanced Insulin Sensitivity of Peripheral Tissues. Diabetes 41:241–253.

110. Hojbjerre L, Skov-Jensen C, Kaastrup P, et al (2009) Effect of insulin catheter wear-time on subcutaneous adipose tissue blood flow and insulin absorption in humans. Diabetes Technol Ther 11:575–580. doi: 10.1089/dia.2009.0058

111. Bergman RN (2003) Insulin Action and Distribution of Tissue Blood Flow. J Clin Endocrinol Metab. doi: jc.2003-031431

112. Groth L, Serup J (1998) Cutaneous Microdialysis in Man: Effects of Needle Insertion Trauma and Anaesthesia on Skin Perfusion, Erythema and Skin Thickness. Acta Derm Venerol 78:5–9.

113. Pickup JC, Sherwin RS, Tamborlane W V, et al (1985) Conference on insulin pump therapy in diabetes. Multicenter study of effect on microvascular disease. The pump life. Patient responses and clinical and technological problems. Diabetes 34 Suppl 3:37–41.

114. Thomsen M, Hernandez-Garcia A, Mathiesen J, et al (2014) Model study of the pressure build-up during subcutaneous injection. PLoS One 9:e104054. doi: 10.1371/journal.pone.0104054

115. Mader JK, Birngruber T, Korsatko S, et al (2013) Enhanced absorption of insulin aspart as the result of a dispersed injection strategy tested in a randomized trial in type 1 diabetic patients. Diabetes Care 36:780–5. doi: 10.2337/dc12-1319

116. Pachler C, Ikeoka D, Plank J, et al (2007) Subcutaneous adipose tissue exerts proinflammatory cytokines after minimal trauma in humans. Am J Physiol Endocrinol Metab 293:E690–6. doi: 10.1152/ajpendo.00034.2007

117. Lattermann R, Schricker T, Wachter U, et al (2001) Understanding the mechanisms by which isoflurane modifies the hyperglycemic response to surgery. Anesth Analg 93:121–127.

118. Tanaka K, Kawano T, Tomino T, et al (2009) Mechanisms of impaired glucose tolerance and insulin secretion during isoflurane anesthesia. Anesthesiology 111:1044–51. doi: 10.1097/ALN.0b013e3181bbcb0d

119. Windeløv JA, Pedersen J, Holst JJ (2016) Use of anesthesia dramatically alters the oral glucose tolerance and insulin secretion in C57Bl/6 mice. Physiol Rep 4:e12824. doi: 10.14814/phy2.12824

120. Behdad S, Mortazavizadeh A, Ayatollahi V, et al (2014) The effects of propofol and isoflurane on blood glucose during abdominal hysterectomy in diabetic patients.

Diabetes Metab J 38:311–316. doi: 10.4093/dmj.2014.38.4.311

121. Carroll LA, Koch RJ (2003) Heparin stimulates production of bFGF and TGF-beta 1 by human normal, keloid, and fetal dermal fibroblasts. Med Sci Monit 9:BR97–108.

122. Fan S-Q, Qin L-Y, Cai J-L, et al Effect of heparin on production of basic fibroblast growth factor and transforming growth factor-beta1 by human normal skin and hyperplastic scar fibroblasts. J Burn Care Res 28:734–41.

123. Bicer YO, Koybasi S, Suslu AE, et al (2014) Effect of heparin on inflammation: An animal model of tracheal stents. Laryngoscope 124:E368–E372. doi: 10.1002/lary.24684

124. Ikeoka DT, Pachler C, Mader JK, et al (2011) Lipid-heparin infusion suppresses the IL-10 response to trauma in subcutaneous adipose tissue in humans. Obesity (Silver Spring) 19:715–21. doi: 10.1038/oby.2010.227

125. Dal Molin A, Allara E, Montani D, et al (2014) Flushing the central venous catheter: is heparin necessary? J Vasc Access 15:241–248. doi: 10.5301/jva.5000225

126. López-Briz E, Ruiz Garcia V, Cabello JB, et al (2014) Heparin versus 0.9% sodium chloride intermittent flushing for prevention of occlusion in central venous catheters in adults. Cochrane Database Syst Rev. doi: 10.1002/14651858.CD008462.pub2

127. Kobayashi T, Sawano S, Itoh T, et al (1983) The pharmacokinetics of insulin after continuous subcutaneous infusion or bolus subcutaneous injection in diabetic patients. Diabetes 32:331–336. doi: 10.2337/diabetes.32.4.331

128. Heinemann L (2002) Variability of insulin absorpton and insulin action. Diabetes Technol Ther 4:673–682.

129. Binder C (1969) Absorption of Injected Insulin. ACTA Pharmacol. E T Toxicol.

130. Hildebrandt P (1991) Subcutaneous absorption of insulin in insulin-dependent diabetic patients. Influence of species, physico-chemical properties of insulin and physiological factors. Dan Med Bull 38:337–46.

131. Freckmann G, Pleus S, Westhoff A, et al (2012) Clinical Performance of a Device That Applies Local Heat to the Insulin Infusion Site: A Crossover Study. J Diabetes Sci Technol 6:320–327. doi: 10.1177/193229681200600215

132. Dunn MF (2005) Zinc-Ligand Interactions Modulate Assembly and Stability of the Insulin Hexamer - A Review. BioMetals 18:295–303. doi: 10.1007/s10534-005-

3685-y

133. Supersaxo A, Hein WR, Steffen H (1990) Effect of molecular weight on the lymphatic absorption of water-soluble compounds following subcutaneous administration. Pharm Res 7:167–9.

134. Brange J, Ribel U, Hansen JF, et al (1988) Monomeric insulins obtained by protein engineering and their medical implications. Nature 333:679–682. doi: 10.1038/333679a0

135. Kang S, Brange J, Burch A, et al (1991) Subcutaneous Insulin Absorption Explained by Insulin's Physicochemical Properties. Diabetes Care 14:942–948.

136. Hedman CA, Lindstrom T, Arnqvist HJ (2001) Direct Comparison of Insulin Lispro and Aspart Shows Small Differences in Plasma Insulin Profiles After Subcutaneous Injection in Type 1 Diabetes. Diabetes Care 24:1120–1121.

137. Morrow L, Muchmore DB, Ludington EA, et al (2011) Reduction in intrasubject variability in the pharmacokinetic response to insulin after subcutaneous co-administration with recombinant human hyaluronidase in healthy volunteers. Diabetes Technol Ther 13:1039–45.

138. Liu D, Moberg E, Wredling R, et al (1991) Insulin absorption is faster when keeping the infusion site in use for three days during continuous subcutaneous insulin infusion. Diabetes Res Clin Pract 12:19–24.

139. Swan KL, Dziura JD, Steil GM, et al (2009) Effect of Age of Infusion Site and Type of Rapid-Acting Analog on Pharmacodynamic Parameters of Insulin Boluses in Youth With Type 1 Diabetes Receiving Insulin Pump Therapy. Diabetes Care 32:240–244. doi: 10.2337/dc08-0595

140. Olsson PO, Arnqvist H, Asplund J (1993) No Pharmacokinetic Effect of Retaining the Infusion Site up to Four Days During Continuous Subcutaneous Insulin Infusion Therapy. Diabet Med 10:477–480. doi: 10.1111/j.1464-5491.1993.tb00102.x

141. Busuttil SJ, Drumm C, Plow EF (2005) In Vivo Comparison of the Inflammatory Response Induced by Different Vascular Biomaterials. Vascular 13:230–235. doi: 10.1258/rsmvasc.13.4.230

142. Hallab NJ, Bundy KJ, O'Connor K, et al (2001) Evaluation of Metallic and Polymeric Biomaterial Surface Energy and Surface Roughness Characteristics for Directed Cell Adhesion. Tissue Eng 7:55–71. doi: 10.1089/107632700300003297

143. Anderson JM, Jones JA (2007) Phenotypic dichotomies in the foreign body reaction. Biomaterials 28:5114–5120. doi: 10.1016/j.biomaterials.2007.07.010

144. Werner S, Grose R (2003) Regulation of wound healing by growth factors and cytokines. Physiol Rev 83:835–70. doi: 10.1152/physrev.00031.2002

145. Grayson LS, Hansbrough JF, Zapata-Sirvent RL, et al (1993) Quantitation of cytokine levels in skin graft donor site wound fluid. Burns 19:401–5.

146. Engelhardt E, Toksoy A, Goebeler M, et al (1998) Chemokines IL-8, GROalpha, MCP-1, IP-10, and Mig are sequentially and differentially expressed during phase-specific infiltration of leukocyte subsets in human wound healing. Am J Pathol 153:1849–60.

147. Iocono JA, Colleran KR, Remick DG, et al (2000) Interleukin-8 levels and activity in delayed-healing human thermal wounds. Wound Repair Regen 8:216–225. doi: 10.1046/j.1524-475X.2000.00216.x

148. Jones KS (2008) Effects of biomaterial-induced inflammation on fibrosis and rejection. Semin Immunol 20:130–136. doi: 10.1016/j.smim.2007.11.005

149. Eming SA, Kaufmann J, Löhrer R, Krieg T (2007) Chronische Wunde. Der Hautarzt 58:939–944. doi: 10.1007/s00105-007-1402-1

150. Veiseh O, Doloff JC, Ma M, et al (2015) Size- and shape-dependent foreign body immune response to materials implanted in rodents and non-human primates. Nat Mater 14:643–51. doi: 10.1038/nmat4290

151. Moshayedi P, Ng G, Kwok JCF, et al (2014) The relationship between glial cell mechanosensitivity and foreign body reactions in the central nervous system. Biomaterials 35:3919–3925. doi: 10.1016/j.biomaterials.2014.01.038

152. Krogh-Madsen R, Plomgaard P, Keller P, et al (2004) Insulin stimulates interleukin-6 and tumor necrosis factor-alpha gene expression in human subcutaneous adipose tissue. Am J Physiol Endocrinol Metab 286:E234–8. doi: 10.1152/ajpendo.00274.2003

153. Wang JF, Olson ME, Reno CR, et al (2001) The pig as a model for excisional skin wound healing: characterization of the molecular and cellular biology, and bacteriology of the healing process. Comp Med 51:341–348.

154. Seaton M, Hocking A, Gibran NS (2015) Porcine models of cutaneous wound

healing. ILAR J 56:127–138. doi: 10.1093/ilar/ilv016

155. Mestas J, Hughes CCW (2004) Of Mice and Not Men: Differences between Mouse and Human Immunology. J Immunol 172:2731–2738. doi: 10.4049/jimmunol.172.5.2731

156. Seok J, Warren HS, Cuenca AG, et al (2013) Genomic responses in mouse models poorly mimic human inflammatory diseases. Proc Natl Acad Sci 110:3507–3512. doi: 10.1073/pnas.1222878110

157. Meyer W, Schwarz R, Neurand K (1978) The skin of domestic mammals as a model for the human skin, with special reference to the domestic pig. Curr Probl Dermatol 7:39–52.

158. Sullivan TP, Eaglstein WH, Davis SC, Mertz P (2001) The pig as a model for human wound healing. Wound Repair Regen 9:66–76.

159. Lindholm JS, McCormick JM, Colton SW, Downing DT (1981) Variation of skin surface lipid composition among mammals. Comp Biochem Physiol -- Part B Biochem 69:75–78. doi: 10.1016/0305-0491(81)90211-X

8. APPENDIX

Table 22: Oligo names and sequences for porcine genes for SYBR Green qPCR

Name	Sequence	Comment
TNFa_fw	GCGTGAAGCTGAAAGACAAC	Gene of interest
TNFa_rv	TGGTGTGAGTGAGGAAAACG	Gene of interest
TGFb_fw	AAAACAGGAAGGCAGTGTGG	Gene of interest
TGFb_rv	TAGGCTGCTTTCTTGGCTTC	Gene of interest
IL10_fw	TGATGGGGAGGATATCAAGG	Gene of interest
IL10_rv	GGCCTTGCTCTTGTTTTCAC	Gene of interest
IL8_fw	AGAAAACAGCCCGTGTCAAC	Gene of interest
IL8_rv	GCTGCAGAAAGCAGGAAAAC	Gene of interest
IL6_fw	CCTGGAAGAAGATGCCAAAG	Gene of interest
IL6_rv	TTCAGTTTTGTCCGGAGAGG	Gene of interest
CD68_fw	ACGTTGGCTGTGCTCTTCTT	Gene of interest
CD68_rv	CTGGTGGTGGTAGCAGGATT	Gene of interest
YWHAZ_fw	CACAGCAAGCATACCAGGAA	Reference gene
YWHAZ_rv	GTTCAGCAATGGCTTCATCA	Reference gene
RPL4_fw	AGGAGGCTGTTCTGCTTCTG	Reference gene
RPL4_rv	TCCAGGGATGTTTCTGAAGG	Reference gene

Table 23: Dye leakage into the CSII catheter's hub, dye leakage onto the skin and insulin pump occlusion alarms for all commercial CSII catheters (CC) and investigational CSII catheters (IC).

Swine	Catheter	No.	Occlusion Alarm	Leak into hub[+]	Leak onto skin[§]
1	C	1	No	None	None
1	C*	2	No	None	Severe
1	C	3	No	None	None
1	C	4	No	None	None
1	C	5	No	None	None
1	C	6	No	None	None
2	C*	1	No	Mild	None
2	C	2	No	None	None
2	C	3	No	None	None
2	C	4	No	None	None
2	C	5	No	None	None
2	C	6	No	Severe	None
3	C	1	Yes	None	None
3	C*	2	No	None	None
3	C	3	No	None	None
3	C	4	No	None	None
3	C	5	No	None	None
3	C	6	No	None	None
4	C*	1	No	None	None
4	C	2	No	None	None
4	C	3	No	None	None
4	C	4	Yes	None	None
4	C	5	No	None	None

4	C	6	No	None	None
5	C	1	No	None	None
5	C*	2	No	None	None
5	C	3	No	None	None
5	C	4	No	None	None
5	C	5	No	None	None
5	C	6	No	None	None
6	C	1	Yes	None	None
6	C*	2	No	Mild	None
6	C	3	No	Mild	None
6	C	4	No	Mild	None
6	C	5	No	None	None
6	C	6	Yes	Mild	None
1	N*	1	Yes	Mild	None
1	N	2	Yes	None	None
1	N	3	No	None	Severe
1	N	4	No	None	None
1	N	5	Yes	None	None
1	N	6	Yes	None	None
2	N	1	Yes	Moderate	None
2	N*	2	No	None	Moderate
2	N	3	No	Mild	None
2	N	4	No	Severe	None
2	N	5	Yes	None	None
2	N	6	Yes	None	None
3	N*	1	Yes	Mild	None
3	N	2	No	Moderate	None
3	N	3	Yes	None	None
3	N	4	No	Mild	None
3	N	5	No	None	Mild
3	N	6	Yes	Severe	None
4	N	1	Yes	None	None
4	N*	2	No	None	None
4	N	3	Yes	None	None
4	N	4	No	Severe	None
4	N	5	Yes	None	None
4	N	6	No	None	None
5	N*	1	No	None	None
5	N	2	Yes	None	None
5	N	3	Yes	None	None
5	N	4	No	Severe	None
5	N	5	No	None	None
5	N	6	Yes	None	None
6	N*	1	No	Moderate	None
6	N	2	Yes	None	None
6	N	3	No	Moderate	None
6	N	4	No	Moderate	None
6	N	5	Yes	None	None
6	N	6	Yes	None	None
[+]indicating a problem with tubing and flow of liquid, [§]indicating a problem with insulin absorption into tissue; *catheters used for PK studies;					

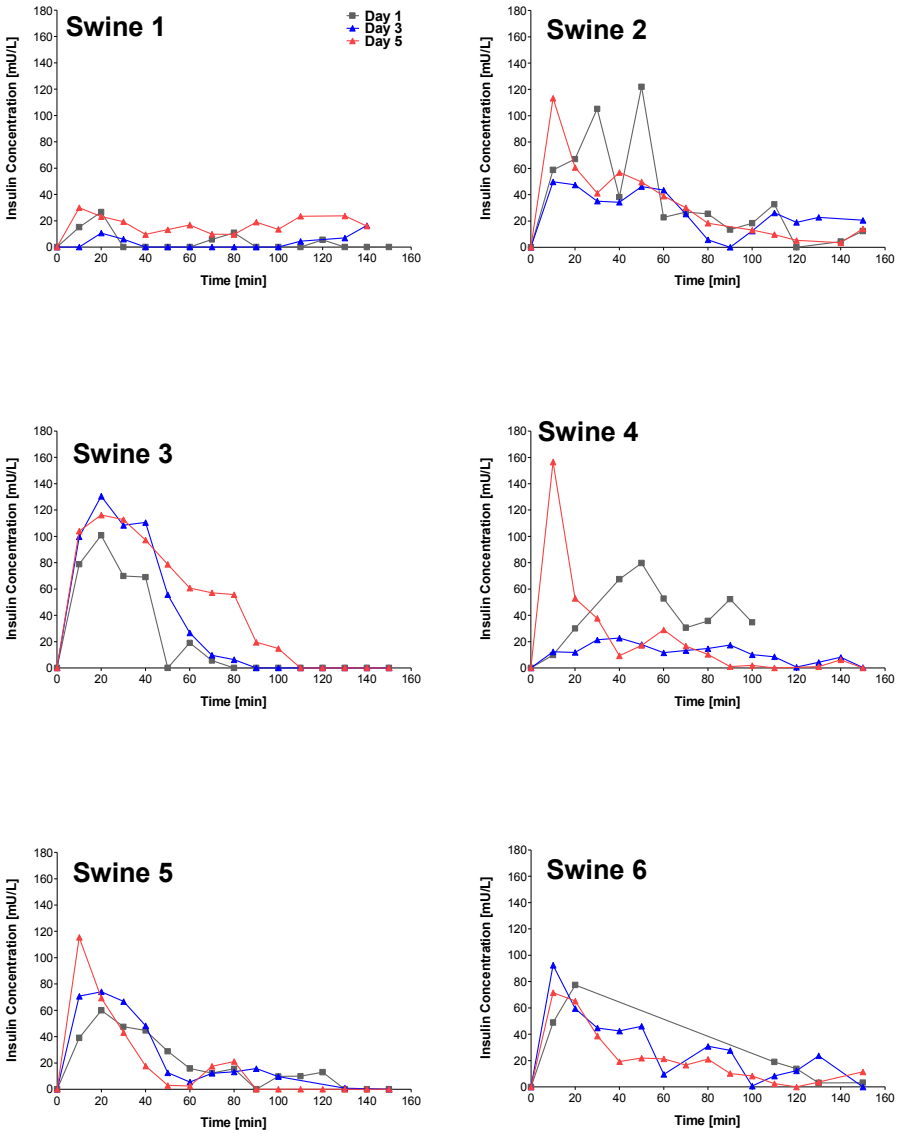

Figure 36: Individual insulin concentration curves over 2.5 hours for insulin administered through the commercial catheter.

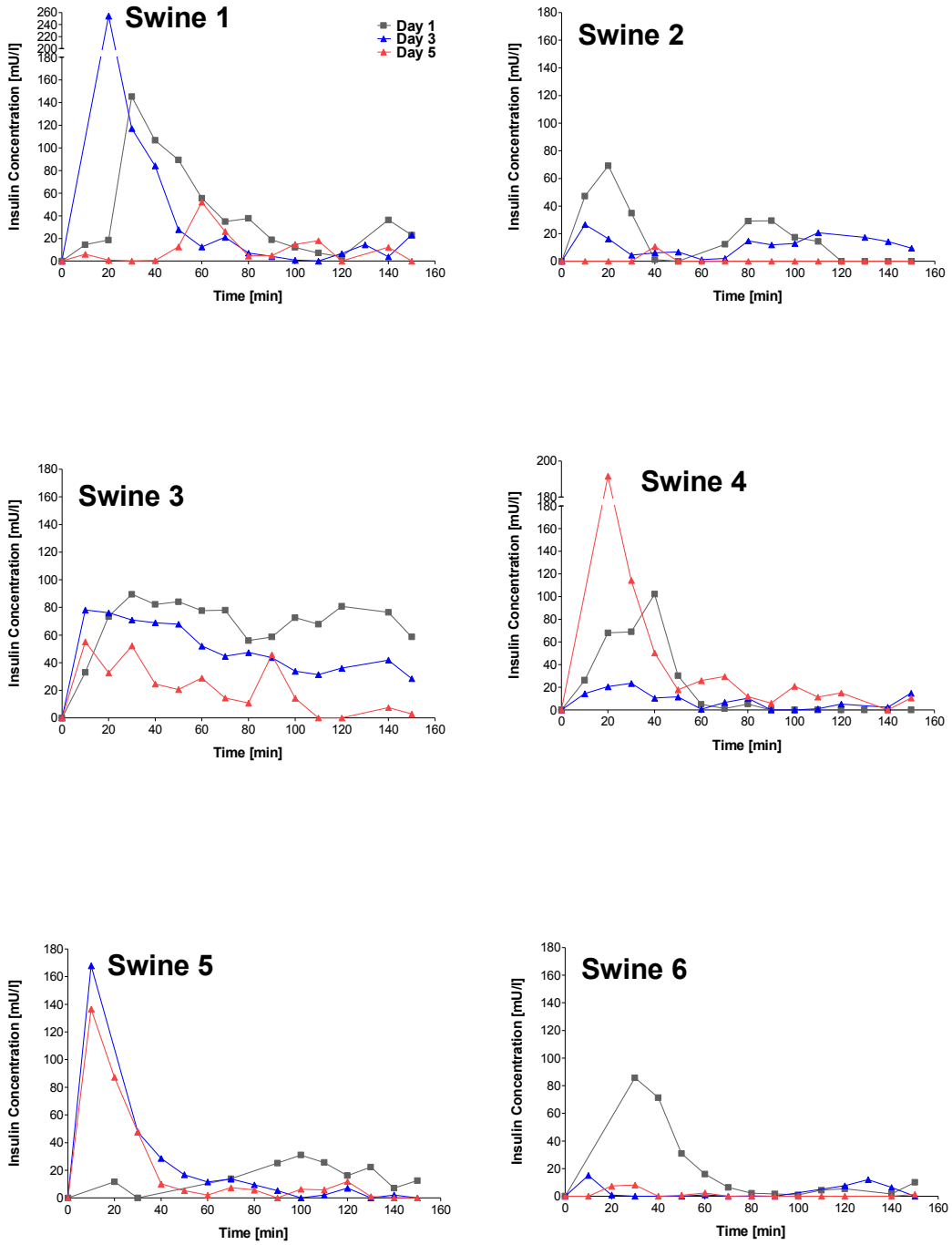

Figure 37: Individual insulin concentration curves over 2.5 hours for insulin administered through the new, experimental catheter.

Table 24: Tissue histology data according to catheter and infusion type

		CSII Catheter	None	Mild	Moderate	Severe	Significance
Reticular Fiber Disruption	Insulin	C	0	9 (82 %)	2 (18 %)	0	§
		N	0	0	4 (33 %)	8 (67 %)	
	Saline	C	0	11 (92 %)	1 (8 %)	0	***
		N	0	2 (17 %)	2 (17 %)	8 (67 %)	
	None	C	0	9 (75 %)	3 (25 %)	0	*
		N	0	4 (33 %)	3 (25 %)	5 (42 %)	
Fibrin Deposition in Reservoir	Insulin	C	0	0	3 (27 %)	8 (67 %)	§
		N	0	2 (17 %)	8 (73 %)	2 (17 %)	
	Saline	C	0	6 (50 %)	5 (42 %)	1 (8 %)	*ns*
		N	0	3 (25 %)	6 (50 %)	3 (25 %)	
	None	C	0	4 (33 %)	7 (58 %)	1 (8 %)	*ns*
		N	0	3 (25 %)	7 (58 %)	2 (17 %)	
Collagen Deposition at Tip	Insulin	C	0	9 (82 %)	2 (18 %)	0	*ns*
		N	1 (8 %)	7 (58 %)	3 (25 %)	1 (8 %)	
	Saline	C	2 (17 %)	8 (67 %)	2 (17 %)	0	*ns*
		N	0	8 (67 %)	4 (33 %)	0	
	None	C	1 (8 %)	9 (75 %)	2 (17 %)	0	§
		N	0	8 (67 %)	4 (33 %)	0	
Fat Necrosis	Insulin	C	0	4 (36 %)	7 (64 %)	0	*
		N	0	1 (8 %)	5 (42 %)	6 (50 %)	
	Saline	C	0	11 (92 %)	1 (8 %)	0	*
		N	0	3 (25 %)	4 (33 %)	5 (42 %)	
	None	C	0	7 (58 %)	5 (42 %)	0	§
		N	0	3 (25 %)	5 (42 %)	4 (33 %)	
Hemorrhage at Tip Base	Insulin	C	0	7 (64 %)	4 (36 %)	0	*ns*
		N	0	6 (50 %)	6 (50 %)	0	
	Saline	C	0	11 (92 %)	1 (8 %)	0	§
		N	1 (8 %)	4 (33 %)	6 (50 %)	1 (8 %)	
	None	C	0	9 (75 %)	3 (25 %)	0	*ns*
		N	0	7 (58 %)	5 (42 %)	0	

Chi-square test applied where possible; §Invalid conditions for Chi-square; Values in brackets are a percent of 12 (11) catheters total; *** $p < 0.001$, * $p < 0.05$, significant difference between catheter types

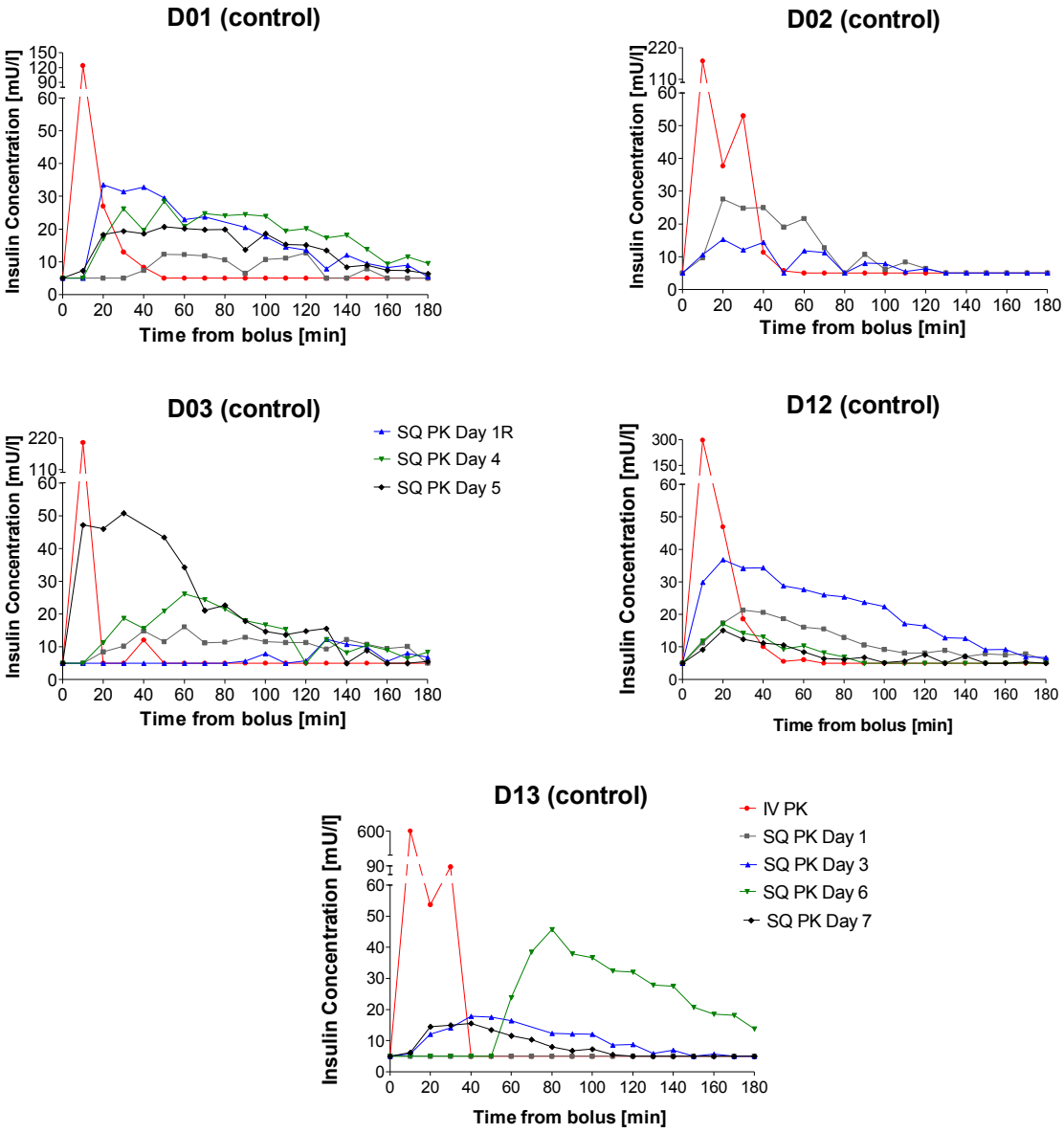

Figure 38: Individual plasma insulin concentration curves over time in control group (canine study).

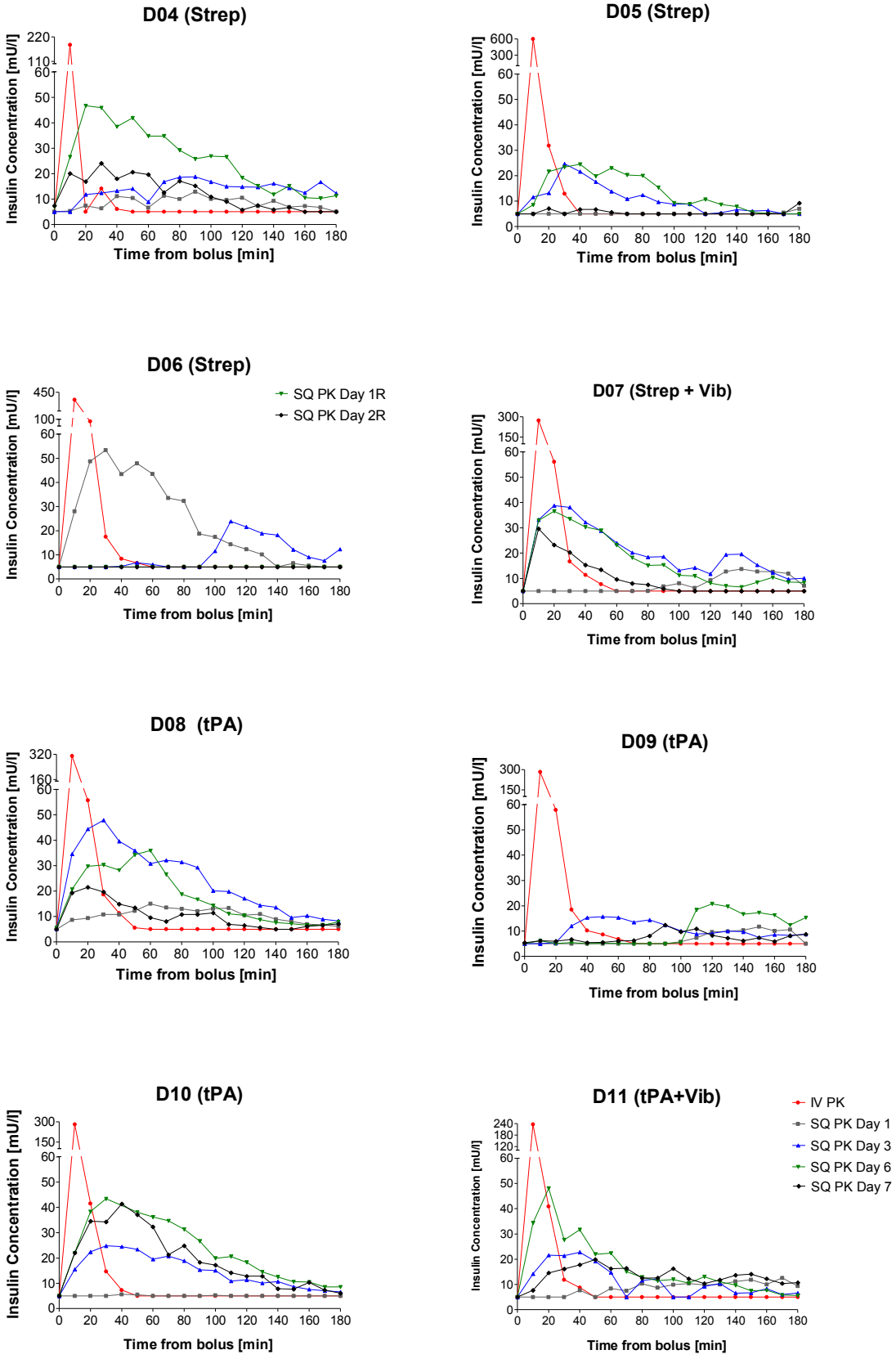

Figure 39: Individual plasma insulin concentration curves over time in treatment group (canine study).